


5-2018

BIOLOGICAL CLOCKS, INFLAMMATION, AND MULTIORGAN DAMAGE IN SICKLE CELL DISEASE

Morayo Adebisi

Follow this and additional works at: https://digitalcommons.library.tmc.edu/utgsbs_dissertations

 Part of the [Molecular Biology Commons](#)

Recommended Citation

Adebisi, Morayo, "BIOLOGICAL CLOCKS, INFLAMMATION, AND MULTIORGAN DAMAGE IN SICKLE CELL DISEASE" (2018). *The University of Texas MD Anderson Cancer Center UTHealth Graduate School of Biomedical Sciences Dissertations and Theses (Open Access)*. 846.
https://digitalcommons.library.tmc.edu/utgsbs_dissertations/846

This Dissertation (PhD) is brought to you for free and open access by the The University of Texas MD Anderson Cancer Center UTHealth Graduate School of Biomedical Sciences at DigitalCommons@TMC. It has been accepted for inclusion in The University of Texas MD Anderson Cancer Center UTHealth Graduate School of Biomedical Sciences Dissertations and Theses (Open Access) by an authorized administrator of DigitalCommons@TMC. For more information, please contact digitalcommons@library.tmc.edu.

BIOLOGICAL CLOCKS, INFLAMMATION, AND MULTIORGAN DAMAGE IN
SICKLE CELL DISEASE

By

Morayo G. Adebisi, B.S.

APPROVED:

Yang Xia, M.D., Ph.D.

Advisory Professor

Rodney E. Kellems, Ph.D.

Darren F. Boehning, Ph.D.

Dorothy E. Lewis, Ph.D.

Edgar T. Walters, Ph.D.

APPROVED:

Dean, The University of Texas

MD Anderson Cancer Center UTHealth Graduate School of Biomedical Sciences

BIOLOGICAL CLOCKS, INFLAMMATION, AND MULTIORGAN DAMAGE
INSICKLE CELL DISEASE

A

DISSERTATION

Presented to the Faculty of
The University of Texas
MD Anderson Cancer Center UTHealth
Graduate School of Biomedical Sciences
in Partial Fulfillment
of the Requirements
for the Degree of
DOCTOR OF PHILOSOPHY

By

Morayo G. Adebisi, B.S

Houston, Texas

May 2018

Copyright

Approval for incorporating previous published study from FASEB Journal was accepted and will be presented with modifications in this dissertation. Additional unpublished findings presented in this dissertation is awaiting manuscript acceptance.

Dedication

This dissertation is dedicated to my family members and close friends, Mr. Howard Head, Ms. Annie Shina, and Ms. Celestina Young who have genetic trait for sickle cell or who are currently living with sickle cell disease. Additionally, I would like to specially dedicate this dissertation to deceased family members who were affected with sickle cell disease. They have encouraged me to pursue graduate school to study this disease.

To my loving family who have helped me adjust throughout graduate school. Especially my mom, David, and Emmanuel who moved to Houston, Texas in order to support me in my graduate school endeavors.

To my patient and supportive husband who allowed me to pursue my passion and offered every support that allowed me to succeed.

Acknowledgments

I would like to thank my mentor **Dr. Yang Xia** for her mentorship and overseeing my dissertation work. I would also like to thank the members of my advisory committee, **Dr. Xia, Dr. Kellems, Dr. Boehning, Dr. Lewis, Dr. Yoo,** and **Dr. Walters** for their guidance of the work presented in this dissertation. I would like to thank my examination committee, **Dr. Boehning, Dr. Lewis, Dr. Chen, Dr. Lee and Dr. Cunha.** Special thanks to **Dr. Seung-Hee Yoo, Dr. Zheng Chen,** and **Dr. Zhaoyang Zhao** for their expertise in circadian biology and special equipment usage. Thank you to several members of my laboratory, particularly, **Ms. Jeanne Manalo, Dr. Anren Song, and Dr. Xuidong Yang,** who have provided support in animal studies. Special thanks to **Dr. Youqiong Ye, Dr. Jing Gong,** and **Dr. Leng Han** for their bioinformatics expertise.

Special thanks to the **Biochemistry and Molecular Biology** graduate students as well as **Biochemistry and Cell Biology** students who have supported me in preparation for committee meetings, candidacy examination, and overall has been an essential part of my graduate journey. Special thanks to **Dr. Yates** who started the First Generation Graduate Students, a group that I am a member of.

I would also like to thank the **NIH National Heart, Lung, and Blood Institute** for their financial support throughout my graduate school career. Special thanks to the **Graduate School of Biomedical Science** for all of the special workshops that played a part in my personal and career development. I would like to thank the

American Society of Hematology for supporting my travel and expenses that allow me to present my work at national conferences.

BIOLOGICAL CLOCKS, INFLAMMATION, AND MULTIORGAN DAMAGE IN SICKLE CELL DISEASE

Morayo G. Adebisi, B.S.

Advisory Professor: Yang Xia, M.D., Ph.D.

Sickle cell disease (SCD) is a dangerous condition caused by a genetic mutation on the human beta-globin gene that contributes to erythrocyte sickling, the hallmark of the disease. Chronic intravascular sickling in peripheral organs can contribute to systemic inflammation and multiple organ dysfunctions leading to further disease progression. Previous metabolomics studies have confirmed that elevated sphingosine kinase 1 (SphK1) mediates sphingosine-1-phosphate (S1P) production to promote erythrocyte sickling. S1P signals via five S1P receptors (S1PR) that regulates several pathophysiological functions.

In the first chapter of this dissertation, I explored the role of S1PRs in SCD by utilizing pharmacologic and genetic tools. To determine the role of S1P-S1PRs signaling in SCD, I treated humanized Berkeley sickle mice (Berkeley HbS mice), with FTY720, a US Food and Drug Administration (FDA) approved drug. FTY720 can be phosphorylated by SphK1 thus mimicking S1P to regulate S1PRs signaling. Mechanistically, FTY720 can inhibit S1PR signaling in immune cells by the internalization of the receptor. Although FTY720 did not improve erythrocyte life span or reduce sickling in SCD mice, FTY720 treated SCD mice showed further reduction of inflammatory cells in the periphery, reduced mRNA and protein levels of

pro-inflammatory cytokine interleukin 6 (IL-6), improved multiple tissue, and renal function.

Since IL-6 is elevated in SCD due to systemic inflammation, I showed that IL-6 expression in the periphery and local tissues contributes to further upregulation of S1PR1 in sickle mice. To test the role of IL-6 in SCD, I generated global genetic deletion of IL-6 in sickle mice. Sickle mice with IL-6 deficiency had overall improved multiple tissue function, which indicates that IL-6 plays a detrimental role in SCD. To further demonstrate this mechanism, I generated mouse BM-derived macrophages to test whether S1P-mediate S1PRs activation, I showed that FTY720 and W146, S1PR1 specific antagonists, have immunomodulatory functions that results in the reduction of S1PR1 and IL-6 mRNA levels. Moreover, I showed that IL-6 induction contributes to further upregulation of S1PR1 mediated via a JAK2-dependent manner in macrophages.

In the second chapter of this dissertation, I discuss findings generated from a highly robust, unbiased microarray screen performed in sickle lung. Several upregulated gene pathways were identified in sickle lung, which include iron homeostatic genes and inflammatory genes. Unexpectedly, I also discovered elevated expression of rhythmic genes, which play a role in regulating biological clocks in multiple cell types. Amongst the rhythmic genes detected was *Period 2* (*Per2*), which regulates circadian rhythms that promotes biological clock function. To test whether *Per2* mRNA and PER2 protein levels were further induced in sickle lung, I utilized a genetic tool, *Per2^{Luciferase}* (*Per2^{Luc}*) mice, a bioluminescence reporter mouse model to study PER2 circadian expression. I generated *Per2^{Luc}* mice with

SCD or WT phenotype by bone marrow transplantation (BMT) studies. With this genetic tool, I detected PER2 luciferase oscillations in *ex-vivo* lung explant cultures. Upregulation of PER2 (based on luciferase activity) regulated in a circadian manner was detected in SCD lungs compared to WT lungs, which confirms that Per2 contributes to clock function.

Next, I determined whether biological clocks play a role in SCD. To test this, I generated WT and SCD phenotypic *Per1/Per2* deficient mice by BMT studies. *Per1/Per2* deficient mice have abnormal biological clock function, which plays a role in disease. Interestingly, I observed further multiple organ dysfunction, systemic, and local tissue inflammation in SCD \rightarrow *Per1/Per2* *dKO* mice compared to SCD \rightarrow WT mice, which demonstrates that the loss of *Per1/Per2* in SCD is detrimental and contributes to these devastating effects.

In the third chapter of my dissertation, I explored the impact of chronic hemolysis mediating elevated heme and iron induction in sickle mice. Since elevated heme and iron are toxic to the organs and contribute to multiple organ dysfunctions, I explored whether *Per1/Per2* was involved. As expected, I observed heme and iron trafficking to the sickle liver and spleen organs is due to hemolysis-mediated events due to sickling. Chronic inflammation due systemic release of heme in the periphery can contribute to heme and iron overload in peripheral tissues to promote further SCD progression. Interestingly, I observed iron trafficking to the *Per1/Per2* deficient sickle lung. To determine a possible mechanism, I detected heme oxygenase 1 (HO-1), an enzyme that metabolizes heme, in peripheral macrophages in the lung and

discovered further elevated expression of HO-1 in sickle mice with *Per1/Per2* deficiency.

Overall, my work demonstrates the beneficial role of biological clock function in sickle mice. My work will be useful for better understanding biological clocks in the context of a highly complicated disease. Although there are several molecular triggers that can offset biological clocks, my work has further clarified why *Per1/Per2* genes are essential regulators of clock function by promoting protective functions in SCD.

Table of Contents

Approval page.....	i
Title Page.....	ii
Copyright.....	iii
Dedication	iv
Acknowledgments	v
Abstract	vii
List of Figures	xvi
List of Tables.....	xix
List of Illustrations.....	xx
Abbreviations	xxi
I. Introduction	1
1.1. Etiology of Sickle Cell Disease.	1
1.2. Epidemiology of Sickle Cell Disease.....	1
1.3. Systemic hemolysis, iron overload, and inflammatory pathways underlying SCD progression.	2
1.4. Sphingosine-1-phosphate (S1P) signaling mediates sickling and further disease progression.	3
1.5. The role of elevated immune responses contributing to vascular dysfunction in SCD.....	6

1.6. Utilizing a unbiased microarray screen to investigate candidate genes that contribute to tissue damage in SCD.	7
1.7. Circadian <i>Period</i> genes from fruit flies to mammals regulate circadian clock function.	8
1.8. The rationale of this dissertation.	11
II. Methods	13
2.1. Mice generation (Berkeley Human Sickle Cell, SCD- <i>IL-6</i> ^{-/-} , <i>Per1/ Per2</i> dKO, <i>Per2</i> ^{Luciferase} mice).	13
2.2. Pharmacologic treatments in sickle mice.	17
2.3. Hematological assessment in sickle mice.	17
2.4. Erythrocyte lifespan measurements.	17
2.5. Flow cytometric analysis of immune cells isolated from peripheral tissues.	18
2.6. Whole blood detection of circulating inflammatory cytokines by ELISA method.	18
2.7. IL-6 detection in serum, multiple organs, and bronchoalveolar lavage (BAL) fluid.	19
2.8. Bone marrow derived macrophages generation from mouse.	19
2.9. Pharmacologic treatment in macrophage culture for S1P, W146, JTE013, TY52156, CYM50358, and AG490.	20
2.10. Whole lung RNA isolation for gene expression screening.	20
2.11. Irradiation and bone marrow (BM) transplantation.	21

2.12. PER2 luciferase detection in bioluminescence reporter mice.	22
2.13. Hematoxylin and eosin (H&E) staining of multiple tissues.	22
2.14. Perl's Blue Prussian iron staining of multiple tissues.	23
2.15. Proteinuria detection.	23
2.16. Hemolytic analysis for total bilirubin.	24
2.17. Alanine aminotransferase (ALT) detection.	24
2.18. Neutrophil infiltration in lung tissue.	24
2.19. RNA extraction and semiquantitative polymerase chain reaction (PCR) detection of inflammatory genes in lung.	25
2.20. Immunofluorescence detection of heme oxygenase (HO-1) expression in alveolar macrophages.	26
2.21. Statistical analysis.	27
III. Results	28
3.1. Chapter 1: Chronic inflammation and multiple tissue damage is detrimental in SCD	28
3.1.1. FY720-mediated S1PR1 antagonism has no effect on erythrocyte sickling.	29
3.1.2. Sphingosine-1-phosphate receptor 1 (S1PR1) mediates elevated inflammation in SCD.	32
3.1.3. Elevated interleukin 6 (IL-6) contributes to chronic inflammation and tissue damage in SCD.	35

3.1.4. FTY720 mediates the reduction of S1PR1 in tissue macrophage.	39
3.1.5. Elevated IL-6 contributes to induction of S1PR1 in SCD.	41
3.1.6. S1P-mediated S1PR1 activation upregulates IL-6 to promote further induction of S1PR1 regulated in a JAK2-dependent manner.....	42
3.2. Chapter 2: Elevated circadian <i>Period 2</i> is beneficial in SCD.....	48
3.2.1. Upregulated expression of circadian genes, inflammatory genes, heme and iron homeostatic genes in SCD lung.	49
3.2.2. <i>Period 2 (Per2)</i> induction in SCD lung underlines molecular clock function to deter further inflammatory response and tissue damage.....	54
3.2.3. Molecular clock dysfunction contributes to further tissue damage in SCD..	60
3.2.4. Systemic inflammation contributes to elevated lung neutrophil infiltration due to global genetic deletion of <i>Per1/Per2</i> in sickle mice.....	68
3.2.5. Genetic deletion of <i>Per1/Per2</i> in sickle mice is involved in tissue lung dysfunction as confirmed by further induction of inflammatory <i>Toll-like receptor 4</i> (Tlr4) and <i>IL-6</i> gene expression as well as elevated IL-6 protein levels in bronchoalveolar lavage (BAL) fluid.....	72
Chapter 3: Elevated heme and iron levels in sickle mice is mediated by heme oxygenase 1 (HO-1)	76
3.3.1. Systemic hemolysis mediates heme and iron deposition in lung.	77
3.3.2. Enhanced heme oxygenase 1 (HO-1) expression in macrophages is required for compensation due to elevated inflammation in SCD lung.	81

IV. Discussion	86
4.1. Summary of dissertation chapters.	86
4.2. Overview of circadian clocks mediating physiological processes in normal and disease conditions.	88
4.3. Heme is a circadian clock regulator.	89
4.4. Pharmacologic induction of heme oxygenase 1 (HO-1) for treating SCD.	90
4.5. Macrophages induction of HO-1 contribute to iron overload in SCD.	94
4.6. Elevated adenosine-mediate ADORA2B activation to promote Per2 induction, which improves disease severity..	98
4.7. Evidence of oxidative-reductive stress in sickle lung tissue.	99
4.8. Future directions.	103
V. References	105
VI. Biographical Sketch	125
VII. Vita.....	129

List of Figures

Figure 1. FTY720 does not affect erythrocyte life span in SCD mice.....	30
Figure 2. FTY720-treated SCD mice reduced circulating inflammatory cytokines demonstrated by ELISA assay.....	33
Figure 3. Circulating IL-6 protein levels in spleen, liver, lung, and kidney detected by spectrophotometric analysis.....	34
Figure 4. Global genetic deletion of <i>IL-6</i> in SCD mice abolished IL-6 levels in the circulation.....	36
Figure 5. FTY70 treatment or global genetic deletion of <i>IL-6</i> contributed to overall improved multiple tissue dysfunction in SCD mice.....	38
Figure 6. FTY720 mediate the reduction of S1PR1 in SCD peripheral macrophages.....	40
Figure 7. Reduction of S1PR1 expression in <i>IL-6</i> genetic deletion mice.....	41
Figure 8. S1P-activates S1PR1 to promote IL-6 production, which upregulates IL-6 production, which induces <i>S1pr1</i> mRNA levels in a JAK2-dependent manner in mouse BM-derived macrophages.....	45
Figure 9. Pathway analyses show upregulated lung specific genes in SCD mice.....	50

Figure 10. Unbiased microarray gene expression screen in SCD lung reveals upregulated expression of rhythmic clock genes, iron hemostatic genes, and inflammatory genes.....	53
Figure 11. Circadian gene expression in SCD compared to WT lung.....	55
Figure 12. Circadian <i>Arnt (Bmal)</i> , <i>Per1</i> , and <i>Per2</i> mRNA expression levels detected by semiquantitative real time polymerase chain reaction (qRT-PCR).....	56
Figure 13. PER2 luciferase activity is higher in SCD.....	59
Figure 14. Loss of <i>Per1/Per2</i> contributes to multi-tissue damage in SCD.....	64
Figure 15. Hepatic and renal dysfunction in <i>Per1/Per2</i> deficient sickle mice.....	66
Figure 16. Phenotypic observation of effect of whole body irradiation and worsen irradiation sensitivity in <i>Per1/Per2</i> dKO mice with SCD phenotype.....	68
Figure 17. Loss of <i>Per1/Per2</i> in SCD contribute to increased pulmonary neutrophil infiltration.....	71
Figure 18. Analysis of <i>Tlr4</i> and <i>IL-6</i> inflammatory gene expression in lung tissue and IL-6 protein detection in BAL fluid.....	74
Figure 19. Heme, iron, and bilirubin are increased in sickle mice with <i>Per1/Per2</i> deficiency.....	79

Figure 20. Immunohistochemistry studies reveal HO-1 expression in peripheral lung macrophages.....83

List of Tables

Table 1. Genotype sequences for Berkeley humanized sickle cell, SCD- <i>IL-6</i> ^{-/-} , <i>Per1/Per2</i> dKO, and <i>Per2</i> ^{Luciferase} mice genetic mice strains.....	16
Table 2. Primer sequences for detecting gene expression by semiquantitative real time polymerase chain reaction (qRT-PCR).....	26
Table 3. Complete blood cell analysis in sickle mice treated with FTY720 or saline and global genetic <i>IL-6</i> deficient sickle mice.....	31
Table 4. Complete blood cell analysis in WT or SCD phenotypic mice with or without <i>Per1/Per2</i> genetic deficiency.....	62

List of Illustrations

Illustration 1. Working models to demonstrate the role of adenosine mediating SphK1-S1P production to promote sickling.....	5
Illustration 2. Circadian gene oscillators that contribute to rhythmic processes.....	10
Illustration 3. Summary of unpublished results for chapter 2 and chapter 3.....	83
Illustration 4: Summary of dissertation chapters 1 – 3.....	87
Illustration 5: Mechanism of heme degradation pathway.....	91
Illustration 6. Possible mechanism involving CD163 scavenger macrophage receptor mediating heme degradation by HO-1 induction to promote <i>Per2</i> transcription in SCD.....	93
Illustration 7. Mixed cell populations that are BM-derived <i>Per1^{+/+}/Per2^{-/-}</i> and resident <i>Per1^{-/-}/Per2^{-/-}</i> express HO-1, which regulates heme degradation in macrophages.....	97
Illustration 8. Differential expression of oxidative-reductive genes identified in mRNA sequencing of the lung isolated from SCD or WT BM transplant mice with or without <i>Per1/Per2</i>	102

Abbreviations

A

ACAD8: acyl-coenzyme A dehydrogenase family member 8

ACOX1: acyl-coenzyme A oxidase-like

ADAM8: a-disintegrin and metalloproteinase domain-containing protein 8

ADORA2B: adenosine receptor 2B

AIFM2: apoptosis inducing factor, (mitochondria associated 2)

ALT: alanine aminotransferase

AMPK: 5'-adenosine monophosphate-activated - protein kinase

ANXA1: annexin A1

ATP: adenosine triphosphate

B

BA: basophils

BAL: bronchoalveolar lavage

BHLHE40: basic helix loop helix family member e 40

BLVRA: biliverdin reductase A

BMAL: brain and muscle arnt-like 1

BMT: bone marrow transplantation

C

C4A: complement component 4 A

C4B: complement component 4 B

CBC: complete blood count/cell

CCL5: C-C motif chemokine ligand 5

CCR2: C-C chemokine receptor type 2

CCR4: C-C chemokine receptor type 4

CLOCK: circadian locomotor output cycles kaput

CO: carbon monoxide

CRY1: cryptochrome 1

CXCL1: C-X-C chemokine motif 1

CXCL2: C-X-C motif chemokine ligand 2

CXCL9: C-X-C motif chemokine ligand 9

CXCL10: C-X-C motif chemokine ligand 10

CXCL13: C-X-C motif chemokine ligand 13

CXCL17: C-X-C motif chemokine ligand 17

CYP1A1: cytochrome P450 family 1 subfamily A member 1

CYP26B1: cytochrome P450, family 26, subfamily B, polypeptide 1

D

DAMPs: danger associated molecular patterns

DBP: d-box binding protein

DEGS1: delta(4)-desaturase, sphingolipid 1

DEOXY-HBS: deoxy-hemoglobin S

D2HGDH2: d-2-hydroxyglutarate dehydrogenase

DIO1: deiodinase, iodothyronine, type 1

2,3-DPG: diphosphoglyceric acid

DUS3L: dihydrouridine synthase 3 like

E

EO: eosinophils

ET-1: endothelin 1

F

FDA: US Food and Drug Administration

FECH: ferrochelatase

FITC: fluorescein isothiocyanate

FPN: ferroportin

FTH: ferritin heavy chain

FTL1: ferritin light chain 1

G

GCSF: granulocyte colony stimulating factor

GSH: glutathione

H

HB α : hemoglobin alpha

HB β : hemoglobin beta

HB-HP: hemoglobin-haptoglobin

HBF: hemoglobin fetal

HBS: sickle beta-globin

HCL: hydrochloric acid

HCT: hematocrit

H&E: hematoxylin and eosin

HGB: hemoglobin

HIF1a: hypoxia inducible factor 1 alpha

HMGB1: high mobility group box 1

HO-1: heme oxygenase 1

HRP: horse radish peroxidase

I

ID1: DNA-binding protein inhibitor 1

ID2: DNA-binding protein inhibitor 2

IFI202B: interferon activated gene 202 B

IL-5: interleukin 5

IL-6: interleukin 6

INFy: interferon gamma

J

K

L

LCN2: lipocalin 2

LOXL4: lysyl oxidase-like 4

LTF: lactoferrin

LY: lymphocytes

M

MDH2: malate dehydrogenase 2, nicotinamide adenine dinucleotide (NAD)

MCP-1: monocyte chemoattractant protein 1

MCV: mean corpuscular volume

ME3: malic enzyme 3, nicotinamide adenine dinucleotide phosphate (NADP) (+)-dependent mitochondrial

MMP11: matrix metalloproteinase 11

MO: monocytes

MSRB2: methionine sulfoxide reductase B2

MT1: metallothionein1

N

NAMPT: nicotinamide phosphoribosyltransferase

ND: not determined

NE: neutrophils

NFE2L2: nuclear factor, erythroid 2-like 2

NO: nitric oxide

NOX1: nicotinamide adenine dinucleotide phosphate (NADPH) oxidase 1

NPAS2: neuronal PAS domain protein 2

NR1D1: nuclear receptor subfamily 1 group D member 1

NR1D2: nuclear receptor subfamily 1 group D member 2

O

ORF: open reading frame

P

PAM: peptidylglycine alpha-amidating monooxygenase

PAS: per-arnt-sim

PCR: polymerase chain reaction

PE: phycoerythrin

PER1: period 1

PER2: period 2

PF4: platelet factor 4

PGE2: prostaglandins E2

P4HA3: prolyl 4-hydroxylase subunit alpha 3

PLOD1: procollagen-lysine, 2-oxoglutarate 5-dioxygenase 1

PPOX: protoporphyrinogen oxidase

PTGS1: prostaglandin synthase 1

Q

R

RBC: red blood cell or erythrocyte count

RDW: red cell distribution width

ROS: reactive oxygen species

S

SAH: subarachnoid hemorrhage

SCD: sickle cell disease

SCD1: (iron-binding) stearyl-coenzyme a desaturase 1

SCN: suprachiasmatic nuclei

SEM: standard error mean

SLC25A37: solute carrier family 25, member 37

S1P: sphingosine-1-phosphate

SPHK1: sphingosine kinase 1

S1PRs: S1P receptors

STEAP 2: metalloredutase 2

STEAP 4: metalloredutase 4

T

TEF: thyrotroph embryonic factor

TLR 4: toll-like receptor 4

TLR 6: toll-like receptor 6

TLR 9: toll-like receptor 9

TNF- α : tumor necrosis factor alpha

U

V

W

WBC: white blood cells

X

Y

Z

ZT: zeitgeber time

I. Introduction

1.1. Etiology of Sickle Cell Disease.

Sickle cell disease (SCD) is the first cellular, molecular and genetic disease characterized in history. In 1910, the first case of SCD was described by Dr. James B. Herrick who coined the term “sickle-shaped”, which described the morphology of erythrocytes isolated from a patient with pulmonary symptoms (1). In 1945, Linus Pauling was the first to hypothesize that SCD was due to abnormalities in hemoglobin (2). To demonstrate this, Pauling performed gel electrophoresis to separate hemoglobin in erythrocytes isolated from SCD patients compared to healthy patients. There were striking differences in electrophoretic motilities in sickle hemoglobin versus normal hemoglobin (3). Dr. Harvey Itano’s research group performed electrophoretic and acid–base titration experiments and concluded that there were differences in ionizing properties in the sickle hemoglobin compared to normal hemoglobin (3). Further analysis was conducted on sickle hemoglobin that confirmed an amino acid substitution from glutamine to valine on the sixth position on the β -globin chain (β^6 Glutamate \rightarrow Valine) (4). Thus, the first disease with a molecular basis was identified. Since abnormalities exist in β -globin chain, this was linked to the discovery of a nucleotide change of the human beta globin (*Hbb*) gene, which is the cause of this autosomal recessive disease (5).

1.2. Epidemiology of Sickle Cell Disease.

In the US, approximately 100,000 people are living with SCD (7). There are approximately 300,000 infants born with SCD worldwide each year (9) with the average life expectancy of patients with SCD about 66 years (6). The incidence of SCD has significantly increased particularly in sub-Saharan Africa, the islands of the Caribbean and the US over the past decades thus leading to high health care costs that average more than 488 million dollars in the US alone (6). It is predicted that by the year 2050, there will be nearly 10 million SCD patients that will be treated for their condition (7). Urgent emergency care is required for the majority of SCD patients, which further increases the economic cost. Frequent hospitalizations for patients with life threatening complications can lead to high morbidity. The pathological and clinical consequences of SCD include end organ damage, priapism, chronic pain, infections, acute chest syndrome, and stroke (6). More than half of patients living with severe complications of the disease experience early mortality (8).

1.3. Systemic hemolysis, iron overload, and inflammatory pathways underlying SCD progression.

Sickle erythrocytes adhesion to the endothelium mediates drastic vascular changes, which can contribute to reduced organ function. Systemic hemolysis releases circulating hemoglobin, which can scavenge nitric oxide (NO) thus resulting in endothelial cell dysfunction (9). NO production is essential for anti-inflammation, anti-thrombosis, and vasodilation. Deficiency in NO production is attributed to the abundance of free heme released in the circulation. Elevated heme mediates induction of endothelial heme oxygenase 1 (HO-1) to breakdown heme to form iron,

carbon dioxide, and biliverdin (10). Bilirubin is a further metabolized product of biliverdin. Elevated bilirubin due to systemic hemolysis can result in deposition to the bile ducts in the liver and gallbladder.

Intravascular hemolysis can contribute to elevated heme-bound iron released from hemoglobin. The heme degradation pathway is involved in the metabolism of heme-bound iron mediated by HO-1. Further induction of HO-1 contributes to the generation of the end products that result from heme degradation. In SCD, elevated HO-1 induction mediates heme degradation. Due to chronic hemolysis elevated iron deposition to multiple organs can become toxic, which can interfere with organ function. Since SCD is a condition of oxidative stress, reactive oxygen species (ROS) are generated, a dangerous outcome of systemic hemolysis. Due to the abundance of ROS, excess iron can react with ROS, which has drastic effects in overall organ function (11).

1.4. Sphingosine-1-phosphate (S1P) signaling mediates sickling and further disease progression.

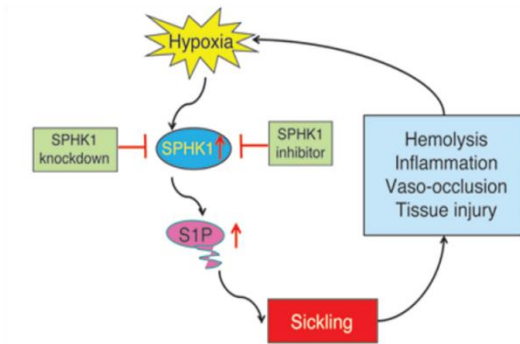
In an unbiased high throughput metabolomics screen, our lab discovered that elevated levels of circulating metabolites adenosine and sphingosine-1-phosphate (S1P) in SCD (12). Our lab discovered that elevated circulating adenosine, a purine nucleoside, mediates erythrocyte sickling through adenosine ADORA2B receptor activation by contributing to 2,3-diphosphoglycerate (2,3-DPG) induction that promotes oxygen release in erythrocytes (13). Due to elevated systemic adenosine in SCD, this signaling pathway contributes to further disease progression. In fact, elevated adenosine-mediated ADORA2B receptor activation in erythrocytes induces

sphingosine kinase 1 (SphK1)-S1P production to contribute to further sickling (14) (Illustration 1).

S1P is a bioactive lipid generated from sphingomyelin, a class of lysophospholipids. Sphingomyelin is metabolized to form ceramide and further metabolized to generate sphingosine. Sphingosine is phosphorylated by two isoforms of sphingosine kinases (SphKs) known as SphK1 and SphK2. Differences in enzymatic activity have been observed in SphKs, such that SphK1 translocate from the cytoplasm to the plasma membrane whereas SphK2 translocate to the nucleus. Although the role of intracellular S1P is not fully understood, elevated extracellular S1P can activate five S1P receptors (S1PRs). Amongst these S1PR subtypes, S1PR1 is ubiquitously expressed in multiple cell types, including immune cells. Since the discovery of S1PRs, pharmacologic advances have been made to target S1PRs. FTY720 is a US Food and Drug Administration (FDA)- approved drug for treating multiple sclerosis and was developed to target and inhibit S1PR1 signaling by internalization of the S1PR1 for its degradation in the proteasome (15).

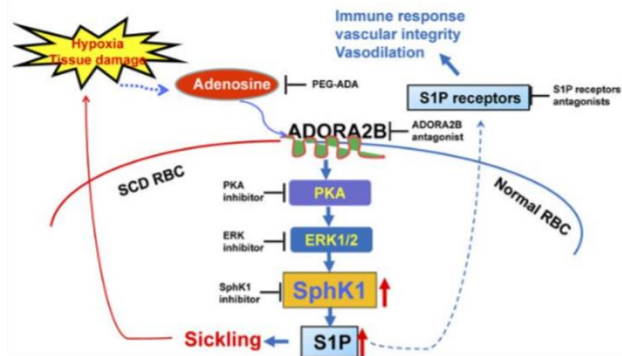
Illustration 1

A



Zhang et.al. *J Clin Invest.* 2014;
124 (6): 2750-2761.

B



Sun et.al. *Blood.* 2015;
125(10):1643-52.

Illustration 1: (A) Working model (Zhang et.al. *J Clin Invest.* 2014) demonstrates that hypoxia mediates sphingosine kinase 1 (SphK1)-sphingosine-1-phosphate (S1P) production to contribute to erythrocyte sickling and SCD progression. **(B)** Working model from (Sun et.al. *Blood.* 2015) demonstrate that hypoxia-mediate elevated adenosine-Adora2B receptor activation in erythrocytes contributes to SphK1-S1P production to promote sickling. In the normal condition, elevated S1P mediate-S1PRs activation to promote biological processes. **Knowledge Gap:** my work demonstrates how S1P-S1PR1 activation contributes to SCD disease progression.

1.5. The role of elevated immune responses contributing to vascular dysfunction in SCD.

Immune cell types, such as neutrophils, macrophages, and lymphocytes, can contribute to the release of inflammatory mediators that promote multiple tissue injuries and disease progression. Systemic and sustained inflammation contributes to further progression of SCD, which affects nearly every organ system of the body. Predictors of mortality in SCD patients can be characterized as elevated circulating levels of inflammatory molecules, such as interleukin 6 (IL-6), monocyte chemoattractant protein (MCP-1), tumor necrosis factor alpha (TNF- α), endothelin-1 (ET-1) (16, 17). In sickle mice, danger associated molecular patterns (DAMPs) such as high mobility group box 1 (HMGB1) can also be released from immune cells or damaged tissues to trigger activation of toll-like receptor 4 (TLR4) signaling pathways in SCD (18).

Since systemic inflammation-mediated by erythrocyte sickling contributes to multiple organ dysfunction, organ specific inflammatory mediators can contribute to the progression of SCD. For instance, in the lung, a mixture of inflammatory cell types can release a milieu of inflammatory mediators that contribute to severe pulmonary complications in SCD. Previous studies have shown increased levels of lymphocytes and cytotoxic T cells in bronchoalveolar lavage (BAL) fluid isolated from sickle mice (19). In addition to elevated immune cells, increased levels of inflammatory mediators released from immune cells including interleukin 5 (IL-5), granulocyte colony stimulating factor (GCSF), and C-X-C chemokine motif 1 (CXCL1) were observed (20).

1.6. Utilizing a unbiased microarray screen to investigate candidate genes that contribute to tissue damage in SCD.

Elevated inflammation and endothelial dysfunction have been well described in SCD. Particularly, pulmonary complications are the leading cause of mortality in SCD due to vaso-occlusive events that occur in the lung (21). To determine whether changes in gene expression patterns underlie pulmonary dysfunction in SCD, I performed a unbiased microarray screen in lung samples isolated from SCD and control mice. The gene categories with the highest log₂ transformation values were inflammatory, heme and iron hemostatic genes, and circadian rhythmic genes. Several inflammatory-related genes identified in the screen include *Ccl5*, *Ccl9*, *Ccl17*, *Cxcl2*, *Cxcl13*, *Ifi202b*, *C4b*, *C4a*, *Cxcl10*, *Pf4*, *Ccr2*, *Nfe212*, *Ccr4*, *Anxa1*, *Ptgs1*, *Tlr6*, and *Adam8*. A series of heme and iron metabolic genes upregulated in SCD lung were *Lpn2*, *Slc25a37*, *Steap2/4*, *Fech*, and *Ltf*. Unexpectedly, I discovered upregulated series of circadian rhythmic genes, which were *Bhlhe40*, *Nr1d1*, *Nr1d2*, *Dbp*, *Per2*, *Id1*, *Id2*, and *Nampt*. Although the reason as to why these genes are enhanced in SCD is unknown. I focused my attention on *Per2*, due to the role that *Per2* gene expression plays in mediating cellular toxicity and inflammation (22-24). Moreover, PER2 is a transcription factor that regulates the transcription of genes responsible for anti-oxidative stress in multiple cell types (25). Overall, PER2 is a major circadian clock gene that regulates biological clocks, which are responsible for generating circadian rhythms in multiple organs.

1.7. Circadian Period genes from fruit flies to mammals regulate circadian clock function.

Period (Per) gene was initially discovered in drosophila in 1971 by Seymour Benzer and Ronald Konopka, which was later characterized as a circadian gene essential for locomotor function. Years later, three scientists, Dr. Jeffrey C. Hall, Dr. Michael Rosbash, and Dr. Michael W. Young earned the Nobel Prize for their pioneering work by identifying the function of *Per* as a circadian clock oscillator. Interestingly, *Per* mutants were identified to have a shortened or lengthened period length, which contributes to complete arrhythmicity in constant darkness (26). *Per* was identified to oscillate in a circadian manner to regulate a transcriptional-translational feedback loop (27). Mammalian *Per* genes were identified and cloned to generate mouse strains with genetically altered *Per* genes. Although there are three *Per* gene homologues that underlie circadian behavior in mice *Per1* and *Per2* are the major genes that function independently in mediating circadian activity in rodents (28). Particularly, *Per2* has been identified to function as a tumor suppressor in age-related toxicity, a contributor to heme biosynthesis, and a regulator of wheel-running locomotive activity in mice (23, 29-31). The function of *Per1* has been demonstrated to be involved in rodent circadian behavior (32) and the role of *Per3* has not been fully understood.

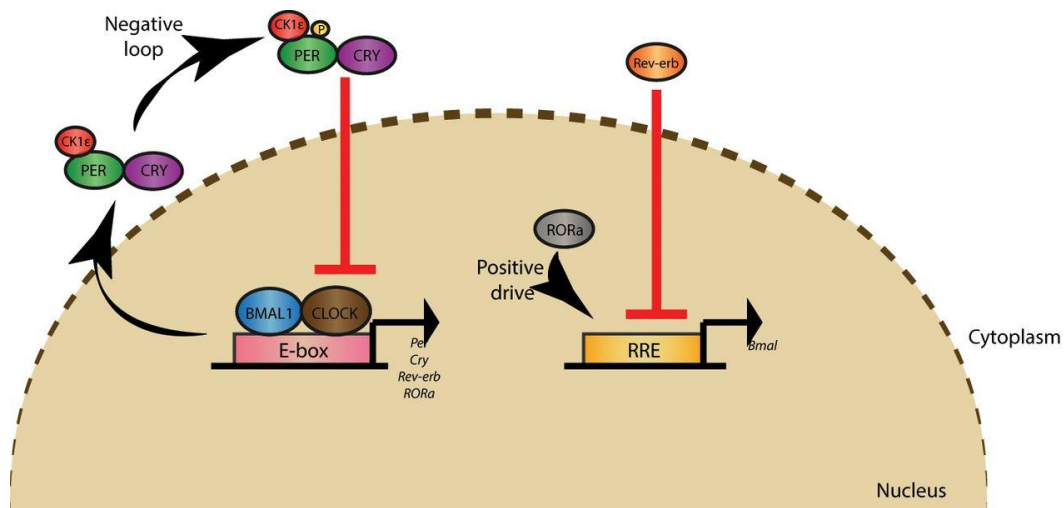
At the transcriptional-translational level, RNA and protein levels of clock-related genes and proteins are circadian regulated. Circadian genes have specific rhythmic expression patterns, which can positively or negatively influence the peripheral clocks. Particularly, brain and muscle arnt-like 1 (BMAL) and circadian

locomotor output cycles kaput (CLOCK), are the upstream oscillators that bind to enhancer box (E-box) regulatory promoter regions (14). Thus, BMAL and CLOCK transcriptionally regulate expression of *Per1* and *Per2* genes, which encode the downstream circadian oscillators. Elevated PER1/PER2 expression can transcriptionally repress BMAL/CLOCK expression in a negative feedback manner (15). *Per* expression can be further enhanced due to elevated enhancers binding to the E-box promoter regions to promote *Per2* transcription (16). Circadian homologues, PER1 and PER2, play a vital role in maintaining the mammalian clock (25) (Illustration 2). In fact, transcriptional repression of *Per2* is detrimental to overall clock function. Persistent repression or genetic deletion of *Per2* impairs vital organ functions and contributes to disease progression (26, 27).

Moreover, disruptions in circadian rhythms mediating biological clocks can contribute to cardiovascular disease, neurological disorders, cancer, and obesity. In addition to *Period* (*Per1* and *Per2*) genes, other genes that regulate circadian rhythms, which includes *Cryptochromes* (*Cry1* and *Cry2*), *Neuronal PAS domain protein 2* (*Npas2*), *Nuclear receptor subfamily 1 group D member 1* (*Nr1d1*), *Brain and muscle arnt-like 1* (*Bmal*) and *circadian locomotor output cycles kaput* (*Clock*) (33). All of these clock genes are ubiquitously expressed in the organism and are necessary for maintaining circadian rhythms (Illustration 2). Circadian rhythms are synchronized globally in the organism; moreover, tissue-specific circadian clocks are regulated in response to stimuli such as hormones, glucose, salt, cytokines, and chemokines (34). The circadian clock regulates expression of the inflammatory response that contributes to the onset of disease (35, 36). Synchronized circadian

rhythms persistently regulates peripheral clocks in tissues. Multiple cell types in tissue also express circadian genes that oscillate based on the time of day. In fact, PER1 and PER2 play a critical role in hematopoiesis, which takes place in the bone marrow (37). At the cellular level, synchronized rhythms can be observed in the erythroid, myeloid, and lymphoid cell lineages (35, 38, 39). However, in erythrocytes *Per2* is not expressed due to enucleation. Besides mature erythroid cells, other hematopoietic lineage cells with a nuclei can transcribe *Per2* DNA, which play a role in various cellular processes (29).

Illustration 2



Biochemical Society Transactions

Illustration 2: Circadian oscillators regulate rhythmic processes in the cell (Biochemical Society Transactions). In the nucleus, BMAL and CLOCK bind to the Enhancer box (E-Box) promoter regions to promote transcription of *Per1 or 2*, *Cry 1 or 2*, and *Ck1ε*. Elevated PER1/PER2 can negatively inhibit BMAL/CLOCK that regulate *Per1 or 2* transcription. Retinoic acid receptor-related orphan receptors (ROR) binding to reverse response elements (RRE) contributes to *Bmal* transcription. However, elevated Rev-erβ can inhibit ROR binding to RRE to inhibit *Bmal* transcription.

1.8. The rationale of this dissertation.

The purpose of this dissertation is to investigate the detrimental impact of chronic hemolysis in SCD that mediates end organ damage. I investigated the role of S1P-mediated S1PR1 signaling in organs that contributes to multiple organ dysfunction. Additionally, I performed a robust and unbiased microarray screen to determine how multiple organ damage due to elevated heme deposition in SCD contributes to changes in gene expression. Unexpectedly, I discovered that circadian *Per2* gene expression was upregulated in SCD, which indicates that *Per2* gene expression mediate molecular clock function, which has an important role in this disease. Extending from the results identified from the unbiased screen, I have generated a hypothesis that elevated *Per2*-mediate biological clock function is required for overall organ maintenance in SCD. By generating sophisticated genetic tools by bone marrow transplantation studies, I will study the expression patterns of *Per2* in sickle and control mice by means of a *Per2* knock-in bioluminescence

reporter mice model to quantify PER2 luciferase activity. Additionally, I will determine whether the differentiation of bone marrow derived cell lineages in the periphery is altered by global deletion of *Period* genes in sickle mice. Overall, I propose that 1) elevated *Per2* plays a beneficial role in SCD due to essential role in regulating biological clocks *in vivo*. 2) Molecular clock dysfunction due to global *Per1*^{-/-}/*Per2*^{-/-} in multiple cell types is detrimental and promotes tissue dysfunction in SCD. 3) Mixture of cell types that are *Per1*^{-/-}/*Per2*^{-/-} in organs or *Per1*^{+/+}/*Per2*^{+/+} progenitor cells from bone marrow can co-induce heme oxygenase 1 (HO-1) activity to regulate heme degradation, which play a protective role in the organ.

II. Methods

2.1. Mice generation (Berkeley Human Sickle Cell, SCD-*IL-6*^{-/-}, *Per1/ Per2* dKO, *Per2*^{Luciferase} mice).

Animals were housed in 12 hour light/12 hour dark (12 L: 12 D) conditions and had access to food and water ad libitum. All animal procedures presented herein were approved by the Animal Welfare Committee at the University of Texas Health Science Center. *IL-6*^{-/-} (*IL-6* dKO) mice were used for mating whereas *Per2*^{Luciferase} (*Per2*^{Luc}) and *Per1*^{-/-}/*Per2*^{-/-} (*Per1/Per2* dKO) mice were used as bone marrow (BM) recipients. WT, *IL-6*^{-/-}, and SCD Berkeley mice were purchased from Jackson laboratory. SCD heterozygous (SCD ^{Tg/+}) females mated with SCD ^{Tg/+} males. Progeny were genotyped to confirm the presence or absence of mutant sickle beta-globin (HbS) gene. About 25% of progeny is predicted to have mutant gene. SCD- *IL-6*^{-/-} mice were generated by mating heterozygous SCD female mice with *IL-6*^{-/-} male mice. Progeny were genotyped and confirmed to be heterozygous for three genes: hemoglobin alpha (Hb α), hemoglobin beta (Hb β), and *IL-6*. Heterozygous *Hb α* ^{+/-}/*Hb β* ^{+/-}/*IL6*^{+/-} females were mated with *IL-6* dKO males (*Hb α* ^{+/+}/*Hb β* ^{+/+}/*IL-6*^{-/-}). Progeny genotype as *Hb α* ^{+/-}/*Hb β* ^{-/-}/*IL-6*^{-/-}, were confirmed and recognized as SCD-*IL-6*^{-/-} mice.

Tails were collected for genomic DNA extraction. Primer sequences for HBB tm1TOW (Sickle cell) sequences were designed as followed (Table1) (40). Thermocycler conditions were set for 40 cyclers at 94 degrees for 5 minutes, 84 degrees for 10 minutes, 94 degrees for 1 minute, 60 degrees for 30 seconds, and 72

degrees for 2 minutes. Followed by 72 degrees for 5 minutes and a final hold temperature at 4 degrees. Mutant and WT DNA fragments were analyzed by gel electrophoresis. Mutant DNA length (398 base pairs) and WT DNA length (291 base pairs). IL-6 primer sequences were designed as follow (Table 1) (41). Thermocycler program was set for 30 cycles for the following 94 degrees at 5 minutes, 84 degrees at 10 minutes, 94 degrees at 1 minute, 60 degrees for 30 seconds, and 72 degrees at 2 minutes. Then 72 degrees for 5 minutes and final holding temperature at 4 degrees. Gel electrophoresis was performed to detect WT (174 base pairs) and Mutant (380 base pairs) DNA fragments.

Per1/Per2 dKO mice were a gift provided by Dr. Cheng Chi Lee and were maintained by mating *Per1/Per2* dKO males and females. Progeny were genotyped to confirm mutated *Per1* and *Per2* gene expression. Mating strategy, homozygous *Per1/Per2* dKO males crossed with homozygous *Per1/Per2* dKO females. Primer sequences for *Per1* WT, *Per1* null DNA, *Per2* WT, and *Per2* null DNA were designed as followed (Table 1) (30). PCR conditions were set for 30 cycles of: 95 degrees for 1 minute, 94 degrees for 38 seconds, and 63 degrees for 38 seconds. Then 72 degrees for 45 seconds and then 3 minutes, and a final hold at 4 degrees. Gel electrophoresis was performed to confirm WT *Per1* DNA length is 440-448 base pairs and Null *Per 1* DNA length is 280-320 base pairs. Primer sequences for *Per2* WT and *Per2* Null DNA were designed as followed (Table 1) (30). PCR thermocycler conditions were set at to repeat for 30 cycles at 95 degrees for 1 minute, 94 degrees for 50 seconds, and 62 degrees for 50 seconds. Followed by 72 degrees for 50 seconds, 72 degrees for 3 minutes, and final hold temperature at 4 degrees. Gel

electrophoresis was performed to validate *Per2* WT DNA (240-280 base pairs) and *Per2* null DNA (600-640 base pairs).

Per2^{Luciferase} mice were provided by Dr. Seung-Hee Yoo. Heterozygous *Per2^{Luciferase}* males mated with heterozygous females. Three primers sequences P1, P2, and P3 were designed to detect progeny genotype: WT (*Per2^{+/+}*), heterozygous (*Per2^{Luc/+}*), and mutant mice (*Per2^{Luc/Luc}*). WT allele (P1) or deleted allele (P2) detection using primer sequences (Table 1) (42). Reverse primer sequences for detecting luciferase knock-in allele (P3) (42). Tails were collected and processed for genomic DNA extraction. PCR thermocycler conditions were run at 95 degrees for 1 minute, 55 degrees for 1 minute, and 72 degrees for 1 minute that repeated for 35 cycles. Gel electrophoresis analysis was carried out to confirm DNA base pair sizes. Heterozygous and homozygous (*Per2^{Luc/+}* and *Per2^{Luc/Luc}*) mice were maintained and used as BM recipients. WT DNA length was 230 base pairs and mutant DNA length 680 base pairs. Heterozygous mice express both WT and mutant DNA.

Table 1

Gene	Sequence 1	Sequence 2
<i>Hbb</i> ^{tm1TOW} (Sickle cell)	WT- 5'-TTA GGT GGT CTT AAA ACT TTT GTG G -3'	WT- 5'-ACT GGC ACA GAG CAT TGT TAT G-3'
	MUT- 5'- AGA TGT TTT TTT CAC ATT CTT GAG C-3'	MUT- 5'-AAT GCC TGC TCT TTA CTG AAG G-3'
<i>IL-6</i> Common	5'-TC CAT CCA GTT GCC TTC TTG G-3'	
<i>IL-6</i> WT	5'-TTC TCA TTT CCA CGA TTT CCC AG-3'	
<i>IL-6</i> Mutant	NeoR: 5'-CCG GAG AAC CTG CGT GCA ATC C-3'	
Null <i>Per1</i>	5'- ACCAGTGAATCTTTGTCAGCAG TTCCC-3'	5'- CAGAGCAGATACATCTTCTCTCACCA TC-3',
WT <i>Per1</i>	5'- GGCCAGACTTCGGGGCTAATAT CTTT-3'	5'- GGTTAGAACTGAGGACCCAAGCTGT A-3'
WT <i>Per2</i>	5'- CAGGTGGGAGGAACTCTTGTA GCAG-3',	5'- CATCAGTAGCCGGTGGATTGTTCTG -3'
<i>Per2gtnlf2</i>	5'- GTTGGGAAACACCACGAGAATG AGATTC-3'	
<i>Per2Neo4</i>	5'- CTCGCTGATCAGCCTCGACTGT G-3',	
<i>Per2</i> (P1)	5'-CTGTGTTTACTGCGAGAGT-3'	
<i>Per2</i> (P2)	5'-GGGTCCATGTGATTAGAAAC- 3'	
<i>Luciferase knock-in allele</i> (P3)	5'- TAAAACCGGGAGGTAGATGAGA -3' (P3)	

Table 1: Genetic sequences for HBB tm1TOW (Humanized sickle cell mice), global deficient *IL-6 dKO*, *Per1/Per2 dKO* (corresponding to gene sequences for null *Per1*, WT *Per1*, WT *Per2*, *Per2gtnlf2*, and *Per2Neo4*), and *Per2^{Luciferase}* bioluminescence reporter mice (gene sequences were designed for detecting *Per2^{Luciferase}* : P1, P2, and P3. Gene sequences were confirmed by Jackson Laboratory.

2.2. Pharmacologic treatments in sickle mice.

Sickle Cell Berkeley mice were treated with Fingolimod (FTY720) supplied by Cayman Chemical Company at a dose of 1 mg/Kg of body weight and injected intraperitoneally (IP) for up to 8 weeks. Drug was prepared in PBS (Invitrogen) used as a vehicle.

2.3. Hematological assessment in sickle mice.

Mice were treated with isoflurane supplemented with oxygen as means of anesthesia during blood collection. Peripheral blood isolated from tail vein was collected in EDTA tubes in order to prevent coagulation. A hemolyzer (IDEXX technologies) was used to detect multiple hematological parameters that pertain to erythrocytes and immunological cells. For sickling assessment, a few drops of blood were smeared on microscope glass slides with positive charges coated on the glass, which improves cell adhesion on the slide. After blood dried on the slide, slides were stained with Wright-Giemsa solution, which stain erythrocytes pink. Sickle cells were captured on a 20X objective using a Zeiss light microscope.

2.4. Erythrocyte lifespan measurements.

Biotinylated-labeled erythrocytes were generated *in vivo* to determine erythrocyte life span in SCD mice. N-hydroxysuccinimide (50 mg/Kg) was injected into the retro-orbital plexus in mice. Next, peripheral blood (5 uL) was collected from mouse tail vein on day 1, 2, 3, 5, and 8 for flow cytometric detection of biotinylated-labeled erythrocytes by expression of streptavidin conjugated fluorochrome and Ter119 (12, 43).

2.5. Flow cytometric analysis of immune cells isolated from peripheral tissues.

Whole tissues were isolated from euthanized mice. Tissues were harvested in culture dishes containing Hank's media and were manually processed with sterilized surgical tools to generate single cell suspensions. Suspensions were transferred to a clean conical tube containing a 40- μ m strainer in order to filter out unprocessed tissue clumps. Single cells were treated with Fc blocking antibody (BD Biosciences) per million cells for 30 minutes at 4 degrees centigrade as previously described (43). Afterwards, cells were stained with fluorophore-conjugated antibodies to detect S1PR1 and F4/80 as previously described (43). Single cell fluorescent expression was detected using a Gallios Flow Cytometer (Beckman Coulter) and analysis was performed using Kaluza software (Beckman Coulter).

2.6. Whole blood detection of circulating inflammatory cytokines by ELISA method.

Whole blood was drawn from anesthetized mice by cardiac puncture and collected in anti-coagulant EDTA tubes. Blood was centrifuged to collect plasma as previously described (43). Multiple analyte ELISA array was performed to detect interleukin (IL): IL- 2, 6, 12, and 17A (MEM-004A; Qiagen).

2.7. IL-6 detection in serum, multiple organs, and bronchoalveolar lavage (BAL) fluid.

Mice were anesthetized and blood was collected by cardiac puncture, blood was centrifuged, serum was flash frozen, and stored at -80 degrees centigrade for future usage. Skin and muscle was removed to expose the trachea. A small hole was cut in the trachea and a gauge needle was inserted. 1% BSA-PBS was injected into the trachea to collect bronchoalveolar lavage (BAL) fluid. BAL fluid was flash frozen and stored until further usage. Afterwards, whole spleen, lung, kidney, and liver were removed from euthanized mice and were properly preserved. Murine IL-6 detection in BAL, blood plasma, and multiple tissues was performed by ELISA assay based on manufacturer's instructions (EZMIL-6, MilliporeSigma).

2.8. Bone marrow derived macrophages generation from mouse.

Mice were IP injected with 2.5% Avertin and euthanized by cervical dislocation. Skin and muscle was removed with sterilized scissors and forceps. Femur and tibia were removed from both hind legs and placed in Hank's solution for further dissection. Excess tissue was removed from the bone and bone was clipped at both ends. Marrow found inside the bone was flushed out in a clean culture dish containing DMEM that is supplemented with FBS, L929, glutamine, and PenStrep. Cells were separated with clean pipet tip to prevent coagulation. Cells were collected from the dish and centrifuged. Then, the cell pellet was collected and resuspended in fresh media. Cells were counted and added to individual petri dishes with additional culture media for 4 days in a 37 degrees centigrade incubator. Additional medium was added to cells in the petri dishes on day 4 and remained in culture

conditions for up to 4 additional days. Culture media was discarded on day 8 and fresh medium was added to petri dish. Cell confluence was determined at 80 to 90%.

2.9. Pharmacologic treatment in macrophage culture for S1P, W146, JTE013, TY52156, CYM50358, and AG490.

Mouse BM derived macrophages were prepared as previously described (43). Macrophage cultures were treated with 1uM of S1P prepared in vehicle and S1PRs antagonists for S1PR1, S1PR2, S1PR3, S1PR4, refer to as W146, JTE013, TY52156, CYM50358, respectfully. Additionally, antagonist for JAK2 is refer to as AG490.

2.10. Whole lung RNA isolation for gene expression screening.

SCD and WT control mice were euthanized by cervical dislocation and whole lung was removed. Lung tissues were completely homogenized in TRIzol (Thermofisher) reagent and kept on ice. Chloroform was added to homogenized samples and centrifuged to create phase separation. RNA was treated with DNase for 30 minutes in order to prevent degradation. RNA was precipitated with isopropanol and RNA samples were transferred to mini columns from RNeasy micro kit (Qiagen) for RNA purification. RNA quality checks were accessed using nanodrop (ThermoFisher) and bioanalyzer (Aligent 2100 technologies). RNA quality control (QC) were based on 260/280 ratio of ≥ 2 and RNA integrity number (RIN) of ≥ 8 . Samples passing all QC requirements were used for microarray analysis. Lung RNA samples were reverse transcribed (RT) to generate cDNA and newly synthesized

cDNA were fluorescently tagged. DNA was hybridized to GeneChip Mouse Exon 1.0 ST (Affymetrix). Data was imported to GeneChip software in order to calculate intensity values based on fluorescence detection. Data files were imported to Affymetrix expression console software to detect probe fluorescence ratios used to confirm quality of library preparation. Intensity values were log₂ transformed and data was imported to software for further statistical analysis. Statistical significance was based on P values of P<0.05 and fold changes of differentially expressed genes were determined in SCD versus WT group.

2.11. Irradiation and bone marrow (BM) transplantation.

WT and SCD humanized Berkley (SCD^{Tg}) mice were used as BM donors. All donors were at least 9 weeks of age prior to BM transplantation (BMT). Recipients with confirmed genotypes were treated with 0.2 % Neomycin for at least 24 hours prior to irradiation and were maintained on Neomycin treatment for up to 2 weeks after irradiation. Recipients were treated with 2 rounds of toxic 2Gy (500 RAD) irradiation that took place 3 hours apart. Irradiated mice were injected retro-orbitally with SCD or WT BM (1 X10⁶ million) cells. At 8 weeks post BMT, 50 uL of whole blood from tail vein was collected in EGTA tubes. Blood cells were lysed using ammonium chloride (NH₄Cl) and washed with phosphate buffered saline (PBS) supplemented with fetal bovine serum (FBS). Cells were stained with leukocyte markers to detect CD45.1- phycoerythrin (PE) and CD45.2- fluorescein isothiocyanate (FITC) expression by flow cytometric analysis. To confirm BM chimeras, SCD transplanted mice typically express high expression of CD45.1

whereas WT control transplant mice groups would express elevated expression of CD45.2 on leukocytes populations.

2.12. PER2 luciferase detection in bioluminescence reporter mice.

Whole lung was isolated from euthanized mice. Lung biopsies were placed on MilliCell membrane inserts then placed inside a culture dish. Biopsies were cultured in DMEM medium that was supplemented with 10 mM HEPES, penicillin/streptomycin (PenStrep), 2% B27, and 0.1 mM of Luciferin. Cultures were tightly sealed with vacuum grease and secured with a coverslip, then placed inside a tightly fasted- light protected 36 degrees incubator for up to 4 days. Tissue sustaining bioluminescence was continuously monitored by LumiCycle 32 (ActiMetrics) photomultiplier tubes for detecting photon counts. Analysis was performed using LumiCycle software (Actimetrics).

2.13. Hematoxylin and eosin (H&E) staining of multiple tissues.

Mice were anesthetized using 2.5% Avertin. Whole blood was collected by means of cardiac puncture. Cardiac perfusion was performed in mice to remove excess blood in the circulation. Whole lung, liver, and spleen were removed from mice and placed in 10% formalin. Organs were processed in a series of ethanol washes that increased to 100% ethanol then placed in histoclear, a wax removing agent. Organs were fastened to a plastic mold for the paraffin wax embedding process. Paraffin embedded organs were allowed to cool over night at room temperature. Tissues were sectioned at 4 microns using a Leticia microtome. Tissue sections were deparaffinized in histoclear followed by a decreasing series of

ethanol solutions. Sections were stained in hematoxylin solution to stain cell nuclei that was followed by eosin solution to stain the cytoplasm and fibers in tissue. Sections were placed in differentiation solution to increase stain quality. Tissue sections were mounted using Cytoseal, a mounting agent, and coverslips were placed to secure the sections. Images were acquired using an Olympus BX60 microscope at a 20X objective. 10 to 15 images were taken for each slide to examine tissue structure, necrotic areas, and inflammatory infiltrate. Images were analyzed using Photoshop and semi-quantification was performed using Image J to examine area density of inflammatory and necrotic regions of the tissues.

2.14. Perl's Blue Prussian iron staining of multiple tissues.

Tissue sections of the lung, liver, and spleen were deparaffinized as previously described in section 2.9. Sections were placed in equal part of hydrochloric acid (HCL) and potassium ferrocyanide $K_4Fe(CN)_6$ solution. Tissues were rinsed in distilled water and placed in nuclear fast red solution then rinsed in water. Tissue iron expression was identified by enhanced blue color and cell nuclei stain as pink.

2.15. Proteinuria detection.

Mice were individually placed in metabolic cages (Tecniplast 3600M021) for 24 hours and had access to food and water ad libitum. Urine was collected and briefly centrifuged to remove feces, food, and other contaminants. Urine samples and standards were placed in a microplate followed by addition of picrate working solutions prepared using 1 M NaOH and Picrate Reagent. Microplate was placed in

a plate reader and absorbance was detected at 500nm. Collected urine and standards were placed in microplate for albumin (Exocell) measurements. Mouse anti- mouse albumin was added to samples and incubated at room temperature. Urine albumin levels were confirmed by chemiluminescent detection using anti-rabbit –horse radish peroxidase (HRP). Color intensity was measured spectrophotometrically. Normalizations were performed by albumin per mg of creatinine.

2.16. Hemolytic analysis for total bilirubin.

Whole blood was collected by means of cardiac puncture from anesthetized mice. Blood was spun down at 2500 RPM for 5 minutes. Blood plasma was collected, buffy coat was discarded, and erythrocytes were stored. Plasma was placed in microplate along with working reagents. Spectrophotometric measurements were detected at 530 nm. Total bilirubin detection was calculated based on manufacturer's instruction (BioAssay).

2.17. Alanine aminotransferase (ALT) detection.

Whole blood was collected and plasma was isolated as previously described in section 2.12. ALT enzyme activity was measured by generation of pyruvate that was assessed by colometric/ fluorometric analysis. Quantifications were performed based on manufacturer's instructions (Sigma Aldrich).

2.18. Neutrophil infiltration in lung tissue.

Lung sections were deparaffinized in a series of ethanol washes and rehydrated as previously described in section 2.9. Tissue sections were heated in

citrate acid antibody retrieval solution for 30 minutes and were allowed to cool to room temperature. Lung tissue sections were incubated in 3% hydrogen peroxide solution to block endogenous peroxidase activity. Tissue sections were then blocked in 2% BSA-PBS solution for 1 hour and were incubated with primary anti-mouse Ly6-G 1:200 diluted (BD Biosciences) antibody overnight at 4 degrees, washed, and incubated in biotinylated anti-mouse antibody. Development was performed using DAB peroxidase substrate solution (Vectastain), counterstained, washed, and mounted. Images were acquired on 20X objective on an Olympus microscope.

2.19. RNA extraction and semiquantitative polymerase chain reaction (PCR) detection of inflammatory genes in lung.

Whole lung tissues were isolated from euthanized mice. Lung were homogenized in TRizol (thermofisher) solution, DNase treated to prevent RNA degradation, and precipitated in isopropanol. RNA were purified using RNeasy micro kit (Qiagen) based on manufacturers' instruction. Quality checks of RNA samples were confirmed by nanodrop (Thermofisher). Absorbance 260/280 ratio of ≥ 2 passed quality check for RNA quality. 1 μg of RNA were reverse transcribed to generate cDNA. Primers for semiquantitative PCR were design using (Integrative DNA technologies) software. Sybr Green (Qiagen) probe were used for gene expression detection for mouse *Bmal* and *Per2* (44). Mouse *IL-6* (45), mouse *Tlr4* (46), and mouse *β -actin* were also detected by RT-PCR. PCR thermocycler conditions were set at 95 degrees for 1 minute, 60 degrees for 30 seconds, and 72 degrees for 15 seconds. Gel electrophoresis were performed to detect DNA fragments for each gene.

Table 2

Gene	Forward	Reverse
<i>Mouse Bmal</i>	5'- CCAAGAAAGTATGGACAC AGACAAA -3'	5'- GCATTCTTGATCCTTCCTTG GT -3'
<i>Mouse Per1</i>	5'- CCCAGCTTTACCTGCAGA AG-3'	5'- ATGGTCGAAAGGAAGCCTC T -3'
<i>Mouse Per2</i>	5'- TGTGCGATGATGATTCGT GA-3'	5'- GGTGAAGGTACGTTTGGTT TGC-3'
<i>Mouse IL-6</i>	5'- TAGTCCTTCCTACCCCAAT TTCC-3'	5'- TTGGTCCTTAGCCACTCCTT C-3'
<i>Mouse Tlr4</i>	5'- TGGCTGGTTTACACATCC ATCGGT-3'	5'-TGG CACCATTGAAGCTGAGGTC TA-3'
<i>Mouse β-actin</i>	5'- CCAGAAGGACTGTTATGT GGGA-3'	5'- GACTCCGTGTTCAATGGGA TAC-3'

Table 2: List of genes for *Bmal*, *Per1*, *Per2*, *IL-6*, *Tlr4*, and *β -actin* in mouse. Primer sequences were designed as previously described (44, 46).

2.20. *Immunofluorescence detection of heme oxygenase (HO-1) expression in alveolar macrophages.*

Whole lung sections were processed for deparaffinization and rehydration followed by antibody retrieval treatment as previously described in sections 2.9 and 2.14. Tissue sections were blocked in 2% BSA-PBS followed by overnight incubation

of diluted antibodies mouse anti- rabbit HO-1 (1:200) (Cell signaling) and mouse anti-rat F4/80 (1:200) (Abcam). Sections were washed several times followed by incubation of diluted (1:1000) goat anti-rabbit IgG and donkey anti-rat IgG (H+L) (Thermofisher). Lung sections were washed to remove excess antibodies and mounted with DAPI SlowFade Gold Antifade reagent (Thermofisher). Clear color nail polish were placed around the perimeter of the section slide to secure coverslip on slide.

2.21. Statistical analysis.

Analyses were performed using Graph Pad software (LaJolla, California). Student t tests for 2 group analyses or one-way ANOVA followed by Tukey multi-comparison tests were performed for multiple group analyses. * $P < 0.05$ were considered significant.

III. Results

3.1. Chapter 1: Chronic inflammation and multiple tissue damage is detrimental in SCD

This chapter is based upon: Zhao S, Adebisi MG, Zhang Y, Couturier JP, Fan X, Zhang H, Kellems RE, Lewis DE, and Xia Y. Sphingosine-1-phosphate receptor 1 mediates elevated IL-6 signaling to promote chronic inflammation and multitissue damage in sickle cell disease. FASEB J. 32,000–000(2018)(43), with permission from the FASEB journal for the usage in this dissertation.

Unbiased metabolomics analysis revealed an increase of sphingosine-1-phosphate (S1P), a highly reactive bio-lipid, in the blood circulation of SCD mice and patients (12). Extracellular S1P signals via five G-protein coupled receptors (GPCRs) known as S1P receptors (S1PRs). S1P-S1PRs signaling has been identified to contribute to disease-related conditions, including vasculature leakage, tissue injury, and pain (47-49). Amongst the five S1PRs, S1PR1 is ubiquitously expressed in multiple cell types and organs and has a high affinity for S1P (50, 51). Although sphingosine kinase 1(SphK1) –mediated S1P production is independent of sickling (12), the question remains whether S1P-mediated S1PR1 activation contributes to sickling and further SCD progression.

3.1.1. FTY720-mediated S1PR1 antagonism has no effect on erythrocyte sickling.

FTY720 is a FDA-approved drug to treat relapsing multiple sclerosis known to have potent anti-inflammatory effects in experimental animal models (15). Sphingosine kinases phosphorylate FTY720 *in vivo*, which mimics the chemical structure of S1P. Thus FTY720 can target S1PRs to either promote recycling of the receptor to membrane or receptor degradation (52). S1PR1 is ubiquitously expressed in multiple cell types including endothelial and immune cells, which contributes to inflammatory responses such as cytokine secretion mediated by inflammatory cell infiltration to multiple organs that promote disease (53).

Sickle erythrocytes have a much higher turnover than normal erythrocytes. I tested whether FTY720 improves erythrocyte life span in sickle mice. To test this, I treated SCD mice with FTY720 (1 mg/Kg/day in vehicle, intraperitoneal injection) or saline-vehicle injection for a duration of 8 weeks. I collected peripheral blood by tail vein extraction from treated mice groups. I used flow cytometry to detect fluorescent streptavidin used to identify biotinylated-labeled erythrocytes generated *in vivo* by means of injecting N-hydroxysuccinimide (50 mg/Kg) in treated SCD mice. Erythrocytes were isolated from the treated mice on day 1, 2, 3, 5, and 8, which followed N-hydroxysuccidnimide injection to monitor erythrocyte life span. No differences were observed in erythrocyte life span in FTY720 treated mice compared to control (Figure 1) (43).

Figure 1

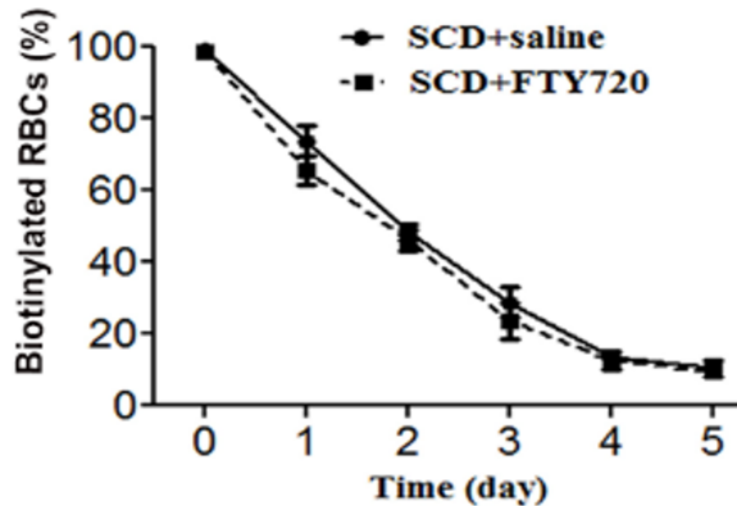


Figure 1. FTY720 does not affect erythrocyte life span in SCD mice. Mice were injected with N-hydroxysuccinimide (50 mg/Kg) to monitor erythrocyte life span. Whole blood was extracted from tail vein on 1, 2, 3, 5, and 8 days to detect biotinylated erythrocytes in sickle mice treated with FTY720 or saline. Analysis revealed that FTY720 or saline treatment has no direct effect on erythrocyte life span in sickle mice; N=6-7 mice per group.

Since I observed no differences in erythrocyte life span in FTY720 treated SCD mice, I examined other hematological parameters such as erythrocyte count (RBC), hemoglobin (HGB), hematocrit (HCT), mean corpuscular volume (MCV), and red cell distribution width (RDW), in the treated groups. Based on the complete blood cell (CBC) analysis, sickle mice express RBC levels of ~4 to 6 M/ μ L, HGB levels of 6 to 8 g/dL, HCT levels of 18 to 27%, MCV levels of 40 to 50 fl, and RDW

levels of ~30 %. By contrast, WT mice typically express RBC levels of ~9 M/ μ L, HGB levels of ~13 (g/dl), HCT levels of 40 to 45 % and MCV levels of ~50 fl. In the FTY720 treated SCD mice, there were no differences in RBC, HGB, HCT, MCV, or RDW compared to saline-treated SCD mice (Table 3) (43). I determined the morphology of erythrocytes in sickle mice to confirm the percentage of sickling in these mice. The analysis revealed that there were no differences in sickling in FTY720 treated mice compared to saline treated mice (Table 3) (43). Altogether, I conclude that FTY720 does not significantly impact erythrocyte life span or reduce erythrocyte sickling in SCD mice.

Table 3

	RBC (M/ μ L)	HB (g/dL)	HCT (%)	MCV (fl)	RDW (%)	WBC (k/ μ L)	LY (k/ μ L)	NE (k/ μ L)	MO (k/ μ L)	EO (k/ μ L)	BA (k/ μ L)
SCD Tg+ saline (N=6)	5.09 \pm 1.70	5.09 \pm 1.70	18.05 \pm 8.04	40.82 \pm 2.59	34.05 \pm 4.54	27.25 \pm 1.31	20.43 \pm 1.60	4.44 \pm 0.4	2.26 \pm 0.31	0.09 \pm 0.02	0.04 \pm 0.02
SCD Tg+ FTY720 (N=6)	5.74 \pm 0.58	6.50 \pm 1.94	23.10 \pm 5.12	40 \pm 5.93	30.47 \pm 5.53	8.14 \pm 0.69 *	5.33 \pm 0.79 *	2.06 \pm 0.36 *	0.62 \pm 0.13 *	0.12 \pm 0.04	0.01 \pm 0.00
SCD Tg- <i>IL-6 dKO</i> (N=6)	6.05 \pm 0.81	6.36 \pm 0.66	20.26 \pm 1.69	48.2 \pm 2.62	34.63 \pm 4.30	15.33 \pm 0.87 *	11.9 \pm 0.49 *	2.41 \pm 0.44 *	1.20 \pm 0.03 *	0.14 \pm 0.02	0.03 \pm 0.00

Table 3: SCD ^{Tg}: sickle cell disease transgenic mice; RBC: red blood cell count; HB: hemoglobin; HCT: hematocrit; MCV: mean corpuscular volume; RDW: red blood cell distribution width; WBC: white blood cells; LY: lymphocyte; NE: neutrophil; MO: monocyte; EO: Eosinophil; BA: basophils. * P<0.05 vs. SCD ^{Tg} mice without treatment.

3.1.2. Sphingosine-1-phosphate receptor 1 (S1PR1) mediates elevated inflammation in SCD.

Although I detected no significant differences in erythrocyte sickling in SCD mice treated with FTY720, I discovered that circulating immune cells in FTY720-treated mice were significantly reduced compared to saline-treated mice. The CBC analysis revealed that the total white blood cells (WBCs) that include lymphocytes (LYs), neutrophils (NEs), monocytes (MOs), eosinophils (EOs), and basophils (BAs) were reduced in FTY720 treated mice. Sickle mice express elevated levels of WBC ~ 27 k/ μ L, LY ~ 20 k/ μ L, NE ~ 4 k/ μ L, MO k/ μ L, ~ 0.09 EO k/ μ L, and BA ~ 0.04 k/ μ L (Table 3) (43). However, FTY720 treated SCD mice express reduced levels of WBC ~ 8 k/ μ L, LY ~ 5 k/ μ L, NE ~ 2 k/ μ L, MO ~ 0.60 k/ μ L, EO ~ 0.12 k/ μ L, and BA ~ 0.01 k/ μ L (Table 3) (43).

Since I revealed that the mechanism of action of FTY720 in SCD functions in an immunomodulation capacity, I hypothesized that elevated S1PR1-mediates cytokine secretion from immune cells to contribute to systemic immune response and further SCD progression. To test this, I detected interleukin (IL)-2, -6, -12, and -17A levels in peripheral blood by ELISA. Although multiple cytokines were increased in SCD mice compared to WT mice, IL-6 was induced to the greatest extent compared to the other cytokines (Figure 2) (43). Additionally, I revealed that all of the cytokines were reduced by FTY720 treatment in SCD mice (Figure 2) (43).

Figure 2

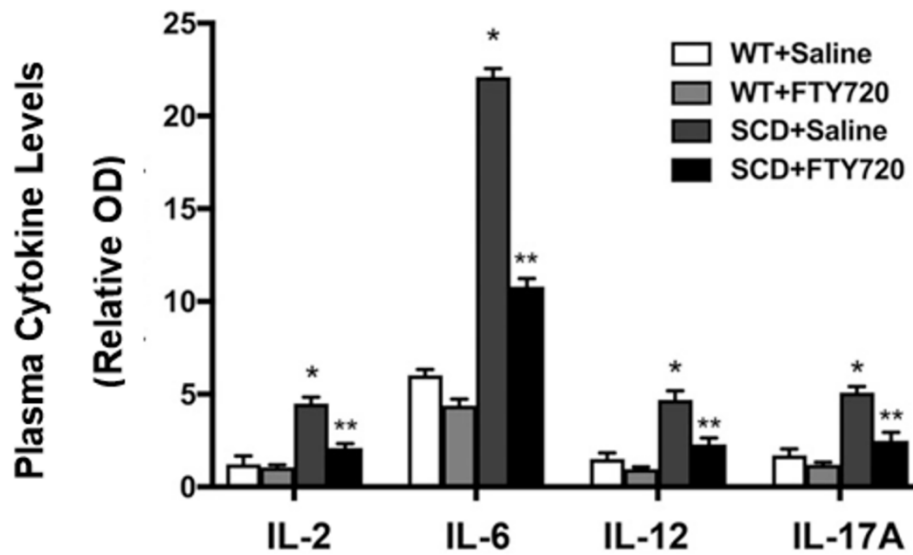


Figure 2. FTY720-treated SCD mice reduced circulating inflammatory cytokines demonstrated by ELISA assay. Values expressed as \pm SEM, * $P < 0.05$, SCD mice treated with FTY720 compared to SCD mice treated with saline. ** $P < 0.01$, SCD mice treated with FTY720 compared to SCD mice treated with saline. $N = 6-9$ mice per treatment group.

Further induction of circulating IL-6 in periphery was identified in SCD mice and reduction of IL-6 was observed in SCD-FTY720 treated mice. Next, I determined whether IL-6 in peripheral tissue levels correlated with plasma levels of IL-6. To test

this, I isolated spleen, liver, lung, and kidney from FTY720 or saline treated WT and SCD mice to determine IL-6 protein levels. In comparison to elevated circulating IL-6 levels in SCD mice, FTY720-treated mice showed a reduction of IL-6 expression in the periphery (Figure 3A). Additionally, IL-6 expression in multiple organs was elevated in SCD mice and reduced by FTY720 (Figure 3B). Taken together, I revealed that elevated FTY720 functions as an immune suppressor to reduce systemic and local inflammatory response in SCD.

Figure 3

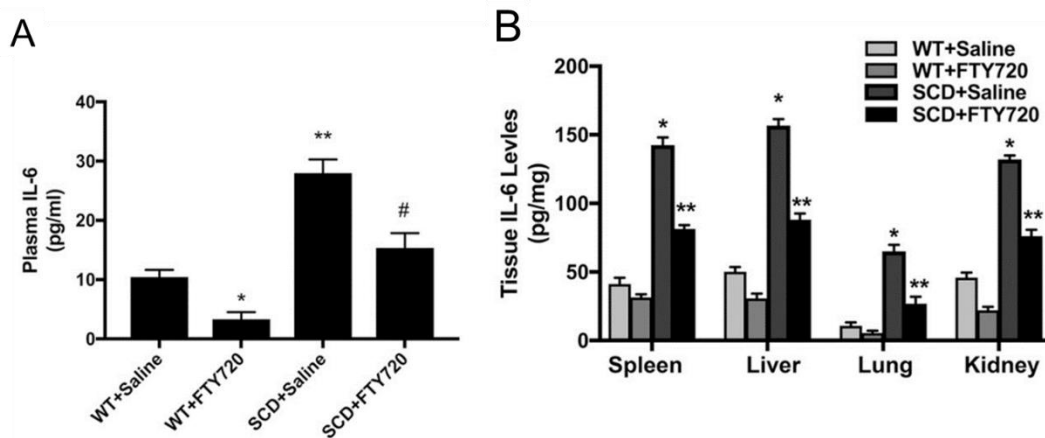


Figure 3. Circulating IL-6 and IL-6 protein levels in spleen, liver, lung, and kidney detected by spectrophotometric analysis. (A&B) Significant reduction of peripheral IL-6 and tissue IL-6 levels in mice treated with FTY720. *P < 0.01, WT mice treated with FTY720 compared to WT mice treated with saline or SCD mice treated saline compared to WT mice treated with saline, respectfully. **P < 0.05, SCD mice treated with saline compared to WT mice treated with saline or SCD mice

treated with FTY720 compared to SCD mice treated with saline. #P<0.001, SCD mice treated with FTY720 compared to SCD mice treated with saline; N=6-9 mice per group.

3.1.3. Elevated interleukin 6 (IL-6) contributes to chronic inflammation and tissue damage in SCD.

Interleukin 6 (IL-6) is a pro-inflammatory cytokine elevated in SCD (54). To determine whether elevated IL-6 mediate an inflammatory responses in SCD, I generated SCD mice with a global deficiency of IL-6 (SCD-*IL6*^{-/-} as described in Methods Section of this dissertation. I analyzed CBC to examine hematological parameters. In SCD-*IL6*^{-/-} mice, RBC counts ~6 M/ μ L, HGB ~6 g/dl, HCT ~20%, MCV ~48, and RDW ~34% (Table 3) (43). I detected erythrocyte sickling in SCD-*IL6*^{-/-} and confirmed that there was no differences in sickling as previously observed (Table 3) (43).

However, I observed that SCD-*IL6*^{-/-} reduction of WBCs ~ 15 k/ μ L, LYs ~ 11 k/ μ L, NEs ~2 k/ μ L, MOs 1 k/ μ L, ~0.09 EO k/ μ L, and BAs ~0.04 k/ μ L (Table 3) (43). This implies that genetic deletion of *IL-6* in sickle mice reduces the immune response. To further confirm *IL-6* global deletion in SCD mice, I detected circulating IL-6 levels and confirmed total elimination of IL-6 in SCD-*IL6*^{-/-} (Figure 4) (43).

Figure 4

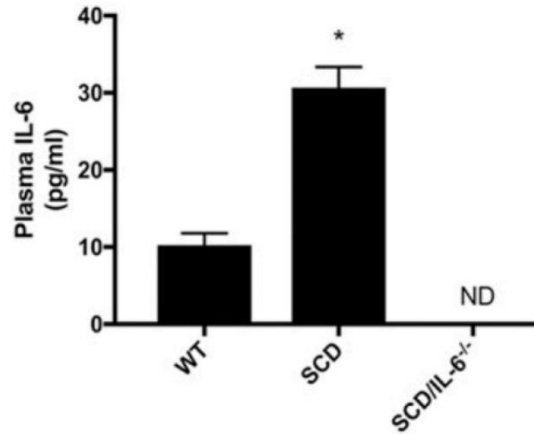


Figure 4. Global genetic deletion of *IL-6* in SCD mice abolished IL-6 levels in the circulation. Although SCD transgenic mice showed increase plasma IL-6 levels compared to WT mice. Sick mice with global genetic deletion of *IL-6* was generated and IL-6 plasma levels were not detectable in these mice. Values shown represent the mean \pm SEM. * $P < 0.01$, SCD mice compared to WT mice. ND means not detected.

Next, I determined whether elevated IL-6 contribute to tissue damage in SCD. Since systemic inflammation is evident in SCD mice and FTY720 mediates anti-inflammatory effects, I hypothesized that FTY720-mediate IL-6 contributes to tissue damage in SCD. To test this, I performed histological assessments in lungs, livers, spleens, and kidneys. I further quantified the areas of interests that indicate severe tissue damage in WT and SCD untreated mice, SCD mice treated with FTY70 or

saline, and SCD-*IL-6*^{-/-} mice. Elevated inflammatory infiltrates in the lungs and necrotic areas in the spleens, livers, and kidneys was identified in SCD mice compared to WT mice (Figure 5 A-D) (43). Moreover, FTY720-treated SCD and SCD-*IL-6*^{-/-} mice showed overall improved tissue structure and decreased inflammatory cell congestion in the lungs (Figure 5A-D) (43). Reduced necrotic regions in spleens, kidneys, and livers was also observed in FTY720 treated SCD mice and SCD-*IL-6*^{-/-} mice (Figure 5A-D) (43).

Sickle mice and patients have severe kidney dysfunction due to abnormal glomerular filtration rates and elevated protein concentrations in the urine (10). I next examined kidney function in the pharmacologic treated SCD mice and SCD mice with IL-6 global deficiency by detecting albumin normalized to creatinine levels in urine isolated from these mice. I first confirmed an increase of albumin in SCD saline treated mice and SCD untreated mice (Figure 5F) (43). In comparison to the untreated and control treated SCD mice, I found that kidney function was improved FTY720 treated SCD mice and SCD-*IL-6*^{-/-} mice (Figure 5F) (43).

Figure 5

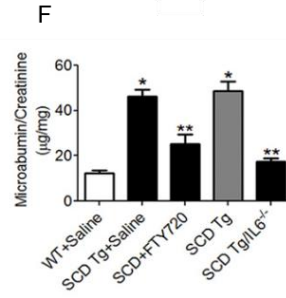
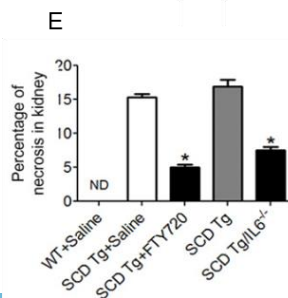
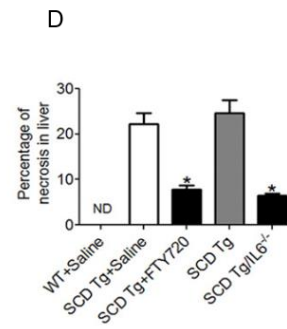
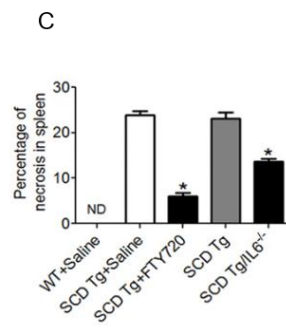
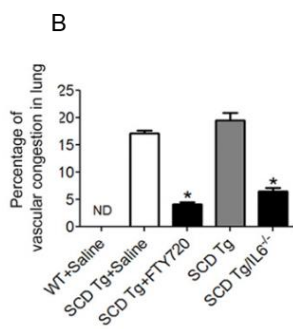
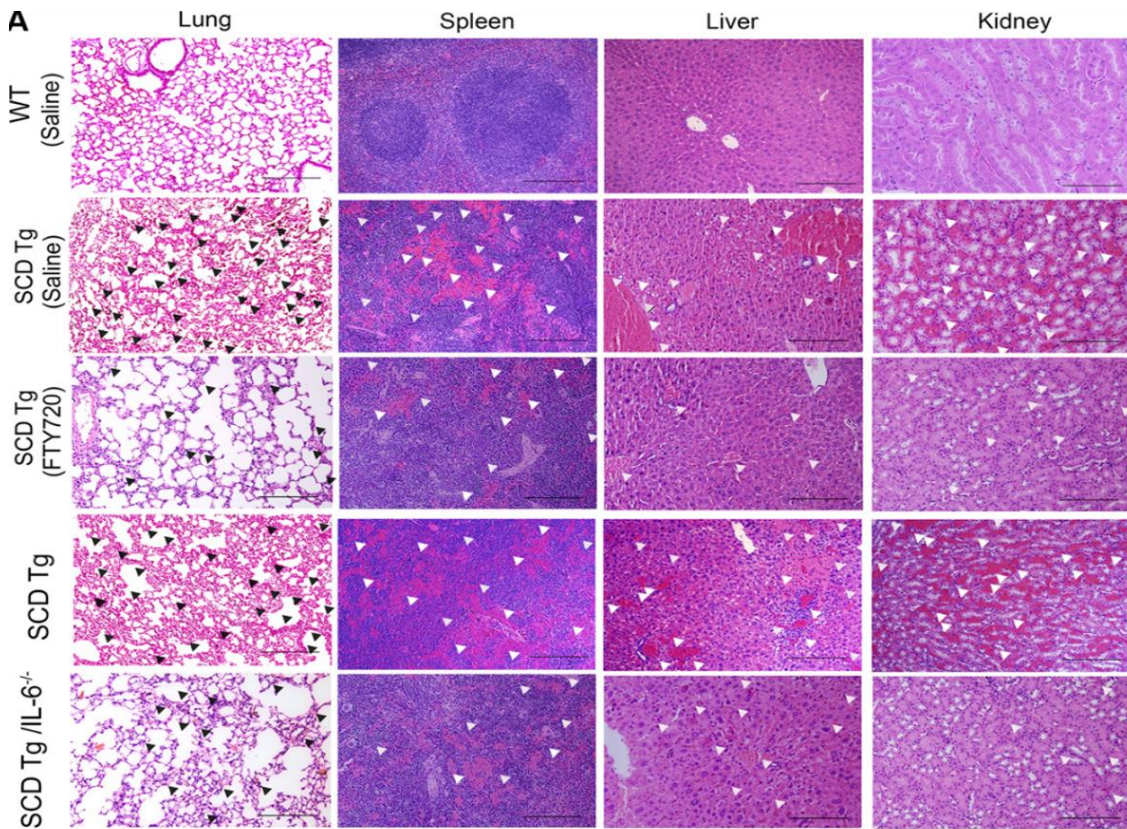


Figure 5. FTY720 treatment or global genetic deletion of *IL-6* contributed to overall improved multiple tissue dysfunction in SCD mice. (A) Histological assessments in untreated WT, untreated and treated SCD mice, and SCD-*IL-6*^{-/-} mice. **(B-E)** Semiquantification of histological areas of interests in lung, spleen, liver, and kidney isolated from the multiple groups. **(F)** Quantification of kidney dysfunction in WT, SCD, and SCD-*IL-6*^{-/-} mice. *P<0.01, saline treated SCD mice compared to saline treated WT mice. **P<0.05, FTY720 treated SCD mice compared to saline treated SCD mice or untreated SCD mice compared to SCD-*IL-6*^{-/-} mice.

3.1.4. FTY720 mediates the reduction of S1PR1 in tissue macrophage.

Since S1PR1 is expressed in various immune cell types and elevated S1P-S1PR1 signaling contributes to chronic disease, I asked whether S1PR1 signaling in macrophages mediate tissue damage in SCD. To test this, I isolated tissue macrophages from kidney and spleen in FTY720 treated mice compared to saline-treated mice. Next, I performed flow cytometric analysis to detect S1PR1 in tissue macrophages isolated from WT and SCD mice. At first, I observed that sickle mice express more S1PR1 on macrophages compared to WT mice (Figure 6A & B) (43). All peripheral macrophages express S1PR1, therefore, I detected S1PR1 expression in macrophages isolated from FTY720 treated SCD mice compared to FTY720 treated WT mice. Taken together, I confirmed a further reduction of macrophages expressing S1PR1 in SCD treated mice (Figure 6A & B) (43).

Figure 6

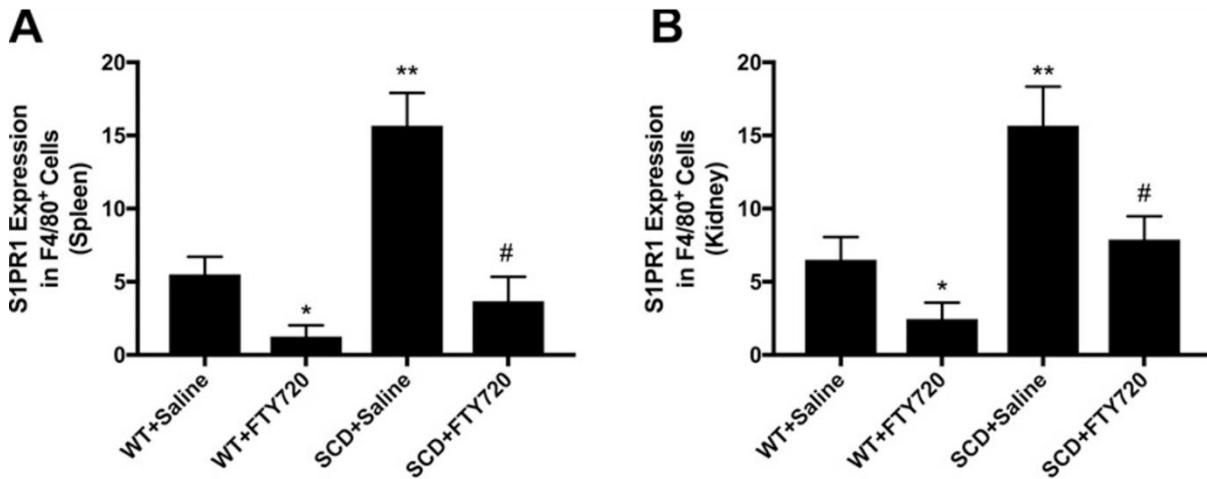


Figure 6. FTY720 mediates reduction of S1PR1 in SCD peripheral macrophages. (A &B) Flow cytometric analysis of F4/80⁺ cells (macrophage marker) in spleen and kidney isolated from WT and SCD mice treated with FTY720 or saline. *P<0.01, WT mice treated with saline versus WT mice treated with FTY720; *P<0.05, SCD mice treated with saline versus WT mice treated with saline. # P<0.001, SCD mice treated with FTY720 versus SCD mice treated with saline.

3.1.5. Elevated IL-6 contributes to induction of S1PR1 in SCD.

As previously demonstrated, S1PR1 in macrophages is elevated in sickle mice and was reduced following FTY720 treatment. Since sickle mice with a genetic deletion of *IL-6* show an overall improved multiple tissue structure and kidney function, I detected S1PR1 expression in kidney and spleen isolated from SCD-*IL-6*^{-/-} mice. By flow cytometric analysis, I detected S1PR1 in tissue macrophages from WT or SCD untreated mice and SCD-*IL-6*^{-/-} mice. As expected, elevated expression of S1PR1 in macrophages were identified in SCD versus WT untreated mice (Figure 7) (43). However, reduced S1PR1 was observed in SCD-*IL-6*^{-/-} mice (Figure 7) (43). Therefore, I demonstrated that IL-6 mediates elevated S1PR1 in SCD tissue macrophages.

Figure 7

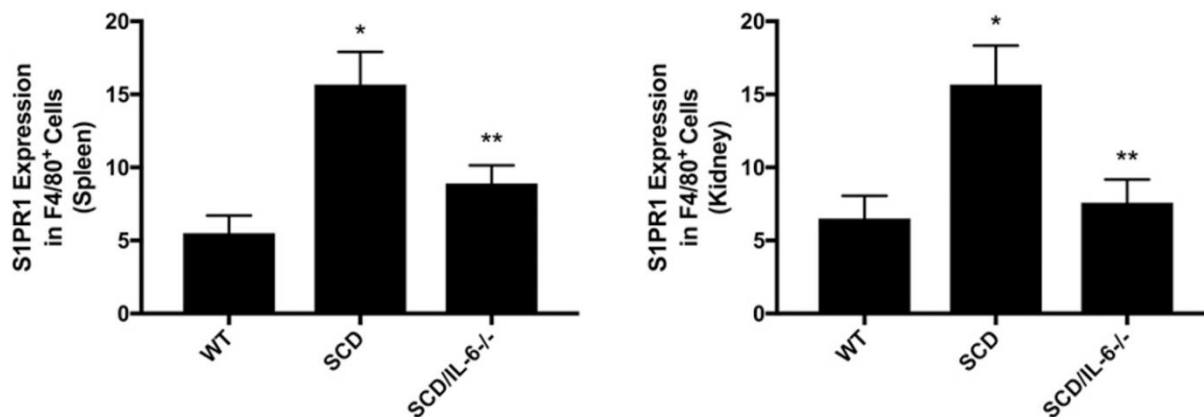


Figure 7. Reduction of S1PR1 expression in *IL-6* genetic deletion mice. (A&B)

Flow cytometric detection of S1PR1 in spleen and kidney tissue macrophages from untreated WT or SCD mice and SCD-*IL-6*^{-/-} mice. Induced S1PR1 expression was detected in SCD mice compared to WT mice. However, reduced S1PR1 expression in tissue macrophages was confirmed in SCD-*IL-6*^{-/-} mice. Values present represent means ±SEM. *P<0.05, WT mice versus SCD mice; **P<0.05, SCD mice versus SCD-*IL-6*^{-/-} mice.

3.1.6. S1P-mediated S1PR1 activation upregulates IL-6 to promote further induction of S1PR1 regulated in a JAK2-dependent manner.

As previously demonstrated, S1PR1 is involved in inducing IL-6 in SCD as identified by pharmacologic and genetic evidence. I determined whether IL-6 can mediate further induction of *S1pr1* gene expression in macrophages. To test this, I generated bone marrow (BM)-derived macrophages from WT mice as described in the Methods Section of this dissertation. I stimulated BM-derived macrophages with S1P and measured *IL-6* mRNA levels. As predicted, I observed induction of *IL-6* mRNA and protein levels in S1P-stimulated macrophages (Figure 8 A &B) (43). To determine whether a specific S1PR mediates induction of IL-6, I treated macrophages with S1P and antagonists for S1PR- 1, 2, 3, and 4 (W146, JTE013, TY52156, and CYM50358), respectively. I discovered that macrophages treated with S1PR1 antagonists W146 and FTY720 reduced *IL-6* mRNA and IL-6 protein level (Figure 8 A &B) (43). For S1P-stimulated macrophages treated with JTE013, TY52156, or CYM50358 expressed no obvious differences in *IL-6* levels (Figure 8 A

&B) (43). This indicates that the other S1PRs have no role in mediating IL-6 induction in WT mice.

To determine whether *IL-6* mediates *S1pr1* mRNA induction, I generated BM-derived macrophages from WT and *IL-6*^{-/-} mice. I stimulated the WT and *IL-6*^{-/-} macrophages with S1P to induce *S1pr1* gene expression. I observed that S1P-stimulated WT macrophages led to further induction of *S1pr1* mRNA levels whereas reduction of *S1pr1* mRNA levels was detected in *IL-6*^{-/-} macrophages (Figure 8 C) (43). Moreover, I treated the S1P-stimulated WT and *IL-6*^{-/-} macrophages with FTY720 and W146 to antagonize S1PR1. I discovered that *IL-6*^{-/-} macrophages expressed reduced *S1pr1* mRNA levels compared to WT macrophages (Figure 8 C) (43).

Additionally, I measured *IL-6* mRNA and IL-6 protein levels in S1P-stimulated WT macrophages. As expected, I discovered that IL-6 levels were further induced in WT macrophages treated with S1P compared to vehicle (Figure 8 D &E) (43). Since I observed an induction of S1P-mediated elevated IL-6 expression in WT macrophages, I asked whether S1P regulates IL-6 signaling. To test this, I stimulated WT macrophages with S1P then treated macrophages with JAK2 specific inhibitor AG490. JAK2 is a tyrosine kinase that stimulates IL-6 production. I found that *IL-6* mRNA and IL-6 protein levels were reduced in S1P-stimulated WT macrophages treated with AG490 (Figure 8 D &E) (43).

Next, I determined whether JAK2 mediates *S1pr1* gene upregulation in WT macrophages. I tested this by stimulating WT macrophages with S1P and *S1pr1* mRNA expression in macrophages with or without addition of AG490. I found that

S1pr1 levels were reduced in WT macrophages treated with AG490 compared to S1P-stimulated macrophages without the addition of AG490 (Figure 8 F) (43).

Overall, I demonstrated that S1P production mediates upregulation of S1PR1 in SCD. By pharmacologic and genetic tools, I have shown that FTY720-treatment and genetic *IL-6* deletion reduces multiple tissue injury, improves overall kidney dysfunction, and reduces chronic inflammation in SCD (Figure 8 G) (43). Mechanistically, I provided pharmacologic evidence that elevated *S1pr1* gene expression can be blocked by S1PR1 antagonism using FTY720 and JAK2-inhibition by AG490 in macrophages (Figure 8 G) (43).

Figure 8

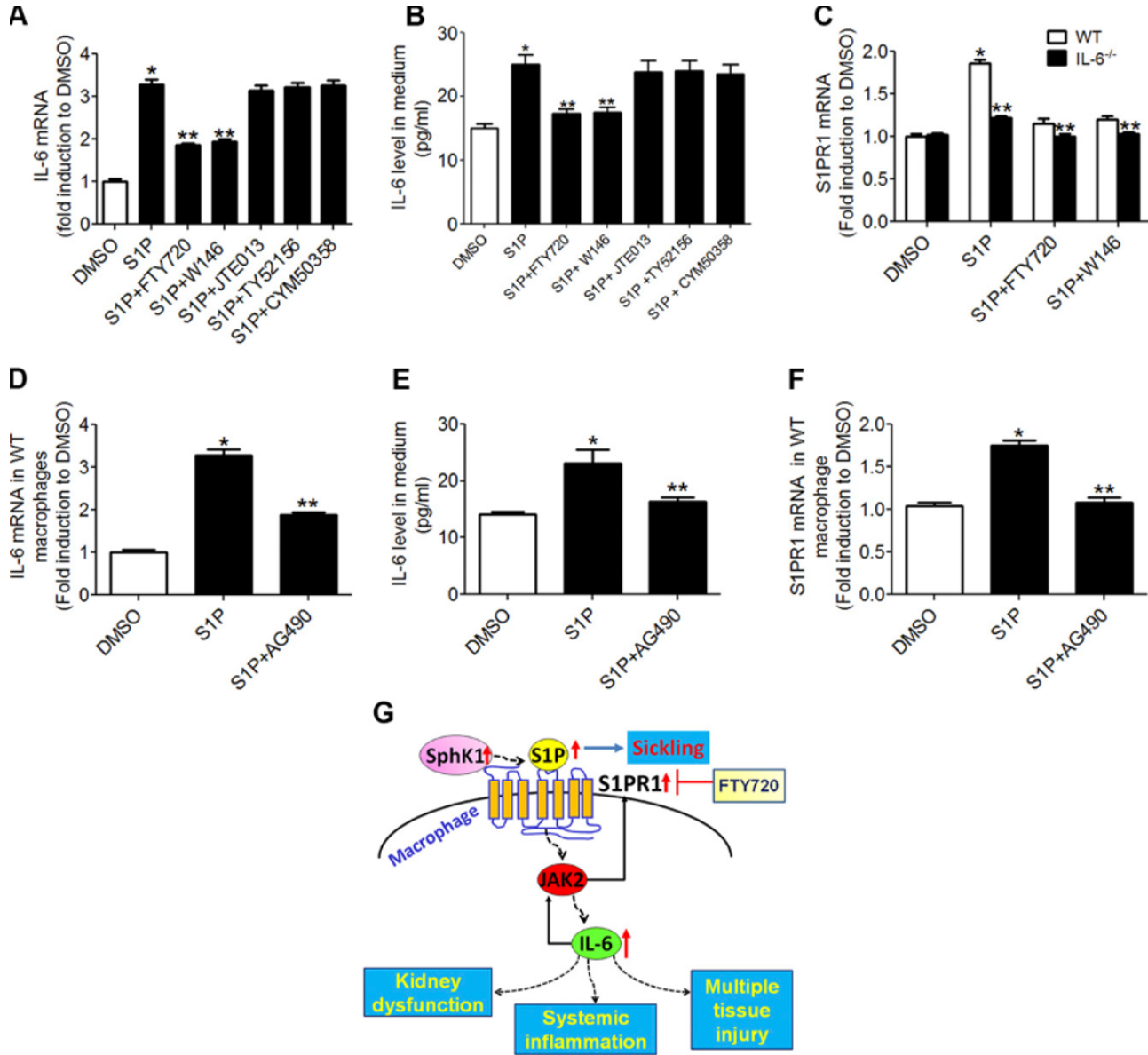


Figure 8. IL-6 production, which induces *S1pr1* mRNA levels in a JAK2-dependent manner in mouse BM-derived macrophages. (A &B) WT BM-derived macrophages were stimulated with S1P in the presence or absence of antagonists for S1PR-1, 2, 3, and 4 followed by a determination of IL-6. **(C)** WT and *IL-6*^{-/-} BM-derived macrophages were generated to detect *S1pr1* mRNA expression. **(D &E)** WT macrophages stimulated with S1P in the presence or absence of JAK2 inhibitor AG490 followed by the determination of *IL-6* mRNA and protein levels. **(F)** *S1pr1* mRNA levels were detected in S1P-stimulated WT macrophages treated with AG490. Values represent mean \pm SEM (N= 6 per group). **(G)** Summary of overall findings in this work. *P <0.01, S1P-treated WT macrophages compared to vehicle-treated group. ** P<0.05, S1P-treated group compared to FTY720-treated group, S1P-treated group compared to W146-treated or FTY720-treated group, and S1P-treated group compared with AG490-treated group (43).

Overall, I provided evidence that elevated S1P-S1PR1-underlines IL-6 induction in macrophage to contribute to systemic and local inflammation in sickle mice. By generating SCD-*IL-6*^{-/-} mice, I demonstrated that IL-6 mediates prolong inflammation, which contributes to further upregulation of *S1pr1* mRNA expression in tissue macrophages. To further demonstrate this mechanism, I generated murine BM-derived macrophages to confirm the roles of S1PR1 and IL-6. By antagonizing S1PRs in macrophages, I detected IL-6 levels and I found that S1PR1 antagonists reduced IL-6 levels whereas the other S1PRs did not. Moreover, I demonstrated that IL-6 mediates the upregulation of *S1pr1* mRNA expression in a JAK2-dependent manner, which confirms the molecular mechanism.

3.2. Chapter 2: Elevated circadian *Period 2* is beneficial in SCD

This chapter is based on unpublished work by Adebiyi MG, Zhao Z, Youqiong Y, Manalo J, Hong Y, Hill R, Gong J, D'Alessandro A, Lee CC, Xian W, McKeon F, Kellems RE, Yoo SH, Han L, and Xia Y.

In this chapter, I will present the robust genetic screen I performed in SCD mice compared to WT control mice. Several upregulated pathways in SCD were identified that involve genes in heme metabolism and inflammation. Unexpectedly, I discovered upregulated expression of circadian clock genes in SCD. The role of circadian genes in SCD has not been previously studied. This chapter will explore the role of a circadian gene *Period 2* and its role in SCD.

3.2.1. Upregulated expression of circadian genes, inflammatory genes, heme and iron homeostatic genes in SCD lung.

Elevated inflammation, vasculature dysfunction, and overall multiple tissue injury is well described in SCD (16, 55). Tissue injury in SCD is a detrimental consequence of the disease progression, which is often irreversible. In fact, changes in gene expression due to chronic tissue injury reveals how an organ functions. To determine whether changes in gene expression underlie tissue dysfunction in SCD, I performed a robust unbiased microarray genetic study as a strategy to examine gene expression profile in SCD mice compared to WT control mice. I selected the lung as an organ of interest because pulmonary complications are the leading cause of SCD patient mortality in the clinic. I isolated RNA from SCD and WT lung then reverse transcribed the RNA to generate cDNA. High quality SCD and WT samples were used to prepare cDNA libraries and screen for gene detection using Affymetrix expression array.

In the screen, I identified ~ 700 genes specific to lung isolated from SCD and WT mice. Amongst the genes identified, I discovered that ~ 200 genes were upregulated in the SCD lung compared to WT lung. By performing pathway analyses, I revealed lung specific genes involved in cilium movement, chemokine-mediated signaling pathway, immune response, axoneme assembly, chemotaxis, inflammatory response, cellular response to interleukin-1, response to virus, neutrophil chemotaxis, response to interferon-gamma, iron ion homeostasis, positive regulation of I-kappaB kinase (NF-kappaB signaling), rhythmic processes, and regulation of lipid metabolic process (Figure 9).

Figure 9

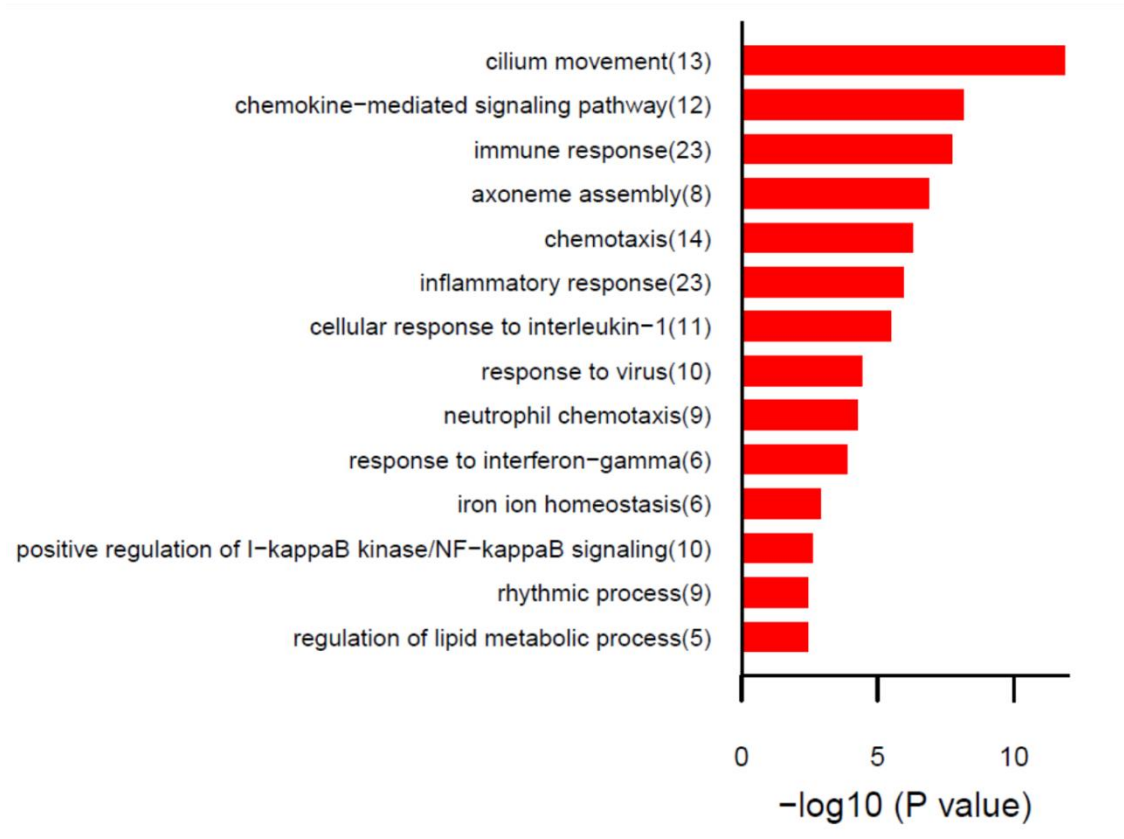


Figure 9. Pathway analyses show upregulated lung specific genes in SCD mice. GO terms for the pathways are shown in the figure and the number of genes for each pathway identified is also indicated in the figure. P values <0.05 were set as cut off and were determined as significant compared to WT.

Although several pathways were upregulated in SCD mice, I became intrigued by series of genes involved in rhythmic processes, heme and iron homeostasis, and inflammatory response as shown in the heat map (Figure 10). The heat map contains expression of genes at a cut off score of $P < 0.05$ in SCD and WT samples. Interestingly, several rhythmic process genes were upregulated at a 1 to 2 fold change in SCD lung, include *Basic helix loop helix family member e 40 (Bhlhe40)*, *D-box binding protein (Dbp)*, *Period 2 (Per2)*, *DNA-binding protein inhibitor 1 (Id1)*, *DNA-binding protein inhibitor 2 (Id2)*, *Nuclear receptor subfamily 1 group D member 1 (Nr1d1)*, *Nuclear receptor subfamily 1 group D member 2 (Nr1d2)*, *Thyrotroph embryonic factor (Tef)*, and *Nicotinamide phosphoribosyltransferase (Nampt)*.

Moreover, I identified that genes pertaining to heme and iron homeostasis, *Lipocalin 2 (Lcn2)*, *Ferrochelatase (Fech)*, *Lactoferrin (Ltf)*, *Solute carrier family 25, member 37 (Slc25a37)*, *Metalloreductase 2 and 4 (Steap 2 and Steap 4)* were elevated in SCD lung (Figure 10). Additionally, the screen revealed elevated inflammatory genes specific to SCD lung. These inflammatory genes were *C-C motif chemokine ligand 5 (Ccl5)*, *C-C motif chemokine ligand 17 (Ccl17)*, *C-X-C motif chemokine ligand 2 (Cxcl2)*, *C-X-C motif chemokine ligand 9 (Cxcl9)*, *C-X-C motif chemokine ligand 10 (Cxcl10)*, *C-X-C motif chemokine ligand 13 (Cxcl13)*, *Interferon activated 202B (Ifi202b)*, *Complement component 4 a (C4a)*, *Complement component 4 b (C4b)*, *Platelet factor 4 (Pf4)*, *C-C chemokine receptor type 2 (Ccr2)*, *C-C chemokine receptor type 4 (Ccr4)*, *Nuclear factor, erythroid 2 like 2, (Nfe2l2)*,

Annexin a1 (Anxa 1), Prostaglandin g/h synthase 1 (Ptgs1), Toll-like receptor 6 (Tlr6), and A-disintegrin and metalloproteinase domain-containing protein 8 (Adam8) (Figure 10).

Using an unbiased approach, I demonstrated elevated expression of lung specific inflammatory, iron homeostasis, and rhythmic genes in SCD. Induced gene expression of several heme and iron metabolic genes and inflammatory genes may provide intrinsic insight on the effect of intravascular hemolysis at the local tissue level.

.

Figure 10

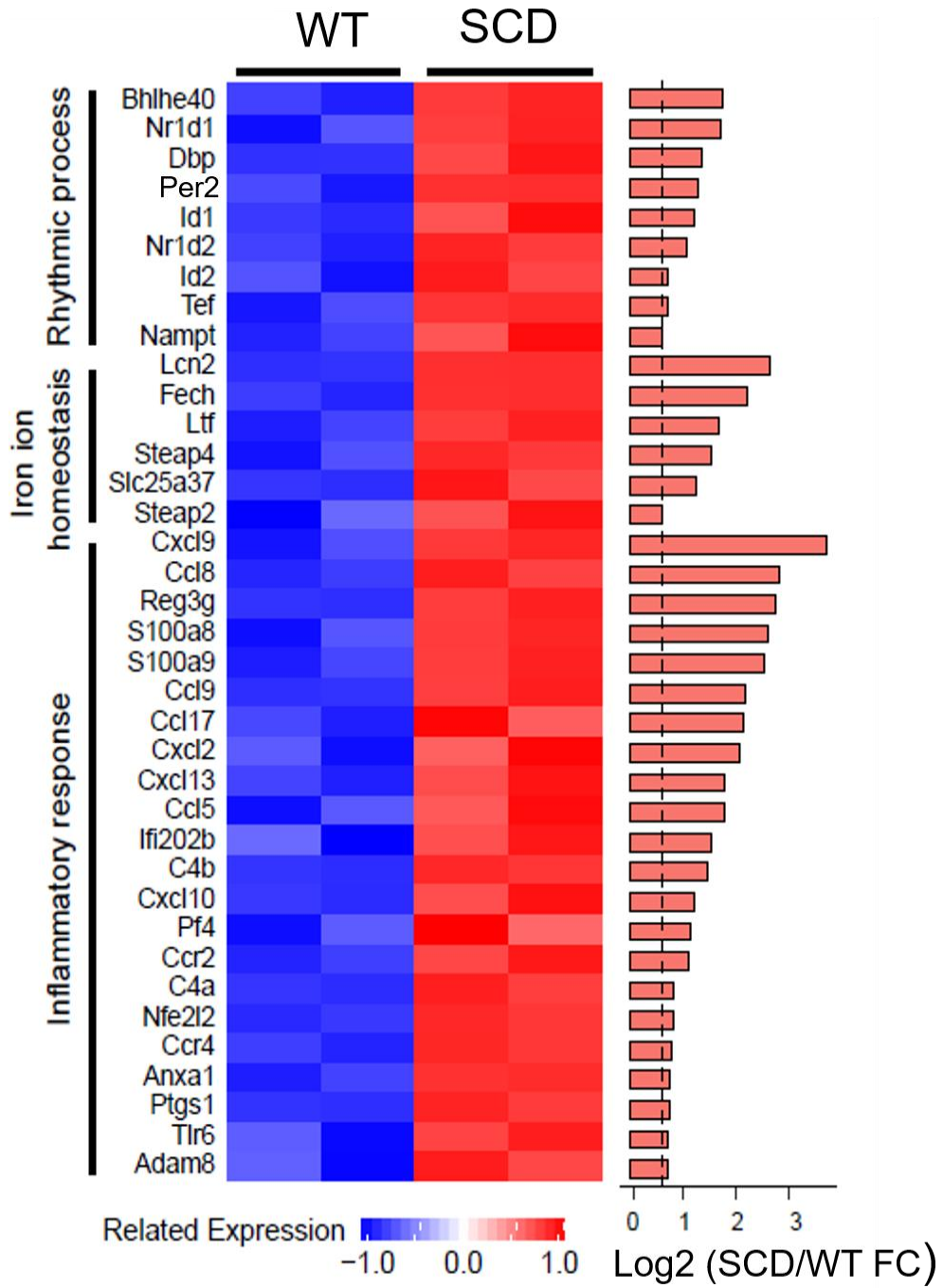


Figure 10. Unbiased microarray gene expression screen in SCD lung reveals upregulated expression of rhythmic clock genes, heme and iron hemostatic genes, and inflammatory genes. Heat map with bar plots correspond to gene expression was generated based on \log_2 -transformation. Gene fold changes was normalized to WT based on $P < 0.05$ cut off score. Upregulated genes were indicated as red and downregulated genes were indicated as blue.

3.2.2. Period 2 (Per2) induction in SCD lung underlines molecular clock function to deter further inflammatory response and tissue damage.

Since I discovered an increase in the expression of rhythmic process genes, I determined whether these genes were further upregulated during a circadian cycle. The core circadian genes that regulates molecular clock function are *Per1*, *Per2*, *Arnt*, and *Clock*. I discovered that *Arnt* gene in WT lung was expressed fold 2 to 3 higher compared to SCD lung (Figure 11).

Figure 11

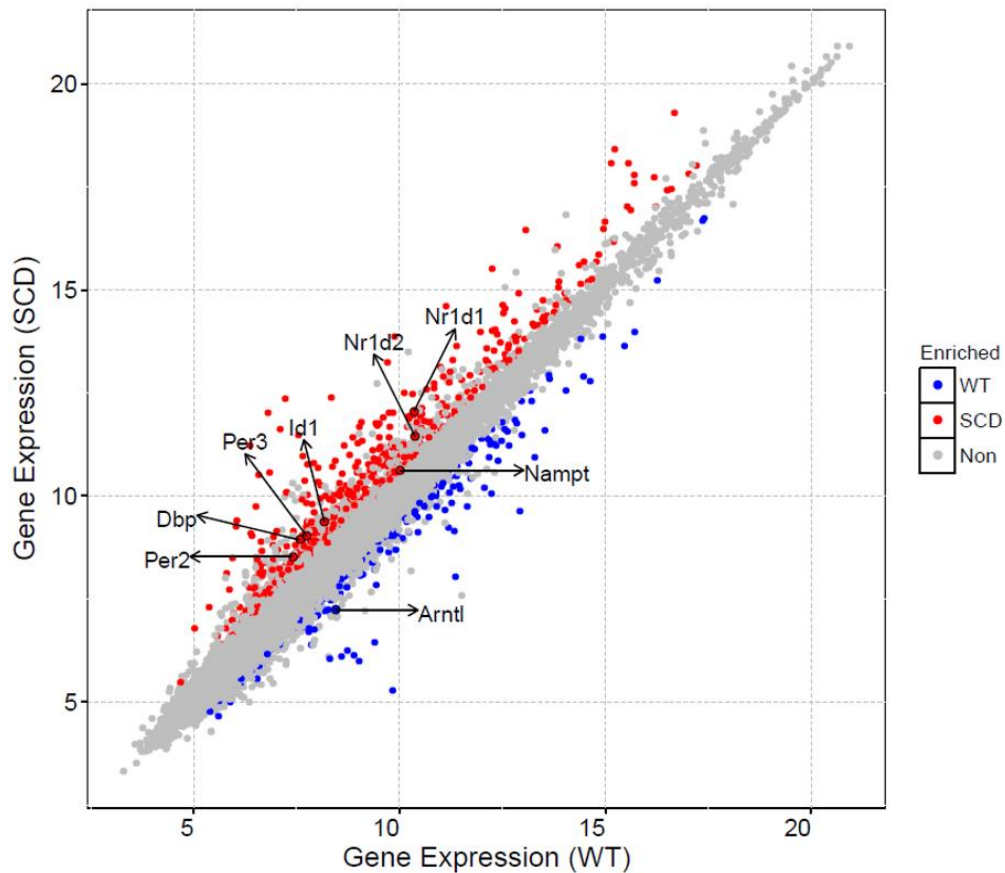


Figure 11. Circadian gene expression in SCD compared to WT lung. Scatter plot of differentially expressed circadian rhythmic genes in SCD and control lung. Red dots show enriched genes in SCD whereas blue dots show elevated genes in WT lung. Circadian gene (s) *Per2*, *Dbp*, *Id1*, *Nr1d1*, and *Nr1d2* were increased by 2 in SCD whereas *Arntl* was increased by 1.5 in WT.

I determined whether *Per2* and *Arnt* could be detected in SCD and WT lung at various time points during the day. To test this, I purified RNA from SCD and WT lung then I performed semiquantification RT-PCR (qRT-PCR) to detect these circadian genes at environmental light and dark conditions, which corresponds to 12 hours light and 12 hours dark also known as zeitgeber time (ZT). Tissue collection was performed as ZT: 1, 7, 13, 19, and 26. When I validated the mRNA expression of *Per2* and *Arnt*, I found that *Per2* gene expression was much higher in SCD lung compared to WT lung during a circadian cycle compared to previous results. During ZT 1-13, *Per2* gene expression change 2 to 3 fold, which increased to a fold change of 3 to 4 at ZT 19-26 (Figure 12B). Moreover, a phase change in *Per2* was apparent in SCD lung.

Figure 12

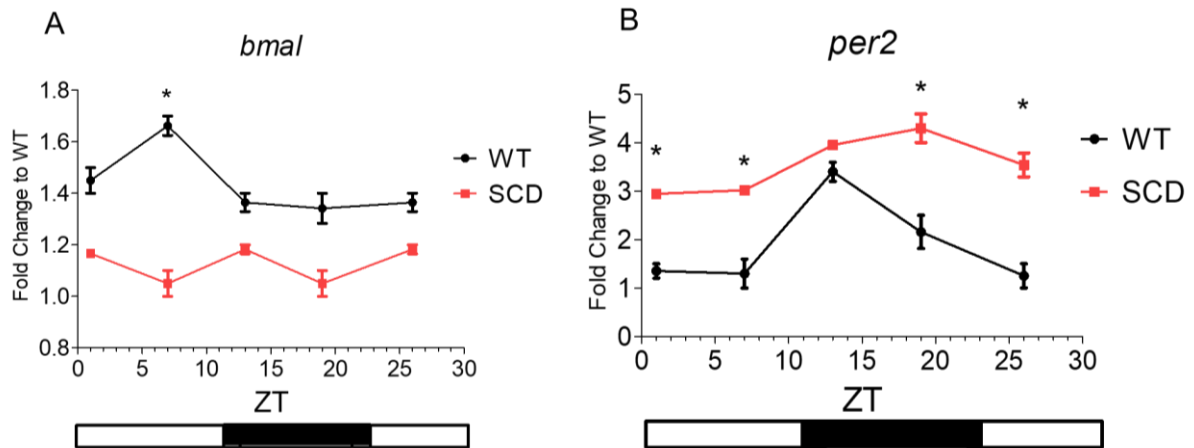


Figure 12. Circadian *Arnt (Bmal)* and *Per2* mRNA expression levels detected by semiquantitative real time polymerase chain reaction (qRT-PCR). Values represented as means \pm SEM, * $P < 0.05$, Fold change represented as SCD normalized to WT.

Since elevated *Per2* mRNA was seen in SCD mice, I confirmed whether PER2 protein levels mimic *Per2* mRNA levels in SCD. To test this, I generated SCD \rightarrow *Per2*^{Luciferase} (SCD \rightarrow *Per2*^{Luc}) mice and WT \rightarrow *Per2*^{Luciferase} (WT \rightarrow *Per2*^{Luc}) mice by means of adoptive SCD or WT bone marrow (BM) cells transfer to lethally irradiated *Per2*^{Luc} bioluminescent reporter mice (Figure 13 A) . *Per2*^{Luc} transgenic mice were created by the insertion of the luciferase reporter into the open reading frame (ORF) of the *Per2* gene (42) . Heterozygous and mutant (*Per2*^{Luc/+} and *Per2*^{Luc/Luc}) mice were used as recipients for the BM transplantation studies. Further details on generation of these mice is found in the Methods Section of this dissertation. I utilized these mice for detecting PER2 luciferase oscillations in tissue cultures isolated from the mice (Figure 13 B). PER2 oscillations in tissue explants are robust even after tissues are removed from the animal (42). The PER2 oscillations reflect a 24 hour cycle that can predict *Per2* mRNA and PER2 protein expression based on the luciferase levels. Cultures were placed in a water jacketed CO₂ incubator that is also light protective and equipped for recording PER2 oscillations in real time (Figure 13 B). Terminology used to describe the PER2

oscillations: amplitude and period. Amplitude refers to the height of the PER2 peaks and the period refers to frequency of the PER2 peaks (Figure 13 B).

Since I previously showed that *Per2* mRNA levels were induced in the SCD lung, I isolated lung from SCD and WT transplanted mice to determine PER2 luciferase activity in lung tissue cultures for up to 36.5 hours. The frequency of the PER2 peaks show no difference in the SCD \rightarrow *Per2*^{Luc} or the WT \rightarrow *Per2*^{Luc} mice. Moreover, I observed increase of luciferase expression based on the intensity of the PER2 peaks in lung cultures isolated from the SCD \rightarrow *Per2*^{Luc} mice compared to control mice. Overall, these results imply that *Per2* mRNA and PER2 protein levels are elevated in SCD mice compared to WT controls.

Figure 13

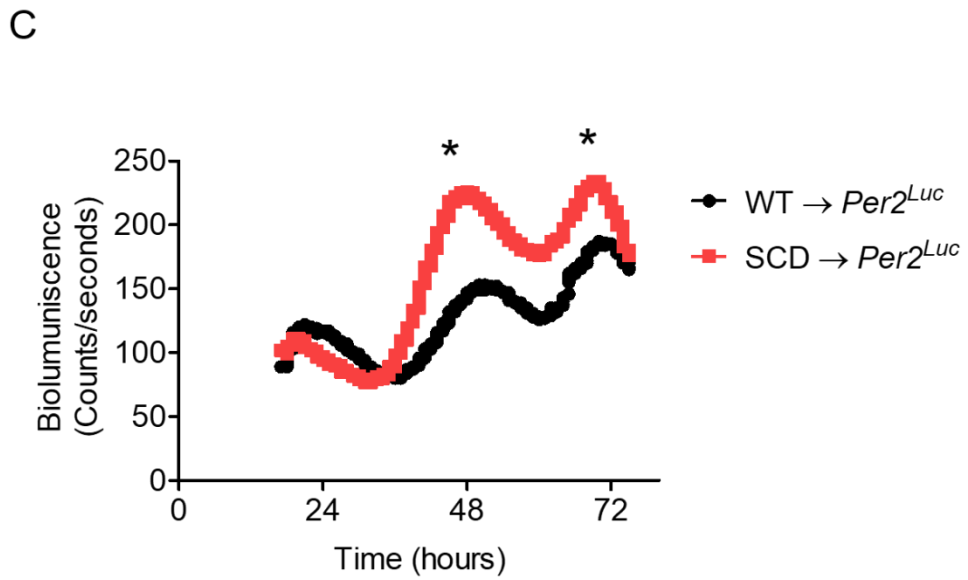
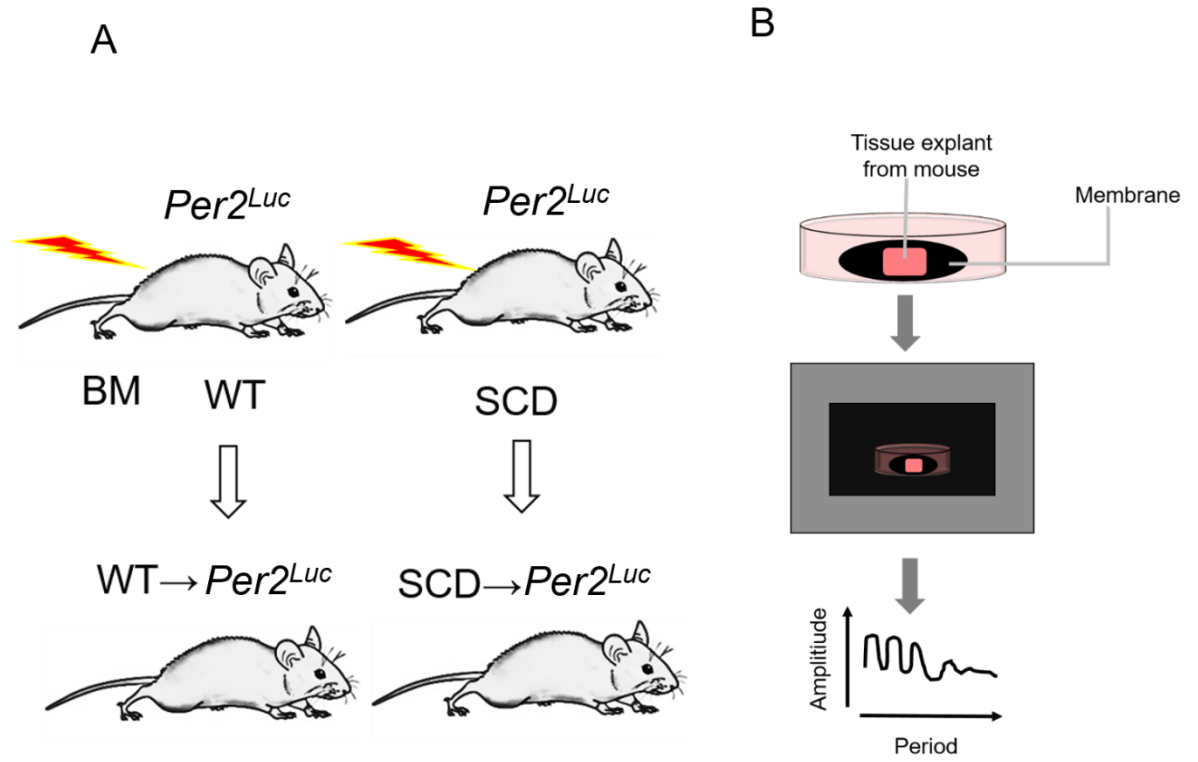


Figure 13. PER2 luciferase activity is higher in SCD. (A) Generation of *Per2^{Luc}* mice with SCD or WT phenotype. **(B)** Schematic of the work-flow for PER2 oscillation recordings performed in tissue explant cultures. **(C)** Data analysis of luminescence detection in lung cultures. Values represents means \pm SEM *P<0.05, SCD versus WT lung. N= 3 per group.

3.2.3. Molecular clock dysfunction contributes to further tissue damage in SCD

Since elevated *Per2* levels were identified in SCD mice, I determined whether the increased *Per2* in SCD plays a role in the disease. *Per1* and *Per2* are homologous genes that are transcriptionally regulated by BMAL and CLOCK genes to promote molecular clock function in multiple organs. The absence of *Period* genes disrupt circadian rhythms due to molecular clock dysfunction (30). To determine whether *Period* genes regulate molecular clocks in SCD, I generated SCD phenotypic *Per1/Per2* double knock out (*dKO*) mice by BM transplantation. WT or SCD BM was transferred to irradiate WT or *Per1/Per2 dKO* mice (Figure 14 A). As such four BM transplant groups, WT \rightarrow WT, WT \rightarrow *Per1/Per2 dKO*, SCD \rightarrow WT, and SCD \rightarrow *Per1/Per2 dKO* mice were generated. After 8 weeks post BM transplantation, peripheral blood was extracted to detect adoptive transfer of WT or SCD leukocytes using fluorescent CD45.1 or CD45.2 expression analyzed by flow cytometry. SCD phenotype mice express high chimerism of CD45.1 ~ 84 to 94 % (Table 4). Control WT phenotype mice typically express high CD45.2 and no CD45.1.

Additionally, I analyzed multiple hematological parameters by performing CBC analyses on SCD and WT chimeric mice. In SCD mice, the RBC counts range was ~ 5.80 to 5.97 x10⁶ cells/ μ l, HB range was ~7.55 to 7.83 g/dl, HCT range was ~35.55 to 36.33 %, RDW range was ~35.33 to 36.33 %, MCV range was ~42.67 to 45.85, and reticulocytes (Ret) range was ~32.42 % (Table 4). These values represent typical hematological parameters for sickle mice. In addition to CBC analysis, I examined the morphology of erythrocytes isolated from the SCD→ WT and SCD→ *Per1/Per2* dKO mice to determine the sickling. I quantified the sickling in SCD BM transplanted mice and observed similar sickling percentages ~13% in both SCD groups. Moreover, there were no significant differences between the WT or *Per1/Per2* dKO mice with SCD phenotype. In comparison to WT mice, RBC counts were ~ 10.94 x10⁶ cells/ μ l, HGB ~ 12.00 g/dl, HCT ~43 %, and Ret ~4 % (Table 4). Chimeric WT or *Per1/Per2* dKO mice generated by BM transplantation showed typical hematological patterns for WT phenotype mice.

Unexpectedly, I observed that white blood cells (WBCs) and neutrophils (NEs) were increased in SCD→ *Per1/Per2* dKO mice. In the WT mice transplanted with SCD BM, WBCs were ~31 k/ μ l, and NEs were ~3.7 k/ μ l whereas *Per1/Per2* dKO mice with SCD phenotype, WBCs were ~ 50.47 k/ μ l and NEs were ~7.03 k/ μ l (Table 4). In comparison to WT or *Per1/Per2* dKO with WT phenotype, expressed normal ranges of WBCs ~ 3 k/ μ l and NEs~ 1 k/ μ l (Table 4). Although *Per1/Per2* does not play a role in sickling, I found that *Per1/Per2* may play a significant role in immune cells in the periphery.

Table 4

	RBC ($\times 10^6$ cells μl^{-1})	HB (g dl ⁻¹)	HCT (%)	RDW (%)	MCV (fL)	WBC (k/uL)	RET (%)	NE (k/uL)	Sickled cells (%)	Chimerism (%)
WT → WT	9.52 ± 2.09	11.13 ± 2.77	42.10 ± 6.27	25.05 ± 3.01	48.18 ± 1.05	3.21 ± .96	4.52 ± 0.47	1.78 ± 0.28	ND	ND
WT → <i>Per1/2</i> <i>dKO</i>	10.94 ± 1.22	12.80 ± 0.80	45.13 ± 4.65	25.53 ± 0.92	50.80 ±3.58	3.39 ± .82	4.08 ± 0.27	1.54 ± 0.68	ND	ND
SCD → WT	5.80 ± 1.10 *	7.83 ± 1.41 *	35.55 ± 2.05 *	34.80 ± 0.91	45.85 ± 1.85	31.68 ± 1.04 *	32.42 ± 1.69 *	3.71 ± 0.48 *	13.15 ± 1.72	87.30 ± 2.61
SCD → <i>Per1/2</i> <i>dKO</i>	5.97 ± 0.32 *	7.55 ± 0.51 *	36.33 ± 2.18 *	37.83 ± 2.27	42.67 ± 1.09	50.47 ± 6.74 *	32.78 ± 4.54 *	7.03 ± 1.46 *	13.08 ± 1.66	89.27 ± 5.52

Table 4: Bone marrow transplantation of wild-type (WT) or sickle cell disease transgenic (SCD ^{Tg}) bone marrow to irradiated *Per1/Per2 dKO* or WT mice recipients; RBC: red blood cell count; HB: hemoglobin; HCT: hematocrit; RET: reticulocytes; WBC: white blood cells, and NE: neutrophils. Confirmation of sickle cells by erythrocyte morphology detection methods and expression of positive CD45.1 leukocyte populations in chimeric sickle transplanted mice. *P < 0.05 versus WT → WT; ** P < 0.01 verses SCD → WT; N=5-7.

Next, I determined whether the loss of *Per1/Per2* plays a role in molecular clock dysfunction in multiple tissues. To test this, I performed histological assessments to analyze tissue damage in lung, liver, and spleen. By comparing histopathology of the SCD and WT transplant groups, I observed that SCD → *Per1/Per2* *dKO* mice had worse lung damage due to increase infiltration of inflammatory cells leading to further lung congestion (Figure 14 B). Evidence of further lung damage was determined in SCD → *Per1/Per2* *dKO* mice compared to SCD→ WT mice (Figure 14 B &C).

In addition to the lung, there was evidence of damage occurring in the spleen and the liver. Sickie mice have elevated intravascular hemolysis due to chronic sickling with severe necrotic areas from chronic accumulation of heme and iron. In this case, I observed more necrosis in the sickie organs derived from *Per1/Per2* *dKO* mice compared WT (Figure 14 B). No observation of liver or spleen necrosis in WT phenotypic mice was observed; but, necrotic regions in liver and spleen were evident in sickie phenotypic mice (Figure 14 D & E). More apoptotic cells could be the reason as to why I observed more lung and liver damage in *Per1/Per2* deficient sickie mice (Figure 14 B-D).

Figure 14

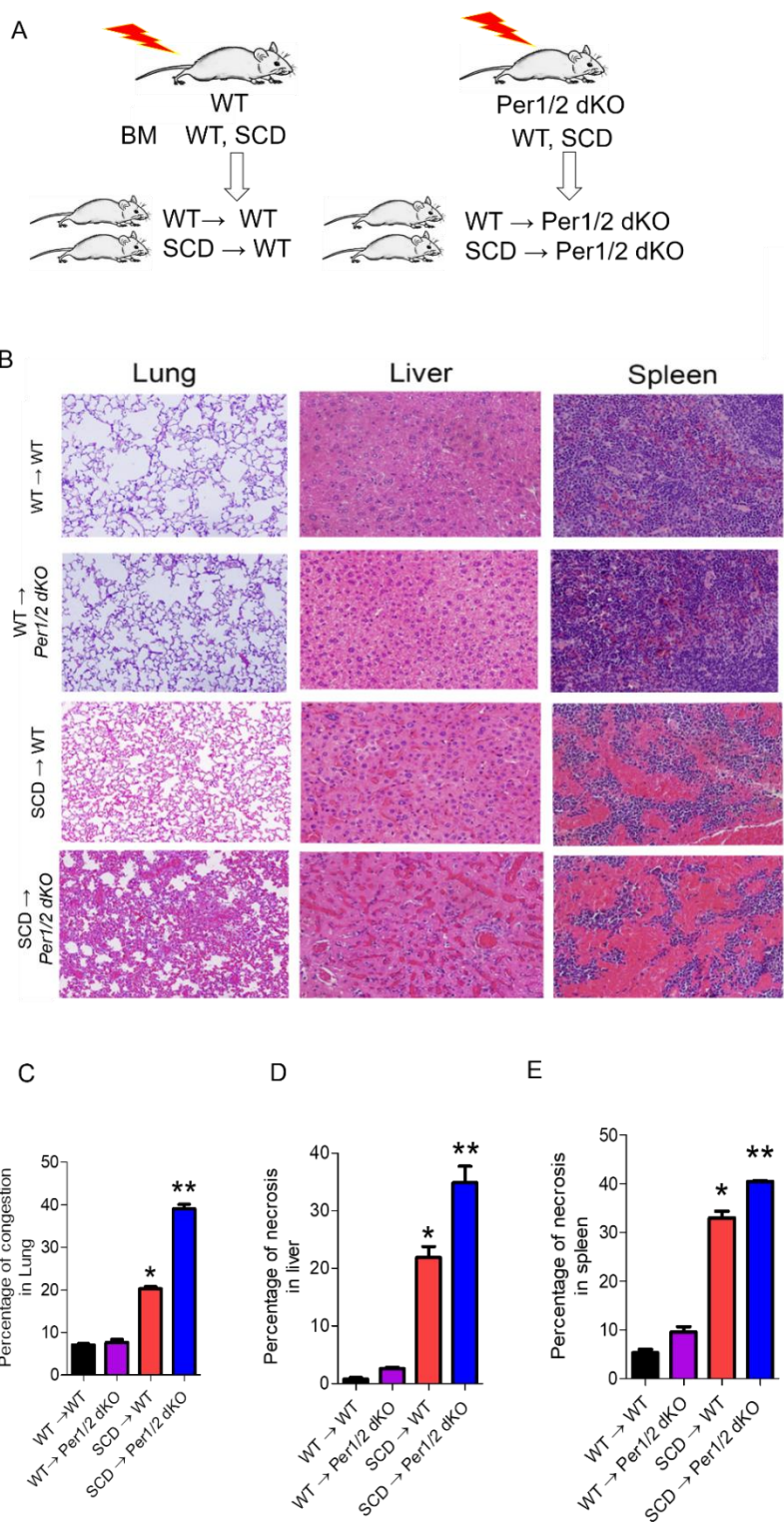


Figure 14. Loss of *Per1/Per2* contributes to multiple tissue damage in SCD.

(A) Cartoon of BM transplant groups generated with WT or SCD phenotype. **(B)** Histopathological assessment of lung, liver, and spleen in BM transplant groups. **(C-E)** Semiquantitative analysis of multiple tissue histological assessment. Values expressed as means \pm SEM, * $P < 0.01$, WT \rightarrow WT or WT \rightarrow *Per1/Per2* dKO versus SCD \rightarrow WT, ** $P < 0.01$, SCD \rightarrow WT versus SCD \rightarrow *Per1/Per2* dKO. N=5 to 6 mice per group.

Severe histopathological outcomes were detected in sickle organs with *Per1/Per2* genetic deletion. I asked whether *Per1/Per2* dKO mice with SCD phenotype also had renal and hepatic dysfunction. To test hepatic function, I measured alanine aminotransferase (ALT) levels in serum isolated from transplant mice. ALT is an enzyme that converts glutamate and pyruvate in order to generate α -ketoglutarate and alanine. This mechanism is essential for liver metabolism. Although ALT is normally expressed in the liver, elevated ALT levels in the serum indicates hepatic dysfunction. In my sickle mice, I observed an increase in serum ALT in SCD \rightarrow *Per1/Per2* dKO mice compared to SCD \rightarrow WT mice (Figure 15 A). This indicates that *Per1/Per2* contributes to hepatic function in sickle mice. Moreover, I tested renal function by detection of albumin levels in the urine. Higher concentrations of albumin in the urine indicates renal dysfunction. Albumin concentrations were normalized to creatinine for each specimen tested. In my analysis of renal function in the sickle mice, I observed higher albumin

concentrations in SCD → *Per1/Per2* dKO mice, which indicates severe renal dysfunction (Figure 15 B). Normal renal function was observed in WT phenotype transplanted mice (Figure 15 B).

Figure 15

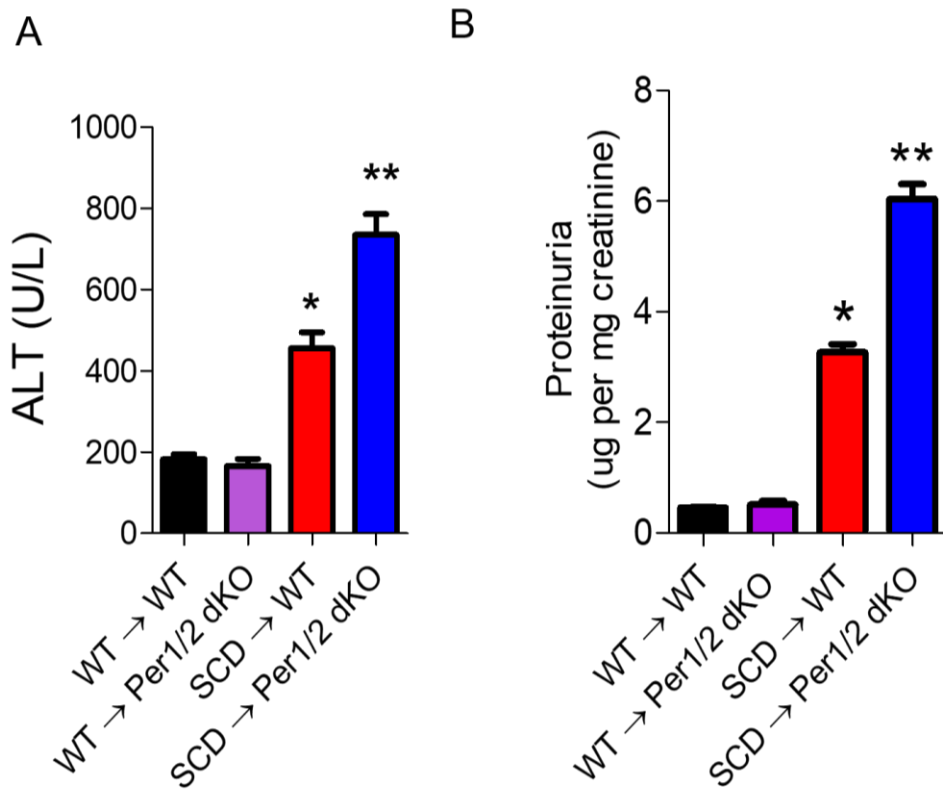


Figure 15. Hepatic and renal dysfunction in *Per1/Per2* deficient sickle mice. **(A)** Analysis of ALT to determine hepatic function in transplant groups. **(B)** Renal dysfunction analysis confirmed by albumin concentration normalized to creatinine. Values expressed as means \pm SEM, * $P < 0.01$, WT \rightarrow WT or WT \rightarrow *Per1/Per2* dKO versus SCD \rightarrow WT, ** $P < 0.01$, SCD \rightarrow WT versus SCD \rightarrow *Per1/Per2* dKO. N=5 to 6 mice per group.

Unexpectedly, I observed increased irradiation sensitivity in *Per1/Per2* dKO mice with SCD phenotype. Although all of the transplant mice were lethally irradiated, the SCD \rightarrow *Per1/Per2* dKO mice were more sensitive due to evidence of irradiation damage in the cranial and dorsal regions (Figure 16). No obvious irradiation damage was found in WT or *Per1/Per2* dKO mice transplanted with WT BM was observed. Similarly, irradiation damage was not evident in WT mice transplanted with SCD BM. This indicates that peripheral *Per1/Per2* has an overall protective role in sickle mice.

Figure 16

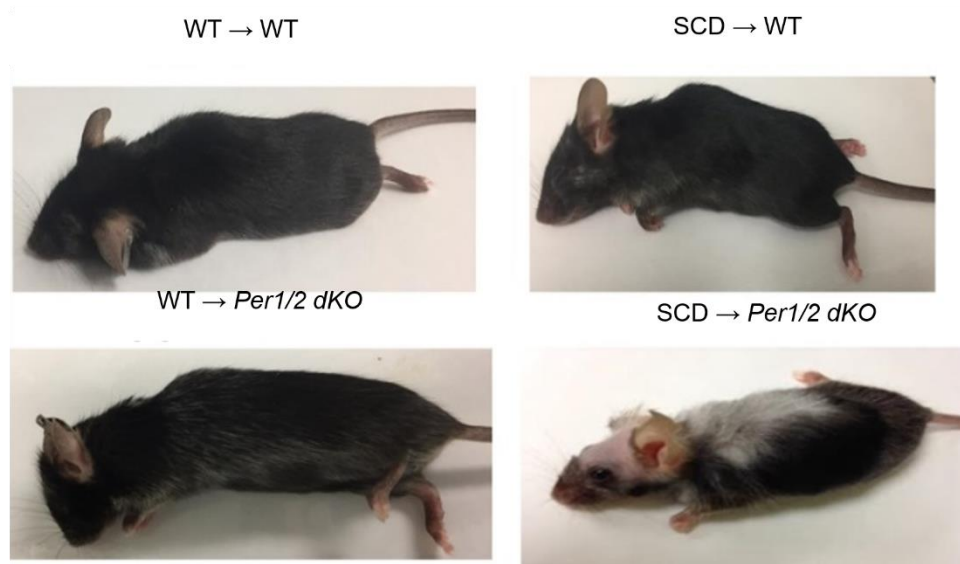


Figure 16. Phenotypic observation of effect of whole body irradiation in transplant groups. Increased irradiation sensitivity in *Per1/Per2* dKO mice with SCD phenotype.

*3.2.4. Systemic inflammation contributes to elevated lung neutrophil infiltration due to global genetic deletion of *Per1/Per2* in sickle mice.*

Neutrophil adhesion to the lung vasculature contributes to endothelium dysfunction in SCD pathophysiology. Since an increase of neutrophils in the circulation was observed in SCD → *Per1/Per2* dKO genetic deficient mice compared to the sickle → WT mice (Table 4), I determined whether peripheral *Per1/Per2* was involved in regulating inflammatory responses in the lung. As indicated by

histological studies, I observed further lung congestion due to increased inflammatory infiltration in the lung. The majority of inflammatory cell types were BM-derived, which can infiltrate to tissues from the periphery. Although mixed populations of BM-derived and resident cell types was found in multiple tissues isolated from *Per1/Per2* *dKO* mice. The role of *Per1/Per2* in multiple immune cell types and systemic inflammation in sickle lung is not fully understood.

Based on the CBC results (Table 4), I generated a hypothesis that *Per1/Per2* *dKO* sickle mice have elevated systemic inflammation, which contributes to further lung tissue damage. To test this, I isolated whole lung from mice transplanted with SCD or WT BM and performed immunohistochemistry to detect neutrophils (Ly6-neutrophil marker). In WT control mice, I detected no neutrophil infiltration to vasculature walls in the lungs (Figure 17 A &B). However, I observed more neutrophils in the sickle lungs as indicated by red arrows (Figure 17 A). My original hypothesis is that neutrophil trafficking due to genetic deletion of *Per1/Per2* were further enhanced in sickle lungs. I demonstrated this by detecting increased numbers of neutrophils in sickle *Per1/Per2* *dKO* lungs (Figure 17 B). Based on

these findings, I conclude that genetic deletion of *Per1/Per2* in sickle mice contributes to more neutrophils in the lung tissue.

Figure 17

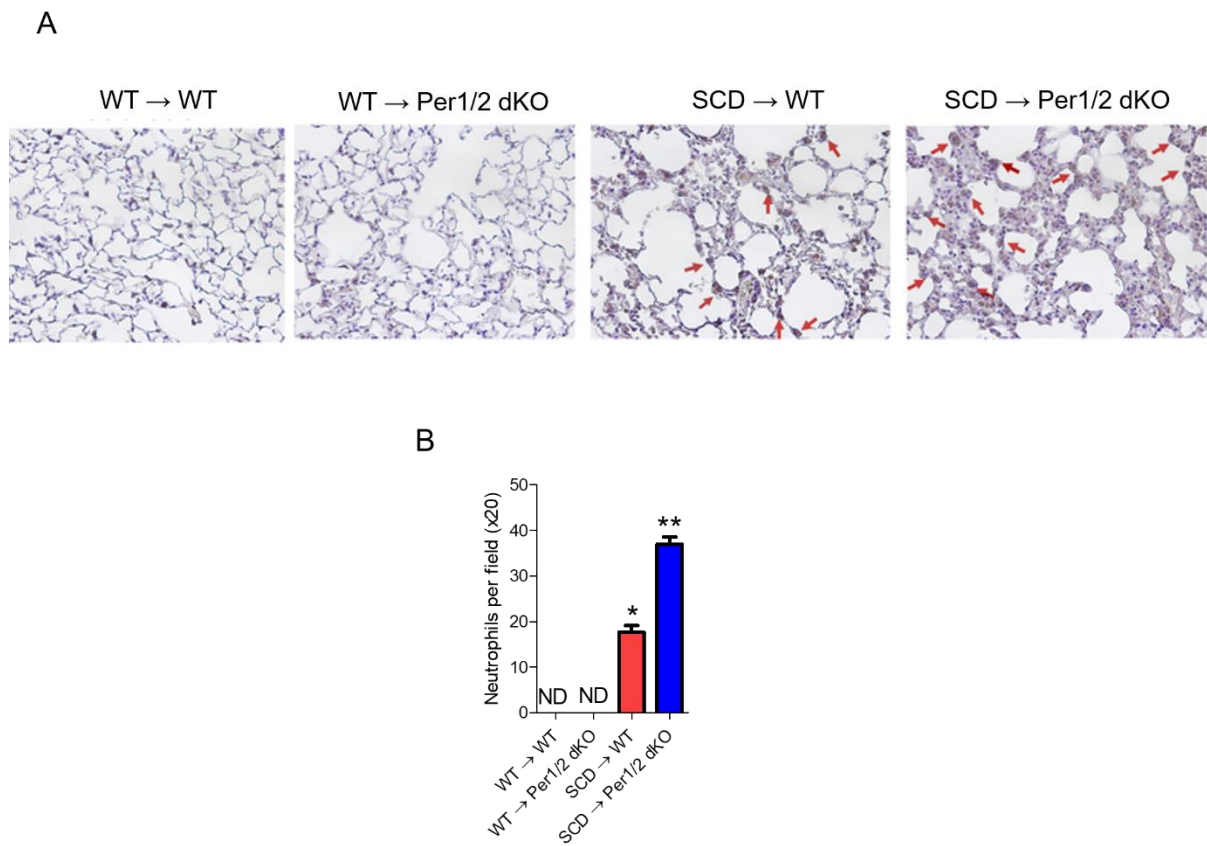


Figure 17. Loss of *Per1/Per2* in SCD contribute to increased pulmonary neutrophil infiltration. (A) Immunohistochemistry images to show Ly6 neutrophil expression in WT→WT, WT → *Per1/Per2* dKO, SCD →WT, and SCD → *Per1/Per2* dKO. Arrows identify presence of neutrophils in the lung vasculature. (B) Images were captured at a 20X objective for counting neutrophils per field. 5 or 6 slides were stained for Ly6 neutrophil marker in WT or SCD transplant groups. For WT →WT and WT → *Per1/Per2* dKO, neutrophils were not detected (ND). *P<0.05, SCD → WT versus WT →WT or WT → *Per1/Per2*dKO; **P<0.05, SCD → WT versus SCD→ *Per1/Per2*dKO.

3.2.5. Genetic deletion of *Per1/Per2* in sickle mice is involved in tissue lung dysfunction as confirmed by further induction of inflammatory Toll-like receptor 4 (*Tlr4*) and *IL-6* gene expression as well as elevated *IL-6* protein levels in bronchoalveolar lavage (BAL) fluid.

In addition to elevated inflammatory cells in the periphery, the presence of neutrophils in the lung indicates that inflammation is further enhanced in *Per1/Per2* deficient sickle mice. To determine whether elevated inflammatory cells in the sickle lung contributes to upregulated inflammatory gene expression, I examined *Tlr4* and *IL-6* mRNA levels to determine whether genes are induced in sickle lung tissue. As

expected, I observed an upregulation of *Tlr4* and *IL-6* mRNA expression in sickle mice compared to control mice (Figure 18 A &B). In fact, I observed further induction of these inflammatory genes in SCD→ *Per1/Per2* *dKO* mice compared to SCD→ WT mice, which indicates that genetic deletion of *Per1/Per2* contributes to this induced inflammatory gene response.

Since I observed further induced *IL-6* mRNA expression in the lung, I validated plasma and systemic IL-6 protein levels in transplanted mice. I measured IL-6 protein levels in BAL fluid isolated extracted from lung, a common technique to diagnose lung damage in mice. In WT BM transplanted mice, I detected ~200 pg/mL of IL-6 protein levels in the lung fluid. In normal mice, this is an acceptable concentration (Figure 17 C). Moreover, in sickle mice, higher levels of IL-6 protein levels were detected, which indicates severe lung dysfunction. In SCD → WT lung, I detected even higher concentration of IL-6 protein levels at ~500 pg/mL (Figure 18 C). In SCD → *Per1/Per2* *dKO* lung, even more IL-6 were detected at ~650 pg/mL (Figure 18 C). Taken together, I conclude that elevated *Tlr4* and *IL-6* inflammatory gene expression and further increase of IL-6 protein levels indicate that genetic deletion of *Per1/Per2* play a role in severe lung dysfunction in SCD mice.

Figure 18

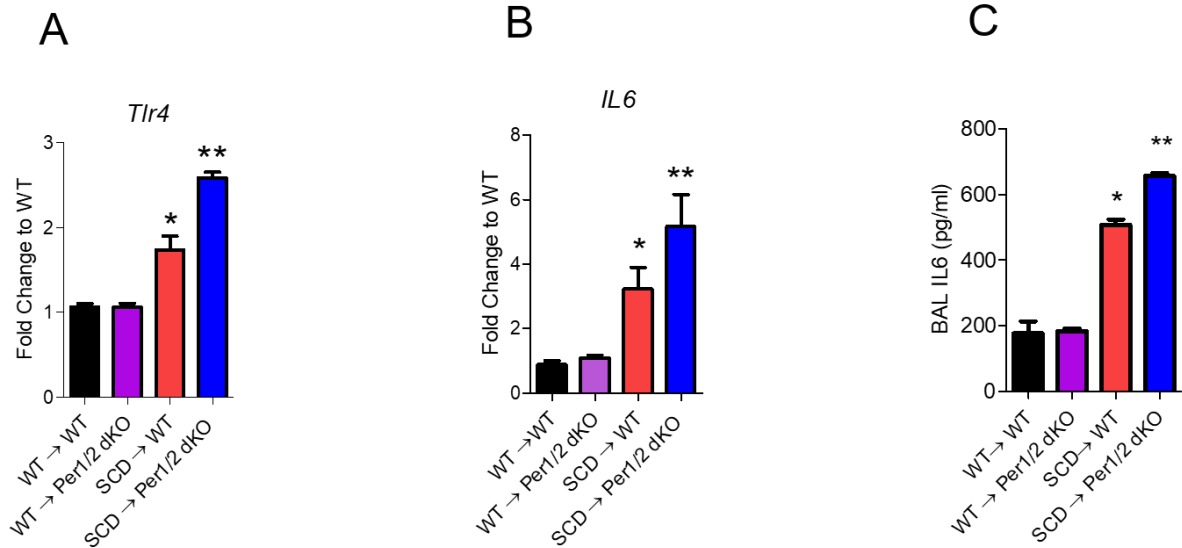


Figure 18. Analysis of *Tlr4* and *IL-6* inflammatory gene expression in lung tissue and *IL-6* protein detection in BAL fluid. Values represent means \pm SEM, *P<0.05, SCD \rightarrow WT versus WT \rightarrow WT or WT \rightarrow *Per1/Per2*dKO; **P<0.01, SCD \rightarrow WT versus SCD \rightarrow *Per1/Per2*dKO.

Since I generated sickle and WT mice with or without *Per1/Per2* deficiency by bone marrow transplantation studies. I speculate that the increased of NEs are BM-derived *Per1^{+/+}/Per2^{+/+}* cells. However, the infiltration of neutrophils to the lung implies a mixed population of cells that are either *Per1^{-/-}/Per2^{-/-}* and *Per1^{+/+}/Per2^{+/+}*. I provide evidence of more lung and liver tissue damage in the sickle mice with *Per1/Per2* deficiency. In addition to this finding, I observed more irradiation damage in sickle phenotypic mice with *Per1/Per2* deficiency, which attributes the importance of *Period* genes in regulating cellular processes required for tissue function. With these observations, I speculate that *Per1/Per2* play a role in regulating systemic inflammation, tissue damage, and dysfunction in SCD.

Chapter 3: Elevated heme and iron levels in sickle mice is mediated by heme oxygenase 1 (HO-1)

This chapter is based on unpublished work by Adebisi MG, Zhao Z, Youqiong Y, Manalo J, Hong Y, Hill R, Gong J, D'Alessandro A, Lee CC, Xian W, McKeon F, Kellems RE, Yoo SH, Han L, and Xia Y.

In this chapter, I will discuss more details as to why sickle mice with *Per1/Per2* deficiency have more severe tissue damage. Since intravascular hemolysis is the cause of multiple tissue dysfunction, I will explore the role of an important enzyme heme oxygenase 1 (HO-1), which mediates heme degradation that contributes to iron release and trafficking to multiple tissues.

3.3.1. Systemic hemolysis mediates heme and iron deposition in lung.

Erythrocyte sickling is the hallmark of SCD. Hemolysis contributes to the release of heme, globin proteins, and iron in the periphery, which can traffic to multiple organs such as the liver. Elevated heme and iron in the organs can promote devastating effects due to increase toxicity that can result in multiple organ dysfunction. Particularly, iron can form dangerous compounds in the presence of reactive oxygen species (ROS), but the mechanism regarding elevated iron in the lungs is not fully understood. To determine whether pulmonary organ dysfunction in sickle mice is due to elevated levels of heme and iron deposition, I performed Perl's Prussian blue iron immunohistochemistry studies to examine local iron content in multiple organs isolated from transplanted mice with WT and SCD phenotype. As expected, I observed more iron in the spleen and liver vasculature in the sickle transplant mice, which indicates that sickling contributes to iron deposition to these organs (Figure 19 A). However, in WT phenotypic transplant mice no increase in iron was observed (Figure 19 A).

I discovered that *Per1/Per2* deficient mice with sickle phenotype expressed more iron in the liver compared to other sickle phenotypic WT transplanted mice (Figure 19 A). I performed analyses to compare iron deposition in the sickle mouse spleen and liver. As revealed from my immunohistological studies, I observed more iron expression in sickle mouse liver with *Per1/Per2* deficiency compared to the other sickle mouse group (Figure 19 B). I did not observe obvious differences in iron levels to the sickle spleens in the WT or *Per1/Per2* deficient sickle mice (Figure 19

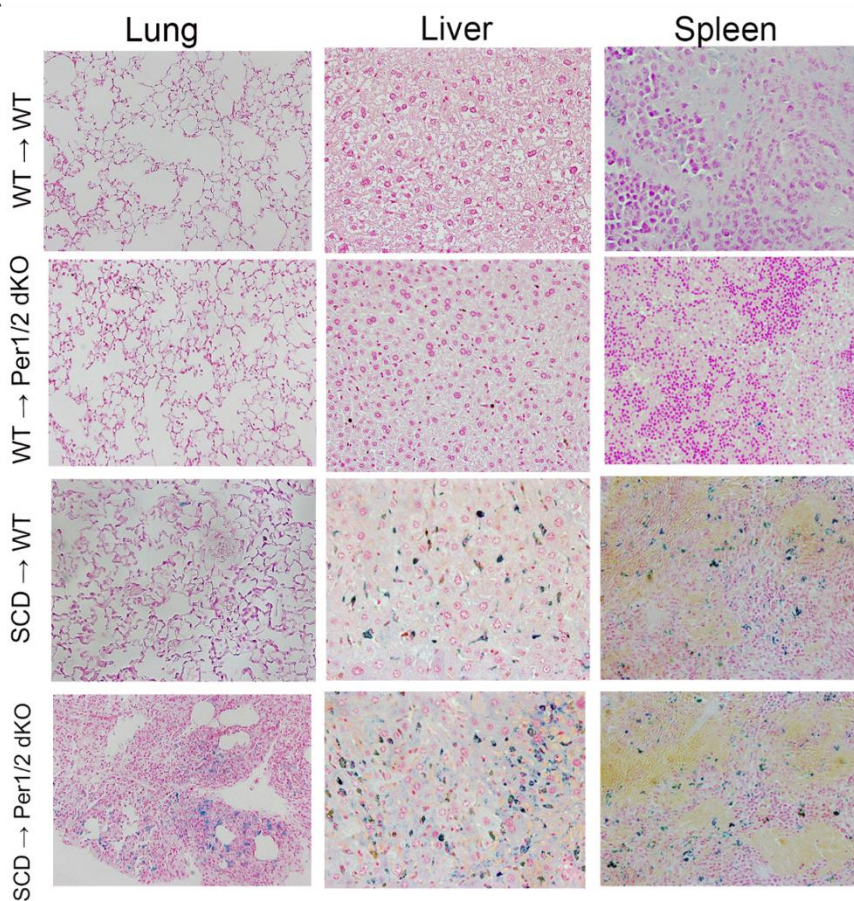
C). As indicated in previous studies, spleen and liver are expected to have more iron since erythrocyte recycling mechanisms take place in these organs. Interestingly, I observed that iron levels can increase in the *Per1/Per2* deficient sickle mouse lung and not in WT sickle mouse lung, which is unexpected (Figure 19 A).

To determine whether elevated heme in the sickle mouse lung contributes to lung dysfunction, I performed biochemical analyses to detect heme levels in WT and sickle lung. As expected, I measured more heme in sickle lung than in the WT lung (Figure 19 D). Interestingly, higher heme was detected in *Per1/Per2* deficient sickle lungs compared to the WT sickle lungs, which indicates that elevated heme content in the lung is associated with the loss of *Per1/Per2* (Figure 19 D).

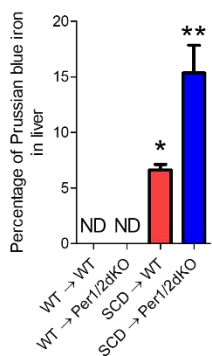
Lastly, heme degradation contributes to generation of iron and bilirubin, products of heme metabolism. Since elevated heme and iron were detected in sickle mice, I measured serum levels of total bilirubin to determine whether chronic hemolysis mediates systemic production of bilirubin release from damaged erythrocytes. As expected, I observed that sickle mice had elevated bilirubin, which was further increased in *Per1/Per2* deficient sickle mice (Figure 19 E). Based on these results, elevated heme, iron, and bilirubin is further induced in *Per1/Per2* deficient sickle mice, which indicates that these dangerous metabolic compounds play a role in multiple organ dysfunction in sickle mice.

Figure 19

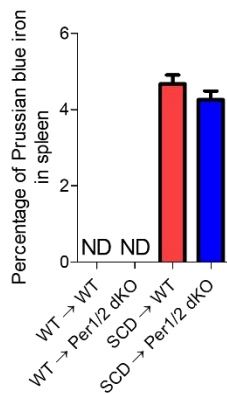
A



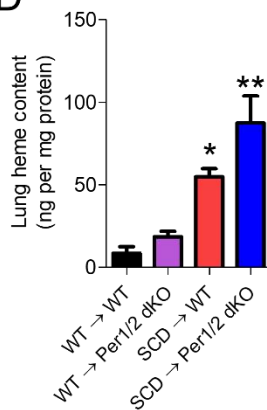
B



C



D



E

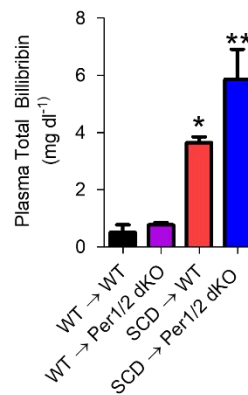


Figure 19. Heme, iron, and bilirubin are increased in sickle mice with *Per1/Per2* deficiency. (A) Perl's Prussian blue iron immunohistochemistry staining of lung, liver, and spleen isolated from WT and SCD phenotypic mice with or without *Per1/Per2* deficiency. (B-C) Semiquantification analyses of liver and spleen. (D) Biochemical detection of heme in the lung. (E) Total serum levels of bilirubin isolated from transplanted mice. Values represented as means \pm SEM, *P<0.05, SCD \rightarrow WT versus WT \rightarrow WT or WT \rightarrow *Per1/Per2* dKO; **P<0.01, SCD \rightarrow WT versus SCD \rightarrow *Per1/Per2* dKO. ND means not detected.

3.3.2. Enhanced heme oxygenase 1 (HO-1) expression in macrophages is required for compensation due to elevated inflammation in SCD lung.

Since systemic hemolysis is evident in sickle mice and contributes to induced heme, iron, and bilirubin levels, I determined whether heme oxygenase 1 (HO-1), which is the enzyme that mediates heme degradation. In sickle mice, HO-1 is widely expressed in multiple cell types including macrophages and endothelial cells, which mediate heme degradation. In fact, further induction of HO-1 is beneficial in SCD due to degradation of heme to generate metabolic products used for essential biological processes such as erythropoiesis.

Although multiple cell types express HO-1 and surprisingly iron deposition was identified in the lung due to the loss of *Per1/Per2* in sickle mice, I determined whether alveolar macrophages express HO-1. As previously shown, I observed iron content that was not widely observed in the *Per1/Per2* deficient sickle mouse lung, therefore, I tested whether alveolar macrophages expressed HO-1 to contribute to iron deposition in the lung. To test this, I isolated WT and SCD mouse lung with or without *Per1/Per2* and performed immunohistochemistry studies. Interestingly, I observed wide distribution of HO-1 expression in sickle mice compared to control mice, which is likely due intravascular sickling events in the organ (Figure 20). In fact, I observed a specific lung vasculature region that distinctly contain HO-1 positive cell types in *Per1/Per2* deficient sickle mice, which confirms that HO-1 mediates heme and iron deposition in these cells (Figure 20). To determine whether macrophages express HO-1, I co-stained lung sections with F4/80, which is a specific macrophage marker. In sickle mice, I observed more F4/80⁺ cells in the

sickle lung, but, I did not observe significant differences in F4/80⁺ expression in WT transplanted mice (Figure 20). Overall, I have observed more HO-1 in lung macrophages in *Per1/Per2* deficient sickle mice.

Figure 20

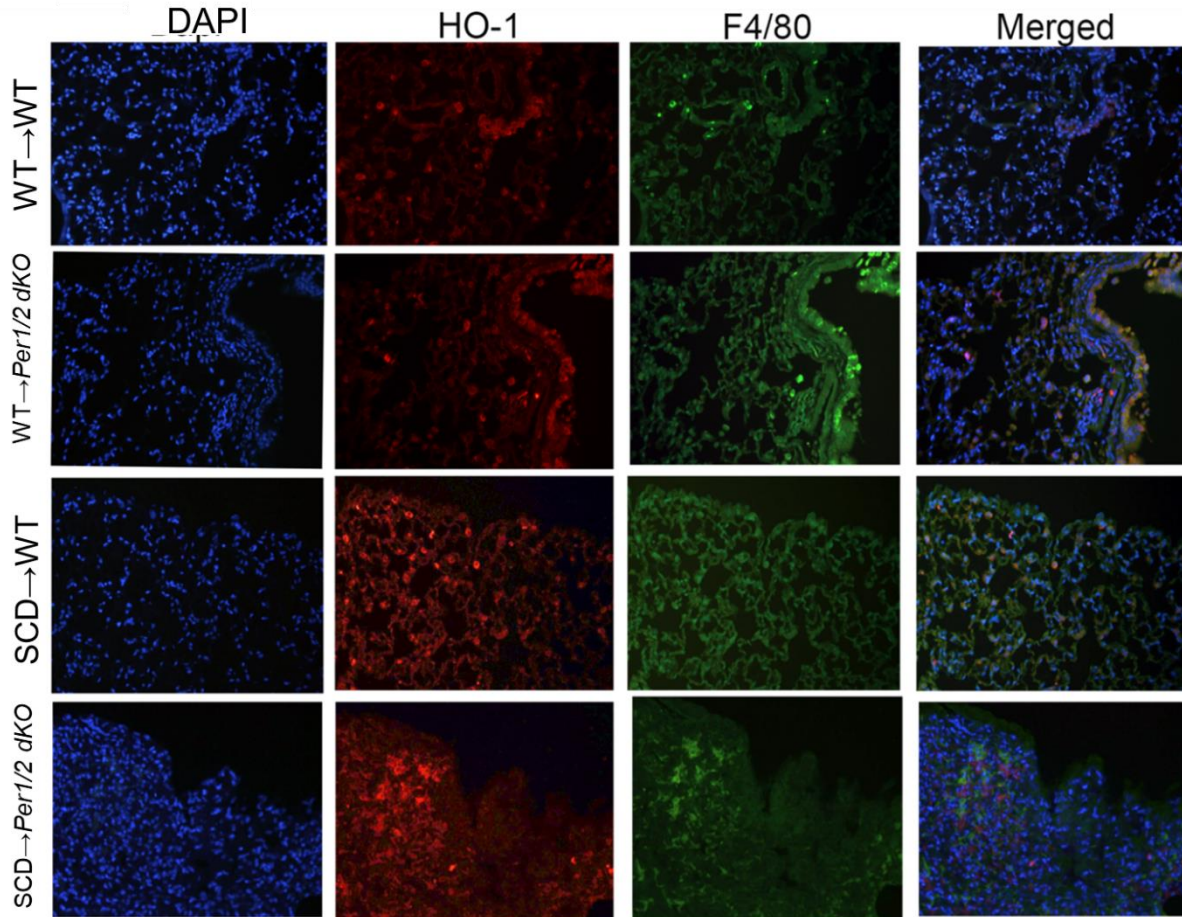


Figure 20. Immunohistochemistry studies reveal HO-1 expression in peripheral lung macrophages. Blue panel show DAPI staining of cellular nuclei, red panel show HO-1, and green panel show F4/80.

Illustration 3

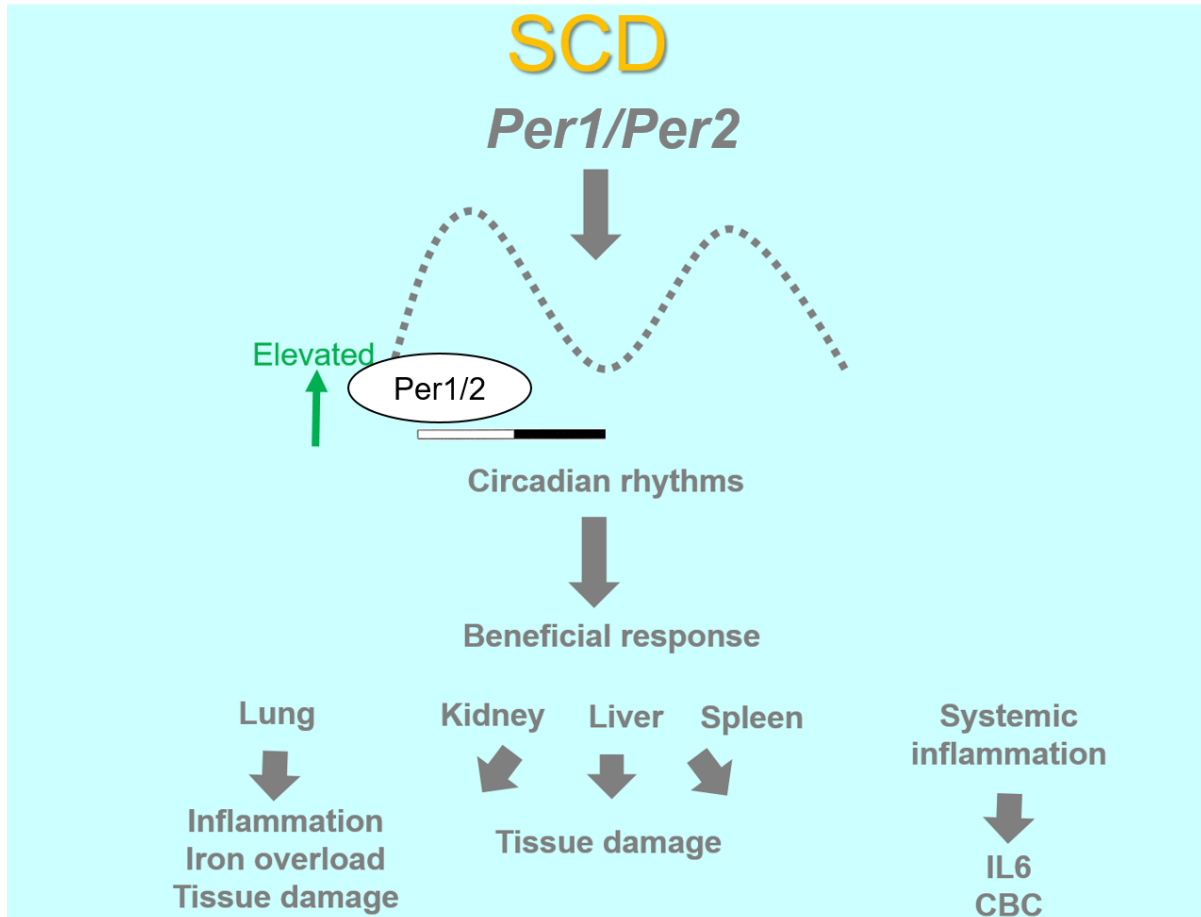


Illustration 3. Summary of unpublished results for chapter 2 and chapter 3. Overall, elevated *Per2* was identified in SCD tissue and has robust circadian rhythmic expression in SCD lung. Additionally, I discovered that when *Per1/Per2* is taken

away this causes further IL-6 levels, iron overload, and further multiple organ damage in SCD.

Systemic hemolysis in SCD contributes to iron and heme deposition in multiple organs. I provide evidence that *Per1/Per2* gene deletion in sickle mice contributes to further heme and iron in multiple organs. Elevated heme and iron can be toxic if not used efficiently for biological processes or if too much heme and iron disrupts overall organ functioning. Based on previous results, I demonstrated that *Per1/Per2* gene deletion contributes to further hepatic dysfunction in sickle mice (Chapter 2). Altered liver metabolism due to increased heme and iron led to further hepatic dysfunction. In the lung, neutrophil infiltration and elevated inflammatory gene expression contribute to tissue damage. Unexpectedly, I discovered elevated levels of iron deposition in the SCD phenotypic *Per1/Per2* deficient lung, which led me to determine whether macrophages either *Per1^{+/+}/Per2^{+/+}* or *Per1^{-/-}/Per2^{-/-}* contributed to iron deposition in the lung. As revealed by my immunohistochemistry studies, I showed that alveolar macrophages in sickle *Per1/Per2* *dKO* mice were also positive for HO-1, which is the enzyme that mediates heme and iron degradation in macrophages. Taken together, I have identified a potential target in macrophages that regulates heme and iron metabolism to promote heme and iron deposition.

IV. Discussion

4.1. Summary of dissertation chapters.

Since elevated SphK1-S1P mediates sickling, hemolysis, and multiple organ damage in SCD. My work addressed how S1P signaling underlines SCD progression. In chapter 1, I discussed how elevated SphK1-S1P production upregulates S1PR1, which can be targeted by FDA-approved drug FTY720. Although targeting S1PR1 does not affect erythrocyte sickling, I discovered that elevated S1PR1 and IL-6 is regulated in a JAK2-dependent manner, which contributes to further multiple tissue damage, systemic inflammation, and tissue dysfunction in SCD. Since multiple organ damage is a severe consequence of SCD patient morbidity and mortality, the mechanism that underlies organ damage is not fully understood. To explore these potential mechanisms, I performed a high throughput unbiased screen, which revealed a series of genes in inflammatory response, heme and iron metabolism, and circadian rhythmic genes. In addition to circadian clock function, *Per1/Per2* genes play a role in organ and cellular function. Therefore, in chapter 2, I discuss how the loss of *Per1/Per2* in SCD contributes to elevated IL-6 to promote systemic inflammation and multiple tissue damage. Furthermore, *Per1/Per2* play a role in heme metabolism. Elevated heme and iron level deposition in SCD can promote organ toxicity. In chapter 3, I discussed how the loss of *Per1/Per2* in SCD contributes to elevated heme deposition in SCD tissue. Due to increase heme content, this can lead to upregulated HO-1 activity, which is required for compensation.

Illustration 4

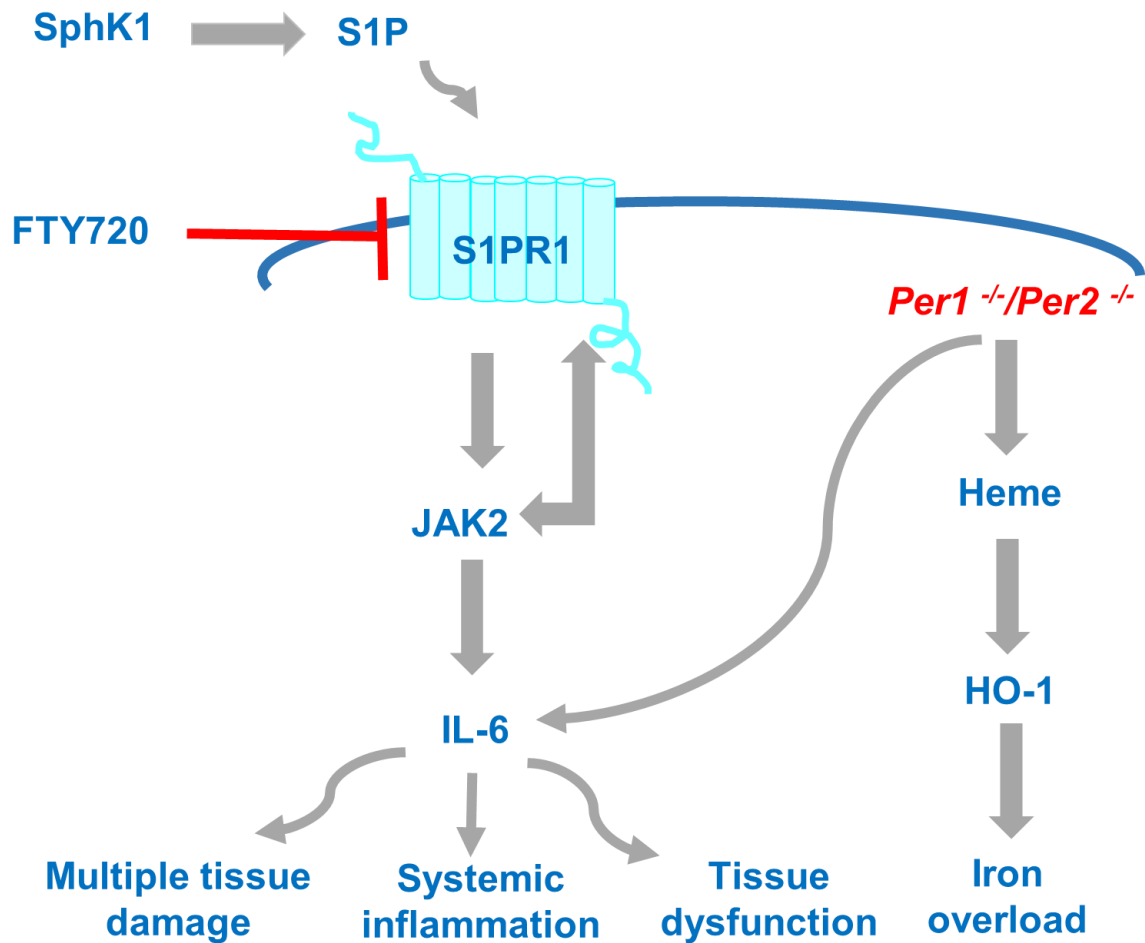


Illustration 4: Summary of dissertation chapters 1-3. In chapter 1, I have identified that elevated S1P-S1PR1 contributes to increase IL-6, which promotes systemic inflammation, multiple tissue damage, and tissue dysfunction. In chapter 2, I discovered that the loss of *Per1/Per2* in SCD contributes to increase IL-6, which

contributes to an increase of multiple tissue damage, systemic inflammation, and tissue dysfunction. In chapter 3, I demonstrated that the loss of *Per1/Per2* in SCD mediates increase heme and iron deposition in multiple organs, which further increases HO-1 activity for compensation.

4.2. Overview of circadian clocks mediating physiological processes in normal and disease conditions.

The circadian clock can regulate physiological processes, such as cardiovascular activity, immunity, hormonal secretion, energy metabolism, and behavior (56-58). Disturbances alter the circadian clock and obstruct multiple processes that are not genetically adaptable and are detrimental (59, 60). Circadian clock synchronizers function to maintain self-sustaining circadian gene oscillation patterns (33). The peripheral clocks are regulated in a diurnal manner, which are not necessarily dependent on environmental light cues (61). Peripheral clocks function independently from the core central clock in the suprachiasmatic nuclei (SCN) located in the hypothalamus. Cells in the SCN are primarily synchronized by external light (62). Multiple cell types in peripheral tissues also orchestrate self-sustaining circadian rhythms that can persist independently of environmental cues, i.e. light (63). Depending on the physiological processes, energy metabolism can be regulated by biological clocks in peripheral organs, such as the pancreas, adrenal glands, and the liver (62). Food consumption is regulated by the circadian clock and functions as a metabolic signal to synchronize rhythms in the liver, but, not in SCN (63, 64). Circadian disturbances and other circadian cycle manipulations, such as

excess light or dim light can restrict feeding, which can obstruct metabolic signals that contribute to disease (65, 66). However, independent of light and metabolic influences, cancer, cardiovascular diseases, and diabetes can result due to endogenous circadian clock defects that promote disease progression (23, 56, 57, 67).

4.3. Heme is a circadian clock regulator.

Metabolites function as signals that regulate circadian clock function (57). These metabolites include heme, glucocorticoids, lipids, insulin, carbohydrates, amino acids, and fatty acids that can function as central and peripheral clock synchronizers (68). For example, glucocorticoids, the steroid hormones, are released from the adrenal glands, but, are regulated by the central clock in the SCN (69). Glucocorticoids are essential for synchronizing rhythms in peripheral organs and have functions in mediating inflammatory responses that contribute to disease (57, 70). Heme is released from erythrocytes and functions to regulate oxygen transport and other biochemical processes. Excess of heme or other metabolites can obstruct proper clock function, which is detrimental (71-73). The biochemical structure of heme contains unique per-arnt-sim (PAS) regions, which function to facilitate ligand binding to receptor, which can mediate signal transduction pathways (74). These heme-PAS domains are ubiquitously expressed including archaea and higher complex eukaryotic species, and have a variety of functions depending on the species (74). Heme-PAS complex can also facilitate transcription of circadian genes such as *Per2*, *Npas2*, *Nr1d1*, and *Nr1d2* (31, 75, 76).

Heme binding to neuronal Per-Arnt-Sim motif 2 (nPAS2) facilitates BMAL1-NPAS2 complex binding to carbon monoxide (CO) sensitive regions on DNA (77). CO suppresses BMAL-NPAS2 binding to promoter regions thus inhibiting transcription of circadian genes, like *Per1/Per2*. Moreover, HO-1 is expressed in a variety of cell types including endothelial and myeloid cells, which function to restore circadian rhythms during tissue injury. In fact, myeloid cells expressing HO-1 confer protection in the brains of subarachnoid hemorrhage (SAH) mice models by suppressing apoptosis (78, 79). It has been demonstrated by pharmacologic inhibition and genetic models that hindering HO-1 activity can alter proper clock function in *Drosophila* and mice (77). When CO production is suppressed this can upregulate BMAL-NPAS2 complex promoting clock gene transcription that can contribute to abnormal glucose metabolism in mouse liver (77). Since complete darkness can function as a metabolic signal in mice (59), a microarray analysis was performed to demonstrate that light pulses in mice kept in darkness can regulate heme and iron metabolic related genes (80). In fact, light exposure functions as a stressor to induce heme oxygenase 2 (HO-2), a homologue to heme oxygenase 1 (HO-1) (80). Other genes discovered from the screen were: Stearoyl-coenzyme A desaturase 1 (SCD1), Ferritin heavy and light chain 1 (FTH and FTL1), Matrix metalloproteinase 11 (MMP11), and Metallothionein1 (MT1) (80). Other detrimental contributions of elevated iron in the tissue includes oxidative stress due to iron oxidation from ferrous to ferric states. Elevated iron increases AMP-activated protein kinase (AMPK) activity thus affecting insulin and glucose signaling in mice (81).

4.4. Pharmacologic induction of heme oxygenase (HO-1) for treating SCD.

Hemin, a ferric protoporphyrin chloride that is a derivative of heme, can alter circadian clock function by obstructing heme transcriptional modulation in cells. Further studies have demonstrated that hemin can be deleterious in cells and mice due to cellular toxicity that affects metabolic functions and pulmonary vaso-occlusive events (72, 73, 82). The mechanism involved requires heme oxygenase-1 (HO-1), which can be induced by heme or hemin. HO-1 is an enzyme that catabolizes heme to generate CO, iron, and biliverdin, which are products of heme degradation (Illustration 5).

Illustration 5

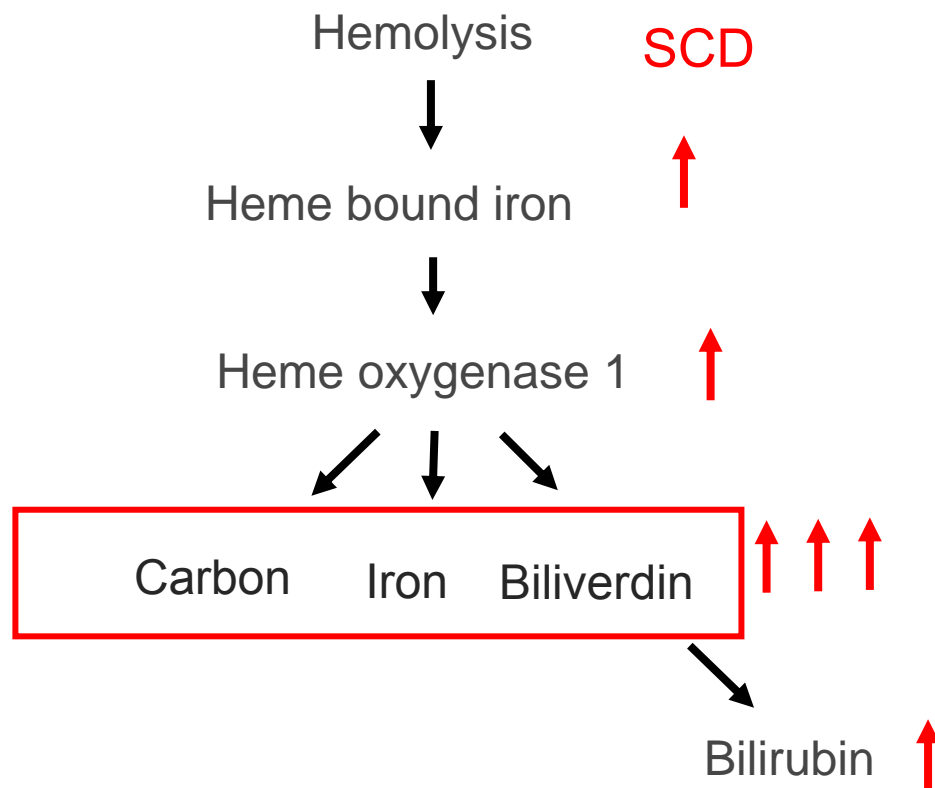


Illustration 5. Mechanism of heme degradation pathway.

Further induction of HO-1-mediating heme degradation is beneficial in SCD. Due to elevated heme content in sickle cell organs, further HO-1 induction is necessary in order to compensate for excess heme, which contributes to vascular inflammation in SCD (83). In SCD, potential therapeutics involving inhaled CO and NO gases to improve vasodilation induce HO-1 expression thus inhibiting stasis in SCD mice. Notably, CO production mediated by HO-1 activity has potent anti-inflammatory and anti-oxidative effects in the vasculature (84). In fact, previous reports have implied that a PEGylated form of hemoglobin saturated with CO gas recognized as MP4CO reduced hypoxia and hemin-induced stasis in SCD mice (85).

HO-1 induction mediates nuclear erythroid factor 2 (Nrf2), which is a transcription factor that regulates HO-1 and other anti-oxidative genes (86). In my study, I discovered that the loss of *Per1/Per2* plays a role in elevated heme and iron deposition in sickle mice, which contributes to further multiple organ damage. I determined whether HO-1 mediates heme and iron degradation in my sickle mice and found that increase of HO-1 expression in *Per1/Per2* deficient sickle mice plays a role in heme and iron deposition in these mice. Thus, I speculate that systemic hemolysis in SCD contributes to release of hemoglobin: haptoglobin (HB:HP) complexes to the circulation. On cellular surfaces of multiple cell types, such as macrophages, contains a CD163, a scavenger hemoglobin receptor, which endocytosis HB:HP complexes from the circulation (87, 88). HB:HP and CD163 receptor gets endocytosed by lysosomes for degradation. Moreover, heme bound iron and globin proteins get released from the lysosomes and HO-1 mediates the

degradation of heme in the cytoplasm. Heme can bind to heme receptors such as BACH 1 or 2 and REV-ER α or REV-ER β located on the nuclear membrane (75). Heme-binding to heme receptors can induce transcription of *Per2* (31). Since iron is released from heme bounded to iron, iron in ferric or ferrous form can be transported within the cell. Elevated iron deposition in organs can be detrimental due to inefficient iron recycling thus causing iron overload as demonstrated in my work. Although, the mechanism that contributes to *Period* genes expression in SCD is still unclear, I hypothesize that elevated heme mediate *Per2* gene expression has a beneficial role in SCD (Illustration 6).

Illustration 6

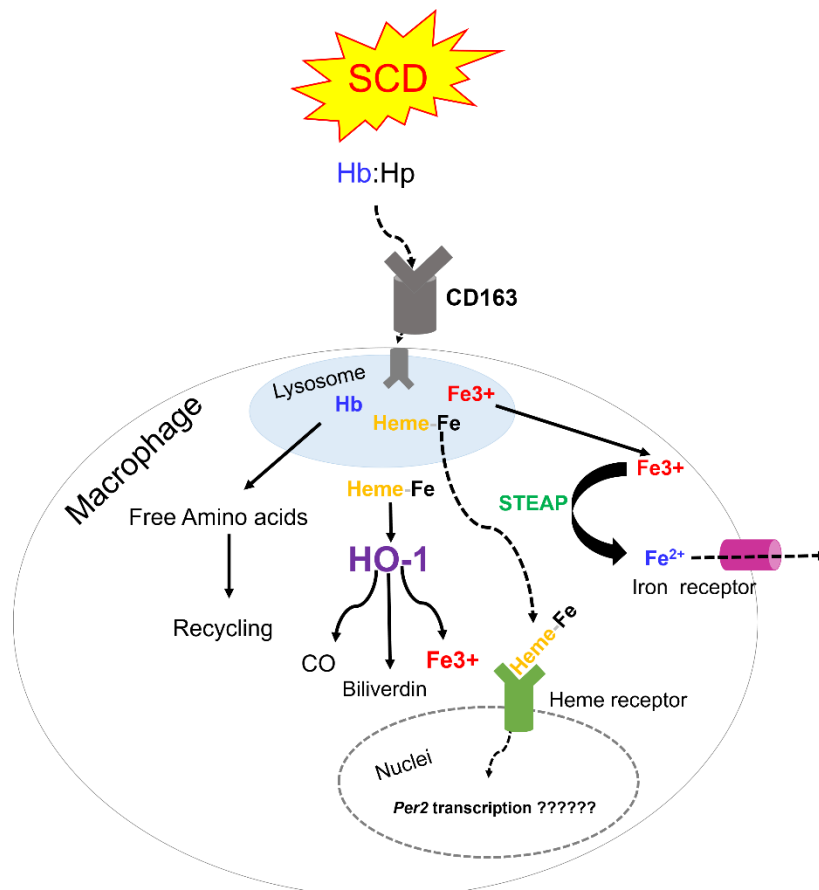


Illustration 6. Possible mechanism involving scavenger CD163 macrophage receptor mediating heme bound iron binding to heme receptors on nuclei to promote Per2 transcription.

Additionally, dimethyl furmate, an agonist for Nrf2 signaling activation, can stimulate a HO-1 response to combat excess heme content in SCD organs (84). One of the functions of dimethyl furmate is to increase fetal hemoglobin (HbF), which reduces HbS polymerization. The chronic administration of dimethyl furmate in SCD mice reduces toxic heme accumulation in local tissues thus reducing heme-mediated inflammatory responses (89). Elevated of HbF in SCD and β -thalassemia can contribute to overall improved conditions in disease (90). In recent years, evidence has indicated that BCL11A protein is a repressor for HbF expression that contributes to elevated HbS polymerization, which mediates hemolytic anemia and end organ damage (91). BCL11A is a transcription factor that is required for B-cell development and expressed in mature erythroid cells (90, 91). In SCD, genetically targeting BCL11A lead to overall improvement in SCD phenotype (91).

4.5. Macrophages induction of HO-1 contribute to iron overload in SCD.

Altered metabolic signals are directly related to molecular clock dysfunction that contribute to cardiovascular, behavioral, endocrine, and immune diseases (10, 11), elevated inflammation in an immune cell dependent manner can result in dampening circadian rhythms that directly affect clock function in diseases such as COPD and inflammatory rheumatoid arthritis (70, 92, 93). In experimental inflammatory conditions, LPS-mediated inflammatory responses can trigger *Per2* gene expression in peripheral blood mononuclear cells (22, 94-96). Additionally, natural killer cells, neutrophils, and macrophages have functional clocks that can be regulated by glucocorticoids and other metabolic signals (39, 97-101). In fact, infiltrating macrophages upregulate transcription of *Per1*, *Per2*, and *N1rd1* circadian gene expression, which can promote inflammatory responses that contribute to tissue destruction (12-14). Although altered metabolic signals in immune cells are directly related to molecular clock dysfunction, this can contribute to abnormal secretion of interleukin 6 (IL-6), tumor necrosis factor alpha (TNF α), chemokine- (C-C motif) ligand 2 (CCL2), interferon gamma (INF γ), prostaglandins E2 (PGE2), and toll-like receptor 9 (TLR9) signaling in macrophages (36, 102-106).

Additionally, macrophages express HO-1, to support a variety of physiological processes that involve heme detoxification and iron recycling required for erythropoiesis. Hemoglobin-haptoglobin (HB-HP) is a complex that induces HO-1 activity in macrophages (87). CD163 is a scavenger receptor expressed on macrophages, which facilitates the uptake of HB-HP complexes via an endocytosis-dependent manner (88, 107, 108). Moreover, heme released from hemoglobin can mediate HO-1 induction in macrophages by upregulating ferroportin (FPN), an iron

transport, to regulate iron metabolism (109). In addition, elevated expression of ferritin, an iron storage protein is mediated by CD163 receptor, which is beneficial for combating iron overload (110).

HO-1 induction in macrophages can have beneficial roles in disease. Excess iron is toxic to the cell due to generation of ROS mediated by Fenton and Harber Weiss reactions that can promote DNA damage, lipid peroxidation, and cross-linking of proteins (111, 112). Furthermore, elevated heme can mediate TLR4 signaling, which can induce the expression of inflammatory cytokines like IL-6 and TNF- α in SCD mice (113, 114).

Sickle mice with biological clock dysfunction have a mixed population of cell types. BM-derived cells that are *Per1^{+/+}/Per2^{+/+}* whereas the peripheral cells in resident tissues are *Per1^{-/-}/Per2^{-/-}*. With this possibility, macrophages expressing HO-1 has a mixed morphology, which may have diverse roles in disease such as M1 or M2 macrophages, which have pro-inflammatory or anti-inflammatory functions in disease (Illustration 7). Taken together, I conclude that elevated HO-1 in macrophages contributes to heme and iron deposition to promote multiple organ dysfunction in sickle mice (Illustration 7).

Illustration 7

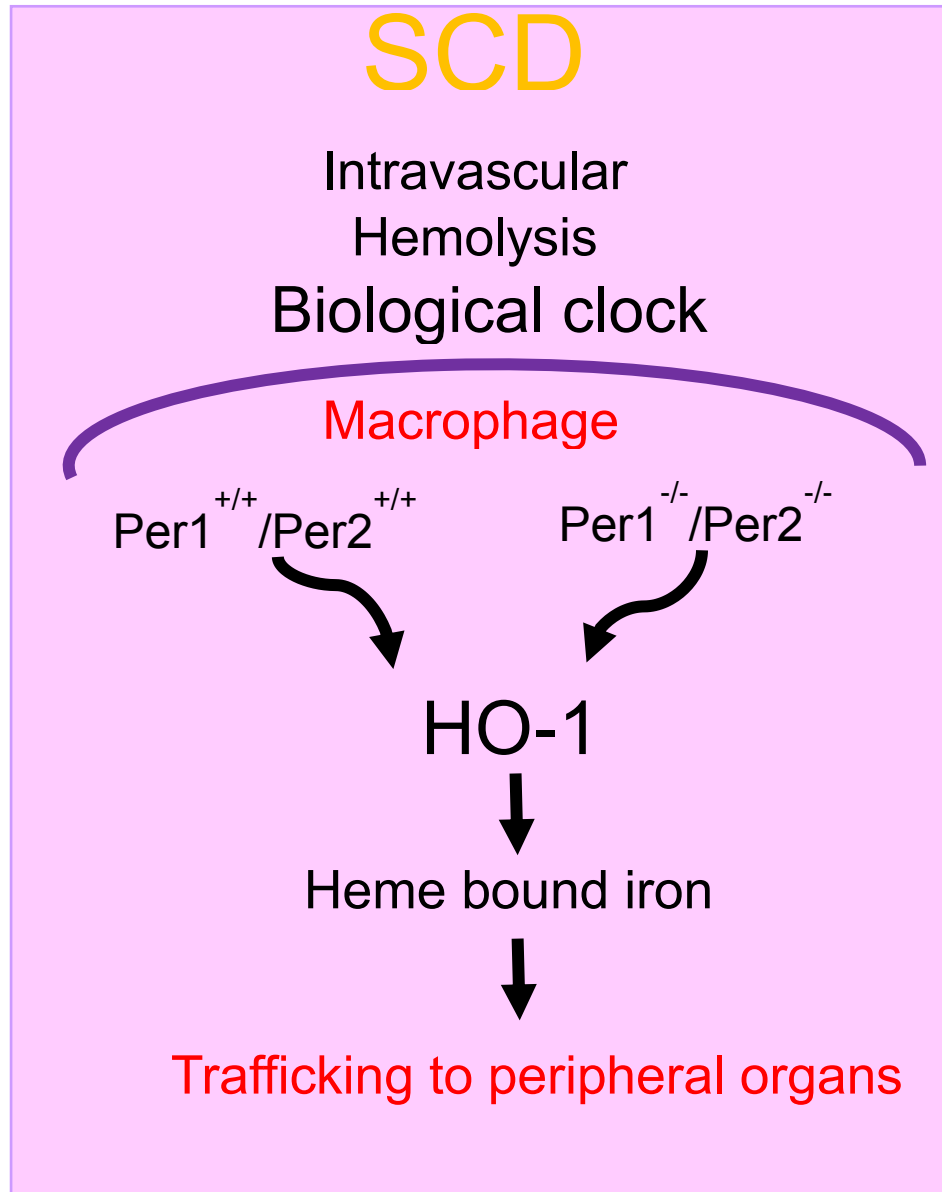


Illustration 7. Mixed cell populations that are BM-derived $Per1^{+/+}/Per2^{-/-}$ and resident $Per1^{-/-}/Per2^{-/-}$ express HO-1, which regulates heme degradation in macrophages.

4.6. Elevated adenosine-mediate ADORA2B activation to promote Per2 induction, which improves disease severity.

Circadian dysfunction contributes to metabolic defects that can promote energy imbalance in the animal (115). In SCD, metabolic changes in the erythrocytes contribute to poor oxygen release and further sickling (13, 116, 117). Metabolite precursors such as adenosine can facilitate 2,3-DPG induction, an allosteric modulator, that prompts oxygen release from hemoglobin (13). Adenosine is derived from adenosine triphosphate (ATP), a nucleoside with three triphosphate groups that regulates energy metabolism. Elevated extracellular adenosine signals via four G-protein coupled receptors that are ubiquitously expressed in a variety of cell types, including epithelial cells, immune cells, and erythrocytes (41). Amongst the four G-protein coupled receptors, ADORA2B has the lowest affinity for adenosine, which is activated due to excess accumulation of extracellular adenosine. In the erythrocytes, elevated adenosine mediated activation of ADORA2B receptor facilitates glycolytic pathways that function in oxygen release. Adenosine signaling via ADORA2B activation has known beneficial roles in hypoxia adaptation under normal conditions (118, 119). However, in inflammatory pulmonary disease and in SCD, elevated adenosine-mediated ADORA2B activation is detrimental and contributes to further disease progression (13, 118, 120). In fact, elevated adenosine mediated ADORA2B activation contributes to further PER2 induction in cardiomyocytes. Further PER2 induction is regulated by upstream

enhancer elements that promote transcription of hypoxia-related genes, such as *hypoxia inducible factor alpha (Hif1 α)* during hypoxic events (121).

Hypoxia is a dangerous condition, in which, systemic deprivation of oxygen can result in inflammatory responses and end organ damage (122, 123). HIF subunits HIF1 α and HIF1 β (also known as BMAL), are key components of hypoxia signaling. Hypoxia can drive glycolytic processes and further contribute to metabolic disease (124). PER2 induction mediated by ADORA2B signaling can regulate glycolytic processes in a HIF1 α dependent manner during ischemic-reperfusion injury (25). Glucocorticoids can mediate PER2 induction to promote clock function (92). In SCD, chronic hypoxia occurs due to systemic oxygen release from hemoglobin S (HbS) mediating sickling (17). In fact, further sickling is regulated by sphingosine kinase 1 (SphK1) in erythrocytes regulated in an adenosine-ADORA2B dependent manner (14). Due to oxygen release events, deoxy-hemoglobin S (deoxy-HbS) forms insoluble polymers that results in enhanced polymerization to promote vaso-occlusion and tissue damage in SCD (117). In the normal setting, SphK1-mediate S1P production contributes to 2, 3-DPG induction in erythrocytes, which plays a role in hypoxia adaptation in individuals at high-altitude (125). In SCD, elevated SphK1-S1P production in erythrocytes mediates sickling and end organ damage (14). Overall, the role of hypoxia contributing to further sickling is known; however, it is still uncertain whether hypoxia-mediate HIF1 α is regulated by further PER2 induction in the periphery to promote SCD progression.

4.7. Evidence of oxidative-reductive stress in sickle lung tissue.

Hypoxia plays a role in the pathophysiological impact of oxidative stress (119, 120), collagen formation (121, 122), mitochondria dysfunction (123), and inflammation (124) in the lung. Hypoxia mediates erythrocyte sickling and further progression of SCD; however, the role of induced erythrocyte sickling and subsequently heme and iron trafficking to organs remains unclear. As a part of my dissertation studies, I determined whether molecular clock dysfunction mediated by the loss of *Per1/Per2* in sickle mice plays a role in lung dysfunction. I have preliminary evidence that indicates that oxidative-reductive process genes are differentially expressed in the sickle lung with *Per1/Per2* deficiency. These results were generated by an unbiased mRNA sequencing of lung tissue isolated from SCD or WT phenotypic mice with or without *Per1/Per2*. Amongst these RNA transcripts detected in sickle lung were: *Procollagen-lysine, 2-oxoglutarate 5-dioxygenase 1 (Plod1)*, *Malic enzyme 3, NADP (+)-dependent mitochondrial (Me3)*, *Apoptosis inducing factor, (mitochondria associated 2) (Aifm2)*, *Malate dehydrogenase 2, NAD (mitochondrial) (Mdh2)*, *NADPH oxidase 1 (Nox1)*, *Lysyl oxidase-like 4 (Loxl4)*, and *Deiodinase, iodothyronine, type I (Dio1)* (Illustration 8A). Upregulated mRNA levels were *Plod1*, *Me3*, *Aifm2*, and *Mdh2* in *Per1/Per2* deficient sickle mouse lung (Illustration 8A).

Further, I also identified several genes that were upregulated in *Per1/Per2* deficient transplant mouse lung compared to WT transplanted lung. WT → *Per1/Per2* dKO lungs were normalized WT → WT lungs. Amongst the transcripts detected were *Prolyl 4-hydroxylase subunit alpha 3 (P4ha3)*, *Biliverdin reductase A (Blvra)*, *Peptidylglycine alpha-amidating monooxygenase (Pam)*, *Dihydrouridine*

synthase 3 like (Dus3l), Acyl-CoA dehydrogenase family member 8 (Acad8), Methionine sulfoxide reductase B2 (Msrb2), Delta(4)-desaturase, sphingolipid 1 (Degs1), Cytochrome P450 family 1 subfamily A member 1 (Cyp1a1) , Protoporphyrinogen oxidase (Ppox), malic enzyme 1, NADP(+)-dependent (Me1), Cytochrome P450, family 26, subfamily b, polypeptide 1 (Cyp26b1), D-2-hydroxyglutarate dehydrogenase (D2hgdh), Acyl-Coenzyme A oxidase-like (Acox1), Scavenger receptor CD163 (Cd163), and Interferon activated gene 202B (Ifi202b) (Illustration 8B). Interestingly, upregulated mRNA expression of *P4ha3, Blvra, Pam, Cd163 and Ifi202b*, was identified in WT→ *Per1/Per2 dKO* mice (Illustration 8B). Specifically, *Blvra* and *CD163* have roles in regulating heme-iron metabolism (20, 126).

Illustration 8

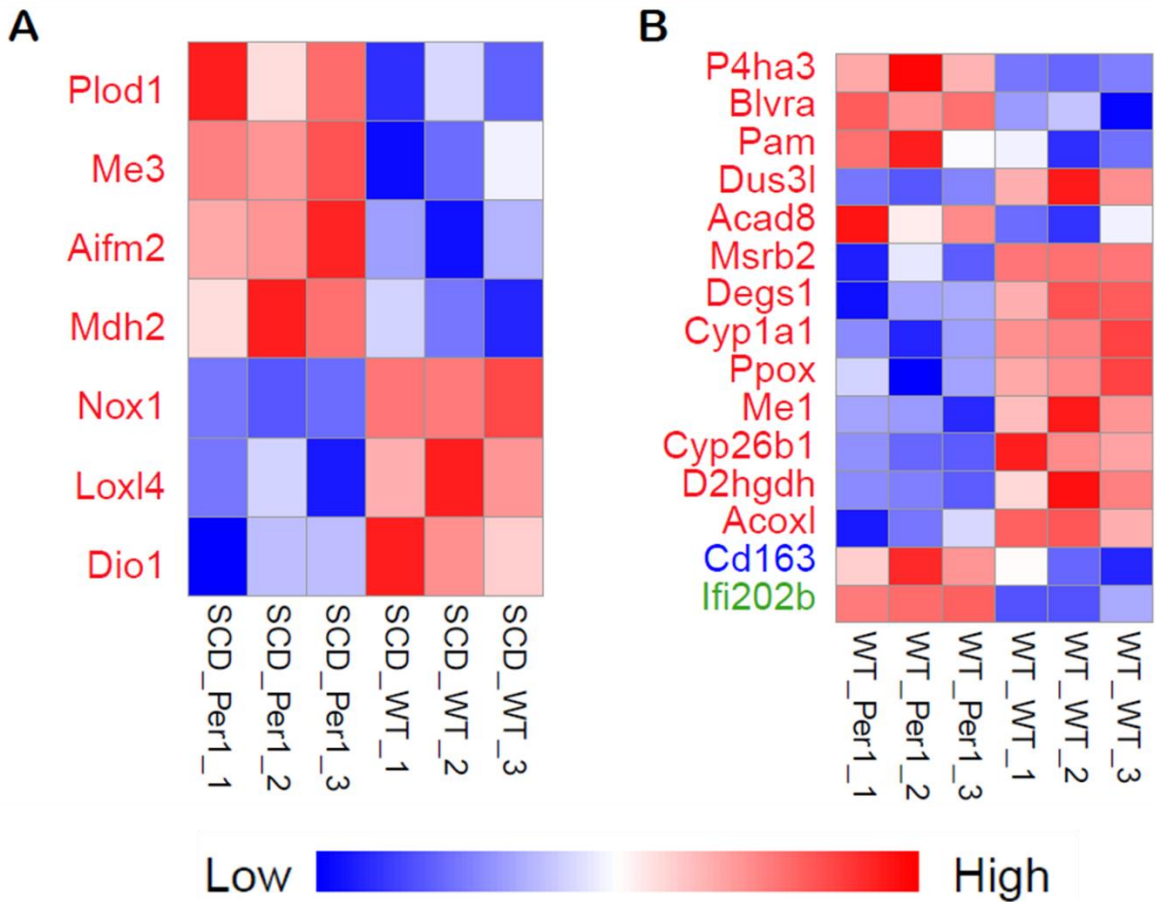


Illustration 8. Differential expression of oxidative-reductive genes identified in mRNA sequencing of the lung isolated from SCD or WT BM transplant mice with or without *Per1/Per2*. $P < 0.05$ cut off score was used to determine significance of genes. Upregulated genes were indicated as red and downregulated genes were

indicated as blue. Analyses revealed differential gene expression in SCD → WT compared to SCD → *Per1/Per2* dKO or WT → WT or WT → *Per1/Per2* dKO mice.

4.8. Future directions.

Oxidative stress, reactive oxidative species, and reduced anti-oxidative responses in SCD can be regulated by *Per 2*. Future directions include performing metabolomics arrays to identify molecular clock functions at the cellular level in my WT and SCD transplanted mice. Since I transplanted SCD or WT bone marrow (BM) to irradiated *Per1/Per2* dKO mice, it is likely that heterogeneous populations of cell types exist in the SCD and WT BM transplant mice due to *Per1/Per2* positive BM-derived cells that are expressed in the periphery. BM cells can differentiate to myeloid, lymphoid, and erythroid progenitor cell lineages that would be *Per1/Per2* positive. These circulating cells can then infiltrate multiple organs causing mixed populations of cells. Since a function of molecular clocks is to regulate metabolism, it would be important to explore metabolic pathways in our SCD and WT BM transplant mice.

Peripheral clocks regulate oxidative stress pathways to promote glutathione (GSH) synthesis and other anti-oxidative responses in *Drosophila* and mammals (127, 128). GSH is a potent anti-oxidant that is circadian regulated. In *Drosophila*, GSH is circadian regulated in WT flies, but, abolished in *Per* mutant flies (127). Thus it will be important to determine whether sickle *Per1/Per2* dKO mice have abnormal metabolic lung profile compare to sickle BM transplanted to WT mice.

At the cellular level, erythrocytes, fibroblasts, immune cells, and liver cells express circadian patterns of anti-oxidant proteins such as peroxiredoxins, which are essential for combating ROS (50, 51). As part of my future studies, I will like to conduct single cell metabolomics by purifying macrophages from peripheral tissues and BM cells isolated from sickle BM transplant mice groups. I am interested to investigate whether elevated presence of ROS in *Per1/Per2* dKO– sickle BM transplant mice results in unique changes in their metabolic profile from BM-derived cells compared to tissue macrophages.

Lastly, heme and iron overload is a serious debilitating condition that can occur due to chronic transfusions in patients with severe hemolytic anemia such as SCD and β -thalassemia. There are two FDA-approved drugs, deferoxamine and deferasirox, which are iron chelators used in the clinic to treat iron overload. Since transplant SCD BM mice express excess iron in peripheral organs, future investigations could be to determine whether these pharmacologic tools can be beneficial for reducing iron levels in *Per1/Per2* dKO sickle mice.

V. References

1. Herrick, J. B. (2001) Peculiar elongated and sickle-shaped red blood corpuscles in a case of severe anemia. 1910. *Yale J Biol Med* **74**, 179-184
2. Pauling, L. (1964) Molecular Disease and Evolution. *Bull N Y Acad Med* **40**, 334-342
3. Pauling, L., Itano, H. A., and et al. (1949) Sickle cell anemia a molecular disease. *Science* **110**, 543-548
4. Ingram, V. M. (1956) A specific chemical difference between the globins of normal human and sickle-cell anaemia haemoglobin. *Nature* **178**, 792-794
5. Ingram, V. M. (1959) Abnormal human haemoglobins. III. The chemical difference between normal and sickle cell haemoglobins. *Biochim Biophys Acta* **36**, 402-411
6. Steiner, C. A., and Miller, J. L. (2006) Sickle Cell Disease Patients in U.S. Hospitals, 2004: Statistical Brief #21. In *Healthcare Cost and Utilization Project (HCUP) Statistical Briefs*, Rockville (MD)
7. Piel, F. B., Hay, S. I., Gupta, S., Weatherall, D. J., and Williams, T. N. (2013) Global burden of sickle cell anaemia in children under five, 2010-2050: modelling based on demographics, excess mortality, and interventions. *PLoS Med* **10**, e1001484
8. Fitzhugh, C. D., Lauder, N., Jonassaint, J. C., Telen, M. J., Zhao, X., Wright, E. C., Gilliam, F. R., and De Castro, L. M. (2010) Cardiopulmonary

- complications leading to premature deaths in adult patients with sickle cell disease. *Am J Hematol* **85**, 36-40
9. Reiter, C. D., Wang, X., Tanus-Santos, J. E., Hogg, N., Cannon, R. O., 3rd, Schechter, A. N., and Gladwin, M. T. (2002) Cell-free hemoglobin limits nitric oxide bioavailability in sickle-cell disease. *Nat Med* **8**, 1383-1389
 10. Nath, K. A., and Katusic, Z. S. (2012) Vasculature and kidney complications in sickle cell disease. *J Am Soc Nephrol* **23**, 781-784
 11. Koduri, P. R. (2003) Iron in sickle cell disease: a review why less is better. *Am J Hematol* **73**, 59-63
 12. Zhang, Y., Berka, V., Song, A., Sun, K., Wang, W., Zhang, W., Ning, C., Li, C., Zhang, Q., Bogdanov, M., Alexander, D. C., Milburn, M. V., Ahmed, M. H., Lin, H., Idowu, M., Zhang, J., Kato, G. J., Abdulmalik, O. Y., Zhang, W., Dowhan, W., Kellems, R. E., Zhang, P., Jin, J., Safo, M., Tsai, A. L., Juneja, H. S., and Xia, Y. (2014) Elevated sphingosine-1-phosphate promotes sickling and sickle cell disease progression. *J Clin Invest* **124**, 2750-2761
 13. Zhang, Y., Dai, Y., Wen, J., Zhang, W., Grenz, A., Sun, H., Tao, L., Lu, G., Alexander, D. C., Milburn, M. V., Carter-Dawson, L., Lewis, D. E., Zhang, W., Eltzschig, H. K., Kellems, R. E., Blackburn, M. R., Juneja, H. S., and Xia, Y. (2011) Detrimental effects of adenosine signaling in sickle cell disease. *Nat Med* **17**, 79-86
 14. Sun, K., Zhang, Y., Bogdanov, M. V., Wu, H., Song, A., Li, J., Dowhan, W., Idowu, M., Juneja, H. S., Molina, J. G., Blackburn, M. R., Kellems, R. E., and Xia, Y. (2015) Elevated adenosine signaling via adenosine A2B receptor

- induces normal and sickle erythrocyte sphingosine kinase 1 activity. *Blood* **125**, 1643-1652
15. Aktas, O., Kury, P., Kieseier, B., and Hartung, H. P. (2010) Fingolimod is a potential novel therapy for multiple sclerosis. *Nat Rev Neurol* **6**, 373-382
 16. Rees, D. C., and Gibson, J. S. (2012) Biomarkers in sickle cell disease. *Br J Haematol* **156**, 433-445
 17. Sun, K., and Xia, Y. (2013) New insights into sickle cell disease: a disease of hypoxia. *Curr Opin Hematol* **20**, 215-221
 18. Xu, H., Wandersee, N. J., Guo, Y., Jones, D. W., Holzhauer, S. L., Hanson, M. S., Machogu, E., Brousseau, D. C., Hogg, N., Densmore, J. C., Kaul, S., Hillery, C. A., and Pritchard, K. A., Jr. (2014) Sickle cell disease increases high mobility group box 1: a novel mechanism of inflammation. *Blood* **124**, 3978-3981
 19. Andemariam, B., Adami, A. J., Singh, A., McNamara, J. T., Secor, E. R., Guernsey, L. A., and Thrall, R. S. (2015) The sickle cell mouse lung: proinflammatory and primed for allergic inflammation. *Transl Res* **166**, 254-268
 20. Thomsen, J. H., Etzerodt, A., Svendsen, P., and Moestrup, S. K. (2013) The haptoglobin-CD163-heme oxygenase-1 pathway for hemoglobin scavenging. *Oxid Med Cell Longev* **2013**, 523652
 21. Stuart, M. J., and Setty, B. N. (1999) Sickle cell acute chest syndrome: pathogenesis and rationale for treatment. *Blood* **94**, 1555-1560

22. Liu, J., Malkani, G., Shi, X., Meyer, M., Cunningham-Runddles, S., Ma, X., and Sun, Z. S. (2006) The circadian clock Period 2 gene regulates gamma interferon production of NK cells in host response to lipopolysaccharide-induced endotoxic shock. *Infect Immun* **74**, 4750-4756
23. Fu, L., Pelicano, H., Liu, J., Huang, P., and Lee, C. (2002) The circadian gene Period2 plays an important role in tumor suppression and DNA damage response in vivo. *Cell* **111**, 41-50
24. Wang, J., Morita, Y., Han, B., Niemann, S., Loffler, B., and Rudolph, K. L. (2016) Per2 induction limits lymphoid-biased haematopoietic stem cells and lymphopoiesis in the context of DNA damage and ageing. *Nat Cell Biol* **18**, 480-490
25. Eckle, T., Hartmann, K., Bonney, S., Reithel, S., Mittelbronn, M., Walker, L. A., Lowes, B. D., Han, J., Borchers, C. H., Buttrick, P. M., Kominsky, D. J., Colgan, S. P., and Eltzschig, H. K. (2012) Adora2b-elicited Per2 stabilization promotes a HIF-dependent metabolic switch crucial for myocardial adaptation to ischemia. *Nat Med* **18**, 774-782
26. Konopka, R. J., and Benzer, S. (1971) Clock mutants of *Drosophila melanogaster*. *Proc Natl Acad Sci U S A* **68**, 2112-2116
27. Hardin, P. E., Hall, J. C., and Rosbash, M. (1990) Feedback of the *Drosophila* period gene product on circadian cycling of its messenger RNA levels. *Nature* **343**, 536-540

28. Bae, K., Jin, X., Maywood, E. S., Hastings, M. H., Reppert, S. M., and Weaver, D. R. (2001) Differential functions of mPer1, mPer2, and mPer3 in the SCN circadian clock. *Neuron* **30**, 525-536
29. Zheng, B., Larkin, D. W., Albrecht, U., Sun, Z. S., Sage, M., Eichele, G., Lee, C. C., and Bradley, A. (1999) The mPer2 gene encodes a functional component of the mammalian circadian clock. *Nature* **400**, 169-173
30. Zheng, B., Albrecht, U., Kaasik, K., Sage, M., Lu, W., Vaishnav, S., Li, Q., Sun, Z. S., Eichele, G., Bradley, A., and Lee, C. C. (2001) Nonredundant roles of the mPer1 and mPer2 genes in the mammalian circadian clock. *Cell* **105**, 683-694
31. Kaasik, K., and Lee, C. C. (2004) Reciprocal regulation of haem biosynthesis and the circadian clock in mammals. *Nature* **430**, 467-471
32. Cermakian, N., Monaco, L., Pando, M. P., Dierich, A., and Sassone-Corsi, P. (2001) Altered behavioral rhythms and clock gene expression in mice with a targeted mutation in the Period1 gene. *EMBO J* **20**, 3967-3974
33. Ko, C. H., and Takahashi, J. S. (2006) Molecular components of the mammalian circadian clock. *Hum Mol Genet* **15 Spec No 2**, R271-277
34. Haus, E., and Smolensky, M. H. (1999) Biologic rhythms in the immune system. *Chronobiol Int* **16**, 581-622
35. Keller, M., Mazuch, J., Abraham, U., Eom, G. D., Herzog, E. D., Volk, H. D., Kramer, A., and Maier, B. (2009) A circadian clock in macrophages controls inflammatory immune responses. *Proc Natl Acad Sci U S A* **106**, 21407-21412

36. Silver, A. C., Arjona, A., Walker, W. E., and Fikrig, E. (2012) The circadian clock controls toll-like receptor 9-mediated innate and adaptive immunity. *Immunity* **36**, 251-261
37. Chen, Y. G., Mantalaris, A., Bourne, P., Keng, P., and Wu, J. H. (2000) Expression of mPer1 and mPer2, two mammalian clock genes, in murine bone marrow. *Biochem Biophys Res Commun* **276**, 724-728
38. Boivin, D. B., James, F. O., Wu, A., Cho-Park, P. F., Xiong, H., and Sun, Z. S. (2003) Circadian clock genes oscillate in human peripheral blood mononuclear cells. *Blood* **102**, 4143-4145
39. Bollinger, T., Leutz, A., Leliavski, A., Skrum, L., Kovac, J., Bonacina, L., Benedict, C., Lange, T., Westermann, J., Oster, H., and Solbach, W. (2011) Circadian clocks in mouse and human CD4+ T cells. *PLoS One* **6**, e29801
40. Hu, X., Adebisi, M. G., Luo, J., Sun, K., Le, T. T., Zhang, Y., Wu, H., Zhao, S., Karmouty-Quintana, H., Liu, H., Huang, A., Wen, Y. E., Zaika, O. L., Mamenko, M., Pochynyuk, O. M., Kellems, R. E., Eltzschig, H. K., Blackburn, M. R., Walters, E. T., Huang, D., Hu, H., and Xia, Y. (2016) Sustained Elevated Adenosine via ADORA2B Promotes Chronic Pain through Neuro-immune Interaction. *Cell Rep* **16**, 106-119
41. Karmouty-Quintana, H., Xia, Y., and Blackburn, M. R. (2013) Adenosine signaling during acute and chronic disease states. *J Mol Med (Berl)* **91**, 173-181
42. Yoo, S. H., Yamazaki, S., Lowrey, P. L., Shimomura, K., Ko, C. H., Buhr, E. D., Siepk, S. M., Hong, H. K., Oh, W. J., Yoo, O. J., Menaker, M., and

- Takahashi, J. S. (2004) PERIOD2::LUCIFERASE real-time reporting of circadian dynamics reveals persistent circadian oscillations in mouse peripheral tissues. *Proc Natl Acad Sci U S A* **101**, 5339-5346
43. Zhao, S., Adebiji, M. G., Zhang, Y., Couturier, J. P., Fan, X., Zhang, H., Kellems, R. E., Lewis, D. E., and Xia, Y. (2018) Sphingosine-1-phosphate receptor 1 mediates elevated IL-6 signaling to promote chronic inflammation and multitissue damage in sickle cell disease. *FASEB J*, fj201600788RR
44. He, B., Nohara, K., Park, N., Park, Y. S., Guillory, B., Zhao, Z., Garcia, J. M., Koike, N., Lee, C. C., Takahashi, J. S., Yoo, S. H., and Chen, Z. (2016) The Small Molecule Nobiletin Targets the Molecular Oscillator to Enhance Circadian Rhythms and Protect against Metabolic Syndrome. *Cell Metab* **23**, 610-621
45. Luo, F., Le, N. B., Mills, T., Chen, N. Y., Karmouty-Quintana, H., Molina, J. G., Davies, J., Philip, K., Volcik, K. A., Liu, H., Xia, Y., Eltzschig, H. K., and Blackburn, M. R. (2016) Extracellular adenosine levels are associated with the progression and exacerbation of pulmonary fibrosis. *FASEB J* **30**, 874-883
46. Qin, Z., Bagley, J., Sukhova, G., Baur, W. E., Park, H. J., Beasley, D., Libby, P., Zhang, Y., and Galper, J. B. (2015) Angiotensin II-induced TLR4 mediated abdominal aortic aneurysm in apolipoprotein E knockout mice is dependent on STAT3. *J Mol Cell Cardiol* **87**, 160-170

47. Doyle, T., Chen, Z., Obeid, L. M., and Salvemini, D. (2011) Sphingosine-1-phosphate acting via the S1P(1) receptor is a downstream signaling pathway in ceramide-induced hyperalgesia. *Neurosci Lett* **499**, 4-8
48. Welch, S. P., Sim-Selley, L. J., and Selley, D. E. (2012) Sphingosine-1-phosphate receptors as emerging targets for treatment of pain. *Biochem Pharmacol* **84**, 1551-1562
49. Xiong, Y., Yang, P., Proia, R. L., and Hla, T. (2014) Erythrocyte-derived sphingosine 1-phosphate is essential for vascular development. *J Clin Invest* **124**, 4823-4828
50. Spiegel, S., and Milstien, S. (2003) Exogenous and intracellularly generated sphingosine 1-phosphate can regulate cellular processes by divergent pathways. *Biochem Soc Trans* **31**, 1216-1219
51. Hla, T., Venkataraman, K., and Michaud, J. (2008) The vascular S1P gradient-cellular sources and biological significance. *Biochim Biophys Acta* **1781**, 477-482
52. Chun, J., and Brinkmann, V. (2011) A mechanistically novel, first oral therapy for multiple sclerosis: the development of fingolimod (FTY720, Gilenya). *Discov Med* **12**, 213-228
53. Liang, J., Nagahashi, M., Kim, E. Y., Harikumar, K. B., Yamada, A., Huang, W. C., Hait, N. C., Allegood, J. C., Price, M. M., Avni, D., Takabe, K., Kordula, T., Milstien, S., and Spiegel, S. (2013) Sphingosine-1-phosphate links persistent STAT3 activation, chronic intestinal inflammation, and development of colitis-associated cancer. *Cancer Cell* **23**, 107-120

54. Keikhaei, B., Mohseni, A. R., Norouzirad, R., Alinejadi, M., Ghanbari, S., Shiravi, F., and Solgi, G. (2013) Altered levels of pro-inflammatory cytokines in sickle cell disease patients during vaso-occlusive crises and the steady state condition. *Eur Cytokine Netw* **24**, 45-52
55. Rees, D. C., Williams, T. N., and Gladwin, M. T. (2010) Sickle-cell disease. *Lancet* **376**, 2018-2031
56. Takeda, N., and Maemura, K. (2016) Circadian clock and the onset of cardiovascular events. *Hypertens Res* **39**, 383-390
57. Gamble, K. L., Berry, R., Frank, S. J., and Young, M. E. (2014) Circadian clock control of endocrine factors. *Nat Rev Endocrinol* **10**, 466-475
58. Paschos, G. K., and FitzGerald, G. A. (2010) Circadian clocks and vascular function. *Circ Res* **106**, 833-841
59. Zhang, J., Kaasik, K., Blackburn, M. R., and Lee, C. C. (2006) Constant darkness is a circadian metabolic signal in mammals. *Nature* **439**, 340-343
60. Karatsoreos, I. N., Bhagat, S., Bloss, E. B., Morrison, J. H., and McEwen, B. S. (2011) Disruption of circadian clocks has ramifications for metabolism, brain, and behavior. *Proc Natl Acad Sci U S A* **108**, 1657-1662
61. Richards, J., and Gumz, M. L. (2012) Advances in understanding the peripheral circadian clocks. *FASEB J* **26**, 3602-3613
62. Buijs, R. M., and Kalsbeek, A. (2001) Hypothalamic integration of central and peripheral clocks. *Nat Rev Neurosci* **2**, 521-526

63. Stokkan, K. A., Yamazaki, S., Tei, H., Sakaki, Y., and Menaker, M. (2001) Entrainment of the circadian clock in the liver by feeding. *Science* **291**, 490-493
64. Lamia, K. A., Storch, K. F., and Weitz, C. J. (2008) Physiological significance of a peripheral tissue circadian clock. *Proc Natl Acad Sci U S A* **105**, 15172-15177
65. Fonken, L. K., Workman, J. L., Walton, J. C., Weil, Z. M., Morris, J. S., Haim, A., and Nelson, R. J. (2010) Light at night increases body mass by shifting the time of food intake. *Proc Natl Acad Sci U S A* **107**, 18664-18669
66. Hara, R., Wan, K., Wakamatsu, H., Aida, R., Moriya, T., Akiyama, M., and Shibata, S. (2001) Restricted feeding entrains liver clock without participation of the suprachiasmatic nucleus. *Genes Cells* **6**, 269-278
67. Gery, S., and Koeffler, H. P. (2007) The role of circadian regulation in cancer. *Cold Spring Harb Symp Quant Biol* **72**, 459-464
68. Bass, J., and Takahashi, J. S. (2010) Circadian integration of metabolism and energetics. *Science* **330**, 1349-1354
69. Dickmeis, T. (2009) Glucocorticoids and the circadian clock. *J Endocrinol* **200**, 3-22
70. Gibbs, J., Ince, L., Matthews, L., Mei, J., Bell, T., Yang, N., Saer, B., Begley, N., Poolman, T., Pariollaud, M., Farrow, S., DeMayo, F., Hussell, T., Worthen, G. S., Ray, D., and Loudon, A. (2014) An epithelial circadian clock controls pulmonary inflammation and glucocorticoid action. *Nat Med* **20**, 919-926

71. Belcher, J. D., Chen, C., Nguyen, J., Milbauer, L., Abdulla, F., Alayash, A. I., Smith, A., Nath, K. A., Hebbel, R. P., and Vercellotti, G. M. (2014) Heme triggers TLR4 signaling leading to endothelial cell activation and vaso-occlusion in murine sickle cell disease. *Blood* **123**, 377-390
72. Gonzalez-Michaca, L., Farrugia, G., Croatt, A. J., Alam, J., and Nath, K. A. (2004) Heme: a determinant of life and death in renal tubular epithelial cells. *Am J Physiol Renal Physiol* **286**, F370-377
73. Goldstein, L., Teng, Z. P., Zeserson, E., Patel, M., and Regan, R. F. (2003) Hemin induces an iron-dependent, oxidative injury to human neuron-like cells. *J Neurosci Res* **73**, 113-121
74. Gilles-Gonzalez, M. A., and Gonzalez, G. (2004) Signal transduction by heme-containing PAS-domain proteins. *J Appl Physiol (1985)* **96**, 774-783
75. Raghuram, S., Stayrook, K. R., Huang, P., Rogers, P. M., Nosie, A. K., McClure, D. B., Burris, L. L., Khorasanizadeh, S., Burris, T. P., and Rastinejad, F. (2007) Identification of heme as the ligand for the orphan nuclear receptors REV-ERBalpha and REV-ERBbeta. *Nat Struct Mol Biol* **14**, 1207-1213
76. Yin, L., Wu, N., Curtin, J. C., Qatanani, M., Szwegold, N. R., Reid, R. A., Waitt, G. M., Parks, D. J., Pearce, K. H., Wisely, G. B., and Lazar, M. A. (2007) Rev-erbalpha, a heme sensor that coordinates metabolic and circadian pathways. *Science* **318**, 1786-1789
77. Klemz, R., Reischl, S., Wallach, T., Witte, N., Jurchott, K., Klemz, S., Lang, V., Lorenzen, S., Knauer, M., Heidenreich, S., Xu, M., Ripperger, J. A.,

- Schupp, M., Stanewsky, R., and Kramer, A. (2017) Reciprocal regulation of carbon monoxide metabolism and the circadian clock. *Nat Struct Mol Biol* **24**, 15-22
78. Schallner, N., Lieberum, J. L., Gallo, D., LeBlanc, R. H., 3rd, Fuller, P. M., Hanafy, K. A., and Otterbein, L. E. (2017) Carbon Monoxide Preserves Circadian Rhythm to Reduce the Severity of Subarachnoid Hemorrhage in Mice. *Stroke* **48**, 2565-2573
79. Lang, D., Reuter, S., Buzescu, T., August, C., and Heidenreich, S. (2005) Heme-induced heme oxygenase-1 (HO-1) in human monocytes inhibits apoptosis despite caspase-3 up-regulation. *Int Immunol* **17**, 155-165
80. Ben-Shlomo, R., Akhtar, R. A., Collins, B. H., Judah, D. J., Davies, R., and Kyriacou, C. P. (2005) Light pulse-induced heme and iron-associated transcripts in mouse brain: a microarray analysis. *Chronobiol Int* **22**, 455-471
81. Huang, J., Simcox, J., Mitchell, T. C., Jones, D., Cox, J., Luo, B., Cooksey, R. C., Boros, L. G., and McClain, D. A. (2013) Iron regulates glucose homeostasis in liver and muscle via AMP-activated protein kinase in mice. *FASEB J* **27**, 2845-2854
82. Ghosh, S., Adisa, O. A., Chappa, P., Tan, F., Jackson, K. A., Archer, D. R., and Ofori-Acquah, S. F. (2013) Extracellular heme crisis triggers acute chest syndrome in sickle mice. *J Clin Invest* **123**, 4809-4820
83. Belcher, J. D., Mahaseth, H., Welch, T. E., Otterbein, L. E., Hebbel, R. P., and Vercellotti, G. M. (2006) Heme oxygenase-1 is a modulator of

- inflammation and vaso-occlusion in transgenic sickle mice. *J Clin Invest* **116**, 808-816
84. Fredenburgh, L. E., Merz, A. A., and Cheng, S. (2015) Haeme oxygenase signalling pathway: implications for cardiovascular disease. *Eur Heart J* **36**, 1512-1518
85. Belcher, J. D., Young, M., Chen, C., Nguyen, J., Burhop, K., Tran, P., and Vercellotti, G. M. (2013) MP4CO, a pegylated hemoglobin saturated with carbon monoxide, is a modulator of HO-1, inflammation, and vaso-occlusion in transgenic sickle mice. *Blood* **122**, 2757-2764
86. Zhu, X., Xi, C., Thomas, B., and Pace, B. S. (2018) Loss of NRF2 function exacerbates the pathophysiology of sickle cell disease in a transgenic mouse model. *Blood* **131**, 558-562
87. Yamazaki, H., Ohta, K., Tsukiji, H., Toma, T., Hashida, Y., Ishizaki, A., Saito, T., Arai, S., Koizumi, S., and Yachie, A. (2007) Corticosteroid enhances heme oxygenase-1 production by circulating monocytes by up-regulating hemoglobin scavenger receptor and amplifying the receptor-mediated uptake of hemoglobin-haptoglobin complex. *Biochem Biophys Res Commun* **358**, 506-512
88. Ugocsai, P., Barlage, S., Dada, A., and Schmitz, G. (2006) Regulation of surface CD163 expression and cellular effects of receptor mediated hemoglobin-haptoglobin uptake on human monocytes and macrophages. *Cytometry A* **69**, 203-205

89. Krishnamoorthy, S., Pace, B., Gupta, D., Sturtevant, S., Li, B., Makala, L., Brittain, J., Moore, N., Vieira, B. F., Thullen, T., Stone, I., Li, H., Hobbs, W. E., and Light, D. R. (2017) Dimethyl fumarate increases fetal hemoglobin, provides heme detoxification, and corrects anemia in sickle cell disease. *JCI Insight* **2**
90. Uda, M., Galanello, R., Sanna, S., Lettre, G., Sankaran, V. G., Chen, W., Usala, G., Busonero, F., Maschio, A., Albai, G., Piras, M. G., Sestu, N., Lai, S., Dei, M., Mulas, A., Crisponi, L., Naitza, S., Asunis, I., Deiana, M., Nagaraja, R., Perseu, L., Satta, S., Cipollina, M. D., Sollaino, C., Moi, P., Hirschhorn, J. N., Orkin, S. H., Abecasis, G. R., Schlessinger, D., and Cao, A. (2008) Genome-wide association study shows BCL11A associated with persistent fetal hemoglobin and amelioration of the phenotype of beta-thalassemia. *Proc Natl Acad Sci U S A* **105**, 1620-1625
91. Sankaran, V. G., Menne, T. F., Xu, J., Akie, T. E., Lettre, G., Van Handel, B., Mikkola, H. K., Hirschhorn, J. N., Cantor, A. B., and Orkin, S. H. (2008) Human fetal hemoglobin expression is regulated by the developmental stage-specific repressor BCL11A. *Science* **322**, 1839-1842
92. Cheon, S., Park, N., Cho, S., and Kim, K. (2013) Glucocorticoid-mediated Period2 induction delays the phase of circadian rhythm. *Nucleic Acids Res* **41**, 6161-6174
93. Yoshida, K., Hashiramoto, A., Okano, T., Yamane, T., Shibamura, N., and Shiozawa, S. (2013) TNF-alpha modulates expression of the circadian clock gene Per2 in rheumatoid synovial cells. *Scand J Rheumatol* **42**, 276-280

94. Murphy, B. A., Vick, M. M., Sessions, D. R., Cook, R. F., and Fitzgerald, B. P. (2007) Acute systemic inflammation transiently synchronizes clock gene expression in equine peripheral blood. *Brain Behav Immun* **21**, 467-476
95. Fukuoka, Y., Burioka, N., Takata, M., Ohdo, S., Miyata, M., Endo, M., and Shimizu, E. (2005) Glucocorticoid administration increases hPer1 mRNA levels in human peripheral blood mononuclear cells in vitro or in vivo. *J Biol Rhythms* **20**, 550-553
96. Leone, M. J., Marpegan, L., Duhart, J. M., and Golombek, D. A. (2012) Role of proinflammatory cytokines on lipopolysaccharide-induced phase shifts in locomotor activity circadian rhythm. *Chronobiol Int* **29**, 715-723
97. Abo, T., Kawate, T., Itoh, K., and Kumagai, K. (1981) Studies on the bioperiodicity of the immune response. I. Circadian rhythms of human T, B, and K cell traffic in the peripheral blood. *J Immunol* **126**, 1360-1363
98. Arjona, A., and Sarkar, D. K. (2005) Circadian oscillations of clock genes, cytolytic factors, and cytokines in rat NK cells. *J Immunol* **174**, 7618-7624
99. Born, J., Lange, T., Hansen, K., Molle, M., and Fehm, H. L. (1997) Effects of sleep and circadian rhythm on human circulating immune cells. *J Immunol* **158**, 4454-4464
100. Fortier, E. E., Rooney, J., Dardente, H., Hardy, M. P., Labrecque, N., and Cermakian, N. (2011) Circadian variation of the response of T cells to antigen. *J Immunol* **187**, 6291-6300
101. Segall, L. A., and Amir, S. (2010) Glucocorticoid regulation of clock gene expression in the mammalian limbic forebrain. *J Mol Neurosci* **42**, 168-175

102. Adams, K. L., Castanon-Cervantes, O., Evans, J. A., and Davidson, A. J. (2013) Environmental circadian disruption elevates the IL-6 response to lipopolysaccharide in blood. *J Biol Rhythms* **28**, 272-277
103. Castanon-Cervantes, O., Wu, M., Ehlen, J. C., Paul, K., Gamble, K. L., Johnson, R. L., Besing, R. C., Menaker, M., Gewirtz, A. T., and Davidson, A. J. (2010) Dysregulation of inflammatory responses by chronic circadian disruption. *J Immunol* **185**, 5796-5805
104. Guan, Z., Vgontzas, A. N., Omori, T., Peng, X., Bixler, E. O., and Fang, J. (2005) Interleukin-6 levels fluctuate with the light-dark cycle in the brain and peripheral tissues in rats. *Brain Behav Immun* **19**, 526-529
105. Sato, S., Sakurai, T., Ogasawara, J., Takahashi, M., Izawa, T., Imaizumi, K., Taniguchi, N., Ohno, H., and Kizaki, T. (2014) A circadian clock gene, Rev-erbalpha, modulates the inflammatory function of macrophages through the negative regulation of Ccl2 expression. *J Immunol* **192**, 407-417
106. Tsuchiya, Y., Minami, I., Kadotani, H., and Nishida, E. (2005) Resetting of peripheral circadian clock by prostaglandin E2. *EMBO Rep* **6**, 256-261
107. Schaer, D. J., Buehler, P. W., Alayash, A. I., Belcher, J. D., and Vercellotti, G. M. (2013) Hemolysis and free hemoglobin revisited: exploring hemoglobin and hemin scavengers as a novel class of therapeutic proteins. *Blood* **121**, 1276-1284
108. Kristiansen, M., Graversen, J. H., Jacobsen, C., Sonne, O., Hoffman, H. J., Law, S. K., and Moestrup, S. K. (2001) Identification of the haemoglobin scavenger receptor. *Nature* **409**, 198-201

109. Kartikasari, A. E., Wagener, F. A., Yachie, A., Wiegerinck, E. T., Kemna, E. H., and Swinkels, D. W. (2009) Heparin suppression and defective iron recycling account for dysregulation of iron homeostasis in heme oxygenase-1 deficiency. *J Cell Mol Med* **13**, 3091-3102
110. Schaer, C. A., Schoedon, G., Imhof, A., Kurrer, M. O., and Schaer, D. J. (2006) Constitutive endocytosis of CD163 mediates hemoglobin-heme uptake and determines the noninflammatory and protective transcriptional response of macrophages to hemoglobin. *Circ Res* **99**, 943-950
111. Braughler, J. M., Duncan, L. A., and Chase, R. L. (1986) The involvement of iron in lipid peroxidation. Importance of ferric to ferrous ratios in initiation. *J Biol Chem* **261**, 10282-10289
112. Birben, E., Sahiner, U. M., Sackesen, C., Erzurum, S., and Kalayci, O. (2012) Oxidative stress and antioxidant defense. *World Allergy Organ J* **5**, 9-19
113. Figueiredo, R. T., Fernandez, P. L., Mourao-Sa, D. S., Porto, B. N., Dutra, F. F., Alves, L. S., Oliveira, M. F., Oliveira, P. L., Graca-Souza, A. V., and Bozza, M. T. (2007) Characterization of heme as activator of Toll-like receptor 4. *J Biol Chem* **282**, 20221-20229
114. Vinchi, F., Costa da Silva, M., Ingoglia, G., Petrillo, S., Brinkman, N., Zuercher, A., Cerwenka, A., Tolosano, E., and Muckenthaler, M. U. (2016) Hemopexin therapy reverts heme-induced proinflammatory phenotypic switching of macrophages in a mouse model of sickle cell disease. *Blood* **127**, 473-486

115. Turek, F. W., Joshu, C., Kohsaka, A., Lin, E., Ivanova, G., McDearmon, E., Laposky, A., Losee-Olson, S., Easton, A., Jensen, D. R., Eckel, R. H., Takahashi, J. S., and Bass, J. (2005) Obesity and metabolic syndrome in circadian Clock mutant mice. *Science* **308**, 1043-1045
116. Darghouth, D., Koehl, B., Madalinski, G., Heillier, J. F., Bovee, P., Xu, Y., Olivier, M. F., Bartolucci, P., Benkerrou, M., Pissard, S., Colin, Y., Galacteros, F., Bosman, G., Junot, C., and Romeo, P. H. (2011) Pathophysiology of sickle cell disease is mirrored by the red blood cell metabolome. *Blood* **117**, e57-66
117. Rogers, S. C., Ross, J. G., d'Avignon, A., Gibbons, L. B., Gazit, V., Hassan, M. N., McLaughlin, D., Griffin, S., Neumayr, T., Debaun, M., DeBaun, M. R., and Doctor, A. (2013) Sickle hemoglobin disturbs normal coupling among erythrocyte O₂ content, glycolysis, and antioxidant capacity. *Blood* **121**, 1651-1662
118. Liu, H., and Xia, Y. (2015) Beneficial and detrimental role of adenosine signaling in diseases and therapy. *J Appl Physiol (1985)* **119**, 1173-1182
119. Liu, H., Zhang, Y., Wu, H., D'Alessandro, A., Yegutkin, G. G., Song, A., Sun, K., Li, J., Cheng, N. Y., Huang, A., Edward Wen, Y., Weng, T. T., Luo, F., Nemkov, T., Sun, H., Kellems, R. E., Karmouty-Quintana, H., Hansen, K. C., Zhao, B., Subudhi, A. W., Jameson-Van Houten, S., Julian, C. G., Lovering, A. T., Eltzschig, H. K., Blackburn, M. R., Roach, R. C., and Xia, Y. (2016) Beneficial Role of Erythrocyte Adenosine A_{2B} Receptor-Mediated AMP-Activated Protein Kinase Activation in High-Altitude Hypoxia. *Circulation* **134**, 405-421

120. Zhou, Y., Mohsenin, A., Morschl, E., Young, H. W., Molina, J. G., Ma, W., Sun, C. X., Martinez-Valdez, H., and Blackburn, M. R. (2009) Enhanced airway inflammation and remodeling in adenosine deaminase-deficient mice lacking the A2B adenosine receptor. *J Immunol* **182**, 8037-8046
121. Yoo, S. H., Ko, C. H., Lowrey, P. L., Buhr, E. D., Song, E. J., Chang, S., Yoo, O. J., Yamazaki, S., Lee, C., and Takahashi, J. S. (2005) A noncanonical E-box enhancer drives mouse Period2 circadian oscillations in vivo. *Proc Natl Acad Sci U S A* **102**, 2608-2613
122. Vespa, P. M. (2016) Brain Hypoxia and Ischemia After Traumatic Brain Injury: Is Oxygen the Right Metabolic Target? *JAMA Neurol* **73**, 504-505
123. Yan, E. B., Hellewell, S. C., Bellander, B. M., Agyapomaa, D. A., and Morganti-Kossmann, M. C. (2011) Post-traumatic hypoxia exacerbates neurological deficit, neuroinflammation and cerebral metabolism in rats with diffuse traumatic brain injury. *J Neuroinflammation* **8**, 147
124. Mirschink, P., and Krek, W. (2016) Hypoxia-driven glycolytic and fructolytic metabolic programs: Pivotal to hypertrophic heart disease. *Biochim Biophys Acta* **1863**, 1822-1828
125. Sun, K., Zhang, Y., D'Alessandro, A., Nemkov, T., Song, A., Wu, H., Liu, H., Adebiyi, M., Huang, A., Wen, Y. E., Bogdanov, M. V., Vila, A., O'Brien, J., Kellems, R. E., Dowhan, W., Subudhi, A. W., Jameson-Van Houten, S., Julian, C. G., Lovering, A. T., Safo, M., Hansen, K. C., Roach, R. C., and Xia, Y. (2016) Sphingosine-1-phosphate promotes erythrocyte glycolysis and oxygen release for adaptation to high-altitude hypoxia. *Nat Commun* **7**, 12086

126. Molzer, C., Wallner, M., Kern, C., Tosevska, A., Zadnikar, R., Doberer, D., Marculescu, R., and Wagner, K. H. (2017) Characteristics of the heme catabolic pathway in mild unconjugated hyperbilirubinemia and their associations with inflammation and disease prevention. *Sci Rep* **7**, 755
127. Beaver, L. M., Klichko, V. I., Chow, E. S., Kotwica-Rolinska, J., Williamson, M., Orr, W. C., Radyuk, S. N., and Giebultowicz, J. M. (2012) Circadian regulation of glutathione levels and biosynthesis in *Drosophila melanogaster*. *PLoS One* **7**, e50454
128. Blanco, R. A., Ziegler, T. R., Carlson, B. A., Cheng, P. Y., Park, Y., Cotsonis, G. A., Accardi, C. J., and Jones, D. P. (2007) Diurnal variation in glutathione and cysteine redox states in human plasma. *Am J Clin Nutr* **86**, 1016-1023

VI. Biographical Sketch

Morayo G. Adebisi

EDUCATION

PhD 2018

MD Anderson Cancer Center UTHealth Graduate School of Biomedical Sciences,
Biochemistry and Molecular Biology, Houston, TX

BS 2012

Spelman College, Environmental Sciences and Studies, Atlanta, GA
Magna cum laude

RESEARCH POSITIONS

06-2013 to current	MD Anderson Cancer Center UTHealth	Graduate Student
07-2012 to 06-2013	University of Chicago	PREP Scholar
08-2011 to 05-2012	Spelman College	Research Technician
05-2011 to 08-2011	Harvard Medical School	SHURP Scholar
05-2010 to 12-2010	Louisiana State University	HHMI Scholar

SPECIAL HONORS AND AWARDS

2015 to 2018	NIH- National Heart, Lung and Blood Diversity Supplement Award
2016 to 2017	Sam Taub & Beatrice Burton Vison and Sensory Award
2016 Award	American Society of Hematology Minority Abstract Achievement
2016	3 rd Place Oral Presentation Biochemistry and Molecular Biology Annual Retreat
2016	Translational Pain Research (TPR) Distinguished Trainee Award
2015	American Society of Hematology Minority Abstract Achievement Award
2012 to 2013	NIH- Post-Baccalaureate Enrichment Research (PREP) Scholar
2009 to 2012	Spelman College Dean's List
2010 to 2012	Spelman STEM Scholar S3

2009 to 2012	United Health Diverse Initiative Scholar
2011 to 2012	United Parcel Service Community Service Scholar
2009 to 2010	Siemens Science Teacher Scholar
2009 to 2010	Thurgood Marshall Scholar
2010	Spelman College Research Day 1 st Place Poster Presentation

PUBLICATIONS

Zhao S* and **Adebiyi M.G.***, Zhang Y, Couturier J, Fan X, Zhang H, Kellems R.E., Lewis D.E. and Xia Y. Sphingosine-1-phosphate receptor 1 mediates elevated IL-6 signaling to promote chronic inflammation and multi-tissue damage in sickle cell disease. *FASEB J.* 2017. In press. [* **First authorship shared**]

Sun K, D'Alessandro A, Ahmed M.H., Zhang Y, Song A, Ko T.P., Nemkov T, Reisz J.A., Wu H, **Adebiyi M**, Peng Z, Gong J, Liu H, Huang A, Wen Y.E., Wen A.Q., Berka V, Bogdanov M.V., Abdulmalik O, Han L, Tsai A.L., Idowu M, Juneja H.S., Kellems R.E., Dowhan W, Hansen KC, Safo M.K., Xia Y. Structural and Functional Insight of Sphingosine 1-Phosphate-Mediated Pathogenic Metabolic Reprogramming in Sickle Cell Disease. *Sci Rep.* 2017 Nov 10;7 (1):15281.

Wu H, Bogdanov M, Zhang Y, Sun K, Zhao S, Song A, Luo R, Parchim N.F., Liu H, Huang A, **Adebiyi M.G.**, Jin J, Alexander D.C., Milburn M.V., Idowu M, Juneja H.S., Kellems R.E., Dowhan W, Xia Y. Hypoxia-mediated impaired erythrocyte Lands' Cycle is pathogenic for sickle cell disease. *Sci Rep.* 2016 Jul 20;6:29637.

Hu X, **Adebiyi M.G.**, Luo J, Sun K, Le T-T.L., Zhang Y, Wu H, Zhao S, Karmouty-Quintana H, Liu H, Huang A, Wen Y.E., Zaika O.L., Mamenko M, Pochynyuk O.M., Kellems R.E., Etszchig H.K., Blackburn M.R., Walters E.T., Huang D, Hu H and Xia Y. Sustained elevation of adenosine-ADORA2B signaling promotes chronic pain through neuro-immune interaction. *Cell Rep.* 2016 Jun 28; 16(1):106-19.

Sun K, Zhang Y, D'Alessandro D, Nemkov T, Song A, Wu H, Liu H, **Adebiyi M**, Huang A, Wen Y.E., Bogdanov M.V., Vila A, O'Brien J, Kellems R.E., Dowhan W, Subudhi A.W., Jameson-Van Houten S, Julian C.G., Lovering A.T., Safo M, Hansen K, Roach R.C. and Xia Y. Sphingosine-1-phosphate promotes erythrocyte glycolysis and oxygen release for adaptation to high-altitude hypoxia. *Nat Commun.* 2016; 7:12086.

Ayalew M, Matheson K, **Adebiyi M**, Robinson S, Elston B. RNA-seq analysis of the effect of kanamycin and the ABC transporter AtWBC19 on *Arabidopsis thaliana* seedlings reveals changes in metal content. *PLoS One.* 2014 Oct 13; 9(10):e109310.

Dharmasiri U, Njoroge S.K., Witek M.A., **Adebiyi M.G.**, Kamande J.W., Hupert M.L., Barany F and Soper S.A. High-Throughput Selection, Enumeration, Electrokinetic Manipulation, and Molecular Profiling of Low-Abundance Circulating Tumor Cells Using a Microfluidic System. *Anal Chem.* 2011 Mar 15; 83 (6):2301-9.

CONFERENCE PRESENTATIONS

Adebiyi M.G., Zhang Y, Manlo J, Zhao Z, Lee C-C. and Xia Y. The role of circadian clock genes *Period1/ 2* in Sickle Cell Disease. Biochemistry and Molecular Biology Annual Retreat, Magnolia, TX, March, 2017

Adebiyi M.G., Sun K, Zhang Y, Hu X and Xia Y. The role and mechanism of Sphingosine-1-Phosphate (S1P) signaling via S1P receptor 1 (S1PR1) in macrophage contributes to pain. American Society of Hematology, San Diego, CA, Dec, 2016

Adebiyi M.G., Sun K, Zhang Y, Hu X and Xia Y. The role and mechanism of Sphingosine-1-Phosphate (S1P) signaling via S1P receptor 1 (S1PR1) in macrophage contributes to pain. Graduate School of Biomedical Science at UTHealth/MD Anderson Research Day, Houston, TX, June, 2016.

Adebiyi M.G., Utilizing rodent models to study chronic pain. Oral presentation delivered for UT-GSBS Summer Research Undergraduate Program (SURP), Houston, TX, June 2016.

Adebiyi M.G., Sun K, Zhang Y, Hu X and Xia Y. The role and mechanism of Sphingosine-1-Phosphate (S1P) signaling via S1P Receptor 1 (S1PR1) contributes to pain in Sickle Cell Disease. Oral presentation delivered at Society of Chinese Bioscientists in America meeting, Houston, TX, May 2016.

Adebiyi M.G. and Xia Y. Studying the role of macrophages in models of inflammatory pain. Oral presentation delivered at seminar series titled, 'I Dream of Flow Cytometry', Houston, TX, January, 2016.

Adebiyi M.G., Sun K, Zhang Y, Hu X and Xia Y. The role and mechanism of Sphingosine-1-Phosphate (S1P) signaling via S1P Receptor 1 (S1PR1) in macrophage mediates inflammatory pain in Sickle Cell Disease. Oral presentation delivered at Translational Pain Research Symposium meeting, Houston, TX, April 2016

Adebiyi M.G., Hu X, Luo J, Sun K, Le T-T.T., Zhang Y, Wu H, Zhao S, Liu H, Huang A, Kellems R.E., Etslzchig H.K., Blackburn M.R., Walters E.T., Hu H and Xia Y. Sustained elevation of adenosine-ADORA2B signaling promotes chronic pain through neuro-immune interaction in Sickle Cell Disease. Poster presentation delivered at American Society of Hematology, Orlando, FL, December, 2015.

Adebiyi M.G. and Ayalew M. The effect of the Arabidopsis ABC transporter Atwbc19 on transcript levels of iron regulated genes. Poster presentation delivered at Southern Regional Conference American Society of Plant Biology Conference, Myrtle Beach, SC, 2012.

Adebiyi M.G., Henke K and Harris M.P. Zebrafish as a Model for Craniosynostosis. Poster presentation delivered at Leadership Alliance Conference, New Haven, Conn, August, 2011.

Shackleford J, **Adebiyi M.G.**, Akinseye A, Mustafa R and Yerokun T. Characterizing How Single Nucleotide Mutations Affect the MSH2 Mismatch Repair Gene and Potential Consequence on the Development of Colorectal Cancer. Poster Presentation delivered at Spelman College Research Day, Atlanta, GA, 2010.

Adebiyi M.G., Dharmasiri U, Njoroge S.K., Witek M, Hupert M and Soper S.A. High-Throughput Selection, Enumeration, Electrokinetic Manipulation, and Molecular Profiling of Low-Abundance Circulating Tumor Cells Using a Microfluidic System. Poster presentation delivered at HHMI Undergraduate Summer Research Symposium, Baton Rouge, LA, 2010.

PUBLIC SERVICE

2014 to 2018	Graduate School Biomedical Science 1 st Generation Student Group at UTHealth/MD Anderson, Voting Member
2013 to 2018	Association of Minority of Biomedical Researchers, Member
2017	Graduate Student Biomedical Science Ambassador
2016 to 2017	Graduate Program of Biochemistry and Molecular Biology Steering Committee
2016 to 2017	Graduate Program of Biochemistry and Molecular Biology Education Committee
2016 to 2017	Biochemistry and Molecular Biology Student Association, President
2015 to 2016	Biochemistry and Molecular Biology Student Association, Vice President

MEMBERSHIPS

Association of Minority Biomedical Researchers, Association of First Generation Students, the Nigerian-American Multicultural Council, Honor Society for Graduate Students, Beta Kappa Chi Scientific Honor Society, National Society of Leadership Success

SKILLSETS

Volunteerism: GSBS Science Night

Course work: Scientific Writing, Life Science entrepreneurship, and Network Leadership

CONTACT PERSONS

- Ph.D advisor: Yang Xia, M.D, Ph.D, Professor, McGovern Scholar, Dept. of Biochemistry and Molecular Biology, UT Health. Email: yang.xia@uth.tmc.edu, Phone: +1 (713) 500-5039
- Advisory committee member: Rodney E. Kellems, Ph.D, Professor and Chairman, Dept. of Biochemistry and Molecular Biology, UT Health. Email: rodney.e.kellems@uth.tmc.edu, Phone: +1 (713) 500-6124 Advisory & Candidacy
- Advisory & Candidacy Examination Committee member: Dorothy E. Lewis, Ph.D, Professor, Dept. of Internal Medicine, UT Health. Email: dorothe.e.lewis@uth.tmc.edu, Phone: +1 (713) 500-6809

VII. Vita

Morayo Gloria Adebisi is the daughter of David Adebisi Sr. and Caroline Aboderin. Her hometown is Atlanta, GA. She is an alumnae of the prestigious Spelman College where she majored in Environmental Sciences and Studies. While at Spelman, she volunteered at Grady Memorial Hospital Sickle Cell Unit and was a Siemens Science Teacher Scholar. Due to her interests in biomedical sciences, she accepted a post-baccalaureate position at the University of Chicago where she learned biochemistry and molecular biology. In the summer of 2013, she enrolled as a graduate student at the University of Texas MD Anderson Cancer Center UT Health Graduate School of Biomedical Sciences.